UNIVERSITY OF AMSTERDAM

UvA-DARE (Digital Academic Repository)

Search for new phenomena in final states with b-jets and missing transverse momentum in √s = 13 TeV pp collisions with the ATLAS detector

The ATLAS Collaboration

DOI
10.1007/JHEP05(2021)093

Publication date
2021

Document Version
Final published version

Published in
Journal of High Energy Physics

License
CC BY

Link to publication

Citation for published version (APA):
The ATLAS Collaboration (2021). Search for new phenomena in final states with b-jets and missing transverse momentum in √s = 13 TeV pp collisions with the ATLAS detector. *Journal of High Energy Physics*, *2021*(05), Article 093. https://doi.org/10.1007/JHEP05(2021)093

General rights
It is not permitted to download or to forward/distribute the text or part of it without the consent of the author(s) and/or copyright holder(s), other than for strictly personal, individual use, unless the work is under an open content license (like Creative Commons).

Disclaimer/Complaints regulations
If you believe that digital publication of certain material infringes any of your rights or (privacy) interests, please let the Library know, stating your reasons. In case of a legitimate complaint, the Library will make the material inaccessible and/or remove it from the website. Please Ask the Library: https://uba.uva.nl/en/contact, or a letter to: Library of the University of Amsterdam, Secretariat, P.O. Box 19185, 1000 GD Amsterdam, The Netherlands. You will be contacted as soon as possible.

UvA-DARE is a service provided by the library of the University of Amsterdam (https://dare.uva.nl)

Download date:10 Nov 2026

Published for SISSA by Springer

Received: *February 1, 2021*
Accepted: *April 19, 2021*
Published: *May 12, 2021*

Search for new phenomena in final states with b-jets and missing transverse momentum in $\sqrt{s} = 13$ TeV pp collisions with the ATLAS detector

The ATLAS collaboration

E-mail: atlas.publications@cern.ch

Abstract: The results of a search for new phenomena in final states with b-jets and missing transverse momentum using 139 fb^{-1} of proton-proton data collected at a centre-of-mass energy $\sqrt{s} = 13$ TeV by the ATLAS detector at the LHC are reported. The analysis targets final states produced by the decay of a pair-produced supersymmetric bottom squark into a bottom quark and a stable neutralino. The analysis also seeks evidence for models of pair production of dark matter particles produced through the decay of a generic scalar or pseudoscalar mediator state in association with a pair of bottom quarks, and models of pair production of scalar third-generation down-type leptoquarks. No significant excess of events over the Standard Model background expectation is observed in any of the signal regions considered by the analysis. Bottom squark masses below 1270 GeV are excluded at 95% confidence level if the neutralino is massless. In the case of nearly mass-degenerate bottom squarks and neutralinos, the use of dedicated secondary-vertex identification techniques permits the exclusion of bottom squarks with masses up to 660 GeV for mass splittings between the squark and the neutralino of 10 GeV. These limits extend substantially beyond the regions of parameter space excluded by similar ATLAS searches performed previously.

Keywords: Hadron-Hadron scattering (experiments), Supersymmetry

ArXiv ePrint: 2101.12527

Open Access, Copyright CERN,
for the benefit of the ATLAS Collaboration.
Article funded by SCOAP^3.

https://doi.org/10.1007/JHEP05(2021)093

JHEP05(2021)093

Contents

1 Introduction **1**

2 ATLAS detector **2**

3 Data collection and simulated event samples **3**

4 Event reconstruction **5**

5 Analysis strategy **8**
- 5.1 Discriminating variables 8
- 5.2 SRA definition 10
- 5.3 SRB definition 11
- 5.4 SRC definition 12
- 5.5 SRD definition 14
- 5.6 Control and validation region definition 14

6 Systematic uncertainties **16**

7 Results and interpretation **18**

8 Conclusions **23**

The ATLAS collaboration **35**

JHEP05(2021)093

1 Introduction

The possible existence of non-luminous matter in the universe, referred to as dark matter (DM), is supported by a wide variety of astrophysical and cosmological measurements [1–5]. However, the nature and properties of the DM remain largely unknown and represent one of the most important unanswered questions in physics. A plausible candidate for cold dark matter [6, 7] is the stable lightest neutralino ($\tilde{\chi}_1^0$) in R-parity-conserving models [8] of electroweak scale supersymmetry (SUSY) [9–14]. In supersymmetric models that naturally address the gauge hierarchy problem [15–18], the scalar partners of the third-generation quarks are light [19, 20]. This may lead to the lighter bottom squark ($\tilde{b}_1$) and top squark ($\tilde{t}_1$) mass eigenstates[1] being significantly lighter than the other squarks and gluinos. As a consequence, the $\tilde{b}_1$ and $\tilde{t}_1$ could be pair produced with relatively large cross-sections in pp

[1]The scalar partners of the left-handed and right-handed chiral components of the bottom quark ($\tilde{b}_L$, $\tilde{b}_R$) or top quark ($\tilde{t}_L$, $\tilde{t}_R$) mix to form two mass eigenstates in each case, of which the $\tilde{b}_1$ and the $\tilde{t}_1$ are defined to be the lighter.

collisions at the Large Hadron Collider (LHC [21]). In most SUSY models, the $\tilde{b}_1$ and the $\tilde{t}_1$ decay into final states incorporating third-generation quarks and invisible $\tilde{\chi}_1^0$ particles.

More generically, the dark matter may be composed of weakly interacting massive particles (WIMPs, generically denoted by χ in the rest of the paper) [22], of which the lightest supersymmetric particle (LSP) is one example. WIMPs can account for the measured relic density of dark matter in the early universe across a broad portion of parameter space [1, 2, 23]. WIMPs could be produced in pairs at the LHC through the decay of a new mediator particle coupling to Standard Model (SM) quarks [24–29]. Should this mediator preferentially couple to third-generation quarks then an excess of events containing such quarks along with invisible dark matter particles could be observed. Such events can be described in the framework of simplified DM models [28, 30, 31] with model assumptions described in refs. [28, 29, 32, 33].

This paper describes a search for the production of invisible dark matter particles in association with bottom quarks. Signal regions (SRs) are developed which target the direct pair production of bottom squarks, each of which decays into a $\tilde{\chi}_1^0$ and a bottom quark, as shown in figure 1a. Additional signal regions target the pair production of DM particles through the decay of a generic scalar (ϕ) or pseudoscalar (a) mediator state produced in association with a pair of bottom quarks (figure 1b). The results of the analysis are also interpreted in the context of beyond-the-SM (BSM) scenarios incorporating pair-produced scalar third-generation down-type leptoquarks LQ_3^d [34–41] decaying to bottom quarks and neutrinos or top quarks and τ-leptons (figure 1c). These models are all characterised by events consisting of jets containing b-hadrons (b-jets), missing transverse momentum ($E_{\mathrm{T}}^{\mathrm{miss}}$), and no charged leptons.

Previous searches by ATLAS [42–45] and CMS [46, 47] using comparable or smaller datasets have targeted similar final states. This analysis extends the regions of parameter space probed by the LHC through the use of a larger dataset than in previous ATLAS searches, new boosted decision tree (BDT) discriminants, and also new selections maximising the efficiency for reconstructing b-jets with low transverse momentum generated by, for instance, SUSY models with small mass-splitting between $\tilde{b}_1$ and $\tilde{\chi}_1^0$.

Section 2 presents a brief overview of the ATLAS detector, section 3 describes the data and simulation samples used in the analysis and section 4 presents the methods used to reconstruct events. An overview of the analysis strategy, including background estimation, is presented in section 5. The systematic uncertainties considered in the analysis are described in section 6. Section 7 presents the results and interpretation thereof. The conclusions of the analysis are presented in section 8.

2 ATLAS detector

The ATLAS detector [48–50] is a multipurpose detector with a forward-backward symmetric cylindrical geometry and nearly 4π coverage in solid angle.[2] The inner detector (ID)

[2]ATLAS uses a right-handed coordinate system with its origin at the nominal interaction point in the centre of the detector. The positive x-axis is defined by the direction from the interaction point to the centre of the LHC ring, with the positive y-axis pointing upwards, while the beam direction defines the

JHEP05(2021)093

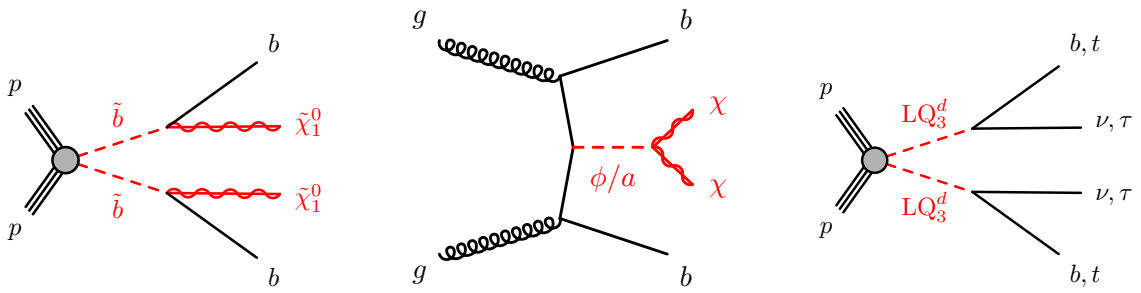

Figure 1. Diagrams illustrating the processes targeted by this analysis: (a) bottom squark pair production, (b) production of DM particles (indicated with χ) through the decay of a scalar or pseudoscalar mediator coupling to bottom quarks, and (c) pair production of scalar third-generation down-type leptoquarks decaying to bottom quarks and neutrinos or top quarks and τ-leptons. BSM particles are indicated in red, while SM particles are indicated in black.

tracking system consists of pixel and silicon microstrip detectors covering the pseudorapidity region $|\eta| < 2.5$, surrounded by a transition radiation tracker, which improves electron identification over the region $|\eta| < 2.0$. The ID is surrounded by a thin superconducting solenoid providing an axial 2 T magnetic field and by a fine-granularity lead/liquid-argon (LAr) electromagnetic calorimeter covering $|\eta| < 3.2$. A steel/scintillator-tile calorimeter provides hadronic coverage in the central pseudorapidity range ($|\eta| < 1.7$). The endcap and forward calorimeters ($1.5 < |\eta| < 4.9$) are made of LAr active layers with either copper or tungsten as the absorber material for electromagnetic and hadronic measurements. The muon spectrometer with an air-core toroid magnet system surrounds the calorimeters. Three layers of high-precision tracking chambers provide coverage in the range $|\eta| < 2.7$, while dedicated chambers allow triggering in the region $|\eta| < 2.4$.

3 Data collection and simulated event samples

The data analysed in this paper were collected between 2015 and 2018 at a centre-of-mass energy of 13 TeV with a 25 ns proton bunch crossing interval. The average number of pp interactions per bunch crossing (pile-up) ranged from 13 in 2015 to around 38 in 2017–2018. Application of beam, detector and data-quality criteria [51] results in a total integrated luminosity of 139 fb^{-1}. The uncertainty in the combined 2015–2018 integrated luminosity is 1.7% [52], obtained using the LUCID-2 detector [53] for the primary luminosity measurements and cross-checked by a suite of other systems.

Events are required to pass a missing transverse momentum trigger [54, 55] with an online threshold of 70–110 GeV, depending on the data-taking period. This trigger is

z-axis. Cylindrical coordinates (r, ϕ) are used in the transverse plane, ϕ being the azimuthal angle around the z-axis. The transverse momentum p_{T}, the transverse energy E_{T} and the missing transverse momentum are defined in the x–y plane unless stated otherwise. The pseudorapidity η is defined in terms of the polar angle θ by $\eta = -\ln\tan(\theta/2)$ and the rapidity is defined as $y = (1/2)\ln[(E + p_z)/(E - p_z)]$ where E is the energy and p_z the longitudinal momentum of the object of interest.

JHEP05(2021)093

found [55] to have an efficiency greater than 95% for events satisfying the offline selections of the analysis. Additional single-lepton triggers requiring the presence of electrons or muons are used in the two-lepton control regions defined in section 5 to estimate the background originating from $Z+$jets production [56, 57]. These triggers yield an approximately constant efficiency in the presence of a single isolated electron or muon with transverse momentum (p_{T}) greater than 27 GeV.

Monte Carlo (MC) simulations are used to model SM background processes and the SUSY, dark matter and leptoquark signals considered in the analysis. Samples of bottom squark and dark matter signal events were generated with MadGraph5_aMC@NLO 2.6.2 [58] at leading order (LO) in the strong coupling constant (α_{S}), with the renormalisation and factorisation scales set to $H_{\mathrm{T}}^{\mathrm{gen}}/2$ (where $H_{\mathrm{T}}^{\mathrm{gen}}$ is the scalar sum of the transverse momenta of the outgoing partons) and parton distribution function (PDF) NNPDF2.3 LO [59]. The matrix element (ME) calculations were performed at tree level and include the emission of up to two additional partons. Bottom squarks decayed directly into a $\tilde{\chi}_1^0$ and a bottom quark with 100% branching ratio, as is the case in R-parity-conserving models in which the lighter bottom squark is the next-to-lightest supersymmetric particle. Leptoquark signal events were generated at next-to-leading order (NLO) in α_{S} with MadGraph5_aMC@NLO 2.6.0 [58], using the leptoquark model of ref. [60] that adds parton showers to previous fixed-order NLO QCD calculations [61, 62], and the NNPDF3.0 NLO [63] PDF set with $\alpha_{\mathrm{S}} = 0.118$. In all cases, simulated signal events were passed to Pythia 8.230 [64] for parton showering (PS) and hadronisation. ME–PS matching was performed following the CKKW-L prescription [65], with a matching scale set to one quarter of the mass of the bottom squark or leptoquark.

Bottom squark pair-production cross-sections were calculated at approximate next-to-next-to-leading-order (NNLO) accuracy in α_{S}, also adding contributions from the resummation of soft gluon emission at next-to-next-to-leading-logarithm accuracy (approximate NNLO+NNLL) [66–69]. The nominal cross-sections and their uncertainties were derived using the PDF4LHC15_mc PDF set, following the recommendations of ref. [70]. For $\tilde{b}_1$ masses ranging from 400 GeV to 1.5 TeV, the cross-sections range from 2.1 pb to 0.26 fb, with uncertainties ranging from 7% to 17%. Leptoquark signal cross-sections were obtained from the calculation of direct top squark pair production, as this process has the same production modes, computed at approximate next-to-next-to-leading order (NNLO) in α_{S} with resummation of next-to-next-to-leading logarithmic (NNLL) soft gluon terms [66–69]. The cross-sections do not include lepton t-channel contributions, which are neglected in ref. [60] and may lead to corrections at the percent level [71].

The production cross-sections for generic scalar and pseudoscalar mediators were evaluated including NLO QCD corrections assuming SM Yukawa couplings to quarks, in a five-flavour scheme, following the prescriptions of ref. [72]. They were calculated with renormalisation and factorisation scales set to $H_{\mathrm{T}}^{\mathrm{gen}}/3$ and the jet p_{T} threshold ('ptj' in ref. [72]) set to 20 GeV. They range from about 29 pb to about 1.5 fb for mediator masses between 10 GeV and 500 GeV.

The SM backgrounds considered in this analysis are: $Z+$jets production; $W+$jets production; $t\bar{t}$ pair production; single-top-quark production; $t\bar{t}$ production in association

JHEP05(2021)093

Process	ME event generator	PDF	PS and hadronisation	UE tune	Cross-section calculation
V+jets ($V = W/Z$)	Sherpa 2.2.1 [73]	NNPDF3.0 NNLO	Sherpa	Default	NNLO [74]
$t\bar{t}$	Powheg-Box v2 [75]	NNPDF3.0 NNLO	Pythia 8.230	A14	NNLO+NNLL [76–81]
Single top	Powheg-Box v2	NNPDF3.0 NNLO	Pythia 8.230	A14	NNLO+NNLL [82–84]
Diboson	Sherpa 2.2.1–2.2.2	NNPDF3.0 NNLO	Sherpa	Default	NLO
$t\bar{t}+V$	aMC@NLO 2.3.3	NNPDF3.0 NLO	Pythia 8.210	A14	NLO [58]
$t\bar{t}H$	aMC@NLO 2.2.3	NNPDF3.0 NLO	Pythia 8.230	A14	NLO [85–88]

Table 1. The SM background MC simulation samples used in this paper. Generator, PDF set, parton shower, tune used for the underlying event (UE), and order in α_S of cross-section calculations used for yield normalisation, are shown for each process considered.

with electroweak or Higgs bosons ($t\bar{t}+X$); and diboson production (WW, ZZ, ZW, ZH and WH). The events were simulated using different MC generator programs depending on the process. Details of the generators, PDF set and underlying-event tuned parameter set (tune) used for each process are listed in table 1.

The EvtGen v1.6.0 program [89] was used to describe the properties of the b- and c-hadron decays in the signal samples and in the background samples, except those produced with Sherpa. For all SM background samples, the response of the detector to particles was modelled with the full ATLAS detector simulation [90] based on Geant4 [91]. Signal samples were prepared using a fast simulation based on a parameterisation of showers in the ATLAS electromagnetic and hadronic calorimeters [92] coupled to Geant4 simulations of particle interactions elsewhere. All simulated events were overlaid with multiple pp collisions simulated with Pythia 8.186 using the A3 tune [93] and the NNPDF2.3 LO PDF set [59]. The MC samples were generated with variable levels of pile-up in the same and neighbouring collisions, and were reweighted to match the distribution of the mean number of interactions observed in data in 2015–2018.

4 Event reconstruction

The analysis identifies events with jets containing b-hadrons or secondary vertices corresponding to b-hadron decays, missing transverse momentum from the χ or $\tilde{\chi}_1^0$, and no charged leptons (electrons or muons). The last requirement is effective in suppressing SM backgrounds arising from $W \to \ell\nu$ decays, including events containing top quark production.

Events are required to have a primary vertex [94, 95] reconstructed from at least two tracks [96] with $p_{\mathrm{T}} > 0.5\,\mathrm{GeV}$. If more than one such vertex is found, the one with the largest sum of the squares of transverse momenta of associated tracks [95] is selected as the hard-scattering collision.

Jet candidates are reconstructed using the anti-k_t jet algorithm [97, 98] with radius parameter $R = 0.4$ [99] using particle-flow objects (PFOs) [100] as inputs. PFOs are charged-particle tracks matched to the hard-scatter vertex with the requirement $|z_0 \sin\theta| <$

JHEP05(2021)093

2.0 mm, where z_0 is the longitudinal impact parameter,[3] and calorimeter energy clusters surviving an energy subtraction algorithm that removes the calorimeter deposits of good-quality tracks from any vertex. Jet energy scale corrections, derived from MC simulation and data, are used to calibrate the average energies of jet candidates to the scale of their constituent particles [101]. Only corrected jet candidates with $p_{\mathrm{T}} > 20\,\mathrm{GeV}$ and $|\eta| < 2.8$ are considered explicitly when selecting events in this analysis, although jet candidates lying within $|\eta| \leq 4.5$ are considered when calculating $E_{\mathrm{T}}^{\mathrm{miss}}$. A set of quality criteria is applied to identify jets which arise from non-collision sources or detector noise [102] and any event which contains a jet failing to satisfy these criteria is removed. Jets containing a large particle momentum contribution from pile-up vertices, as measured by the jet vertex tagger (JVT) discriminant [103] are rejected if they have $p_{\mathrm{T}} \in [20, 60]\,\mathrm{GeV}$, $|\eta| < 2.4$ and a discriminant value of JVT < 0.5.

Selected jets are identified as b-jets if they lie within the ID acceptance of $|\eta| < 2.5$ and are tagged by a multivariate algorithm (`DL1r`) which uses a selection of inputs including information about the impact parameters of ID tracks, the presence of displaced secondary vertices and the reconstructed flight paths of b- and c-hadrons inside the jet [104]. The b-tagging algorithm uses a working point with an efficiency of 77%, determined with a sample of simulated $t\bar{t}$ events. The corresponding misidentification (mis-tag) rate is 20% for c-jets and 0.9% for light-flavour jets. Differences in efficiency and mis-tag rate between data and MC simulation are taken into account with correction factors as described in ref. [104].

To enhance sensitivity to models where low-p_{T} bottom quarks are present in the final state (e.g. bottom squark pair production with nearly mass-degenerate $\tilde{b}_1$ and $\tilde{\chi}_1^0$), a dedicated secondary-vertex finding algorithm (TC-LVT) is used. Documented in ref. [105], this algorithm reconstructs secondary vertices independently of the presence of an associated jet. A new *loose* working point, defined using the same track and vertex variables described in ref. [106] for the *medium* and *tight* working points, was optimised for this analysis. The efficiency to correctly identify the secondary vertex associated with the decay of a b-hadron (ϵ^{vtx}) ranges from 5% for a b-hadron p_{T} of 5 GeV to 40% for a p_{T} of 15 GeV. The corresponding probability (f^{vtx}) to obtain a vertex in an event without a b-hadron depends on the event topology and pile-up conditions, and is 1%–5%. Differences in ϵ^{vtx} (f^{vtx}) between data and MC simulation are taken into account by using correction factors computed in dileptonic $t\bar{t}$ ($W+$jets) production events. The correction factors are compatible with one for ϵ^{vtx} and range between 1.2 and 1.5 for f^{vtx}.

Two different classes ('baseline' and 'high-purity') of reconstructed lepton candidates (electrons or muons) are used in the analyses presented here. When selecting samples for the search, events containing a 'baseline' electron or muon are rejected. When selecting events with leptons for the purpose of estimating $W+$jets, $Z+$jets and top quark backgrounds, additional requirements are applied to leptons to ensure greater purity of these

[3]The transverse impact parameter is defined as the distance of closest approach of a track to the beam-line, measured in the transverse plane. The longitudinal impact parameter corresponds to the z-coordinate distance between the point along the track at which the transverse impact parameter is defined and the primary vertex.

JHEP05(2021)093

backgrounds. These leptons are referred to as 'high-purity' leptons in the following and form a subset of the baseline leptons.

Baseline muon candidates are formed by combining information from the muon spectrometer and ID as described in refs. [107, 108] and are required to possess $p_{\mathrm{T}} > 6\,\mathrm{GeV}$ and $|\eta| < 2.7$. Baseline muon candidates must additionally have a significance of the transverse impact parameter relative to the beam-line $|d_0^{\mathrm{BL}}|/\sigma(d_0^{\mathrm{BL}}) < 3$, and a longitudinal impact parameter relative to the primary vertex $|z_0\ \sin(\theta)| < 0.5\,\mathrm{mm}$. Furthermore, high-purity muon candidates must satisfy the *Medium* identification requirements described in refs. [107, 108] and the *FixedCutTightTrackOnly* isolation requirements, which are described in the same references and use tracking-based variables to implement a set of η- and p_{T}-dependent criteria.

Baseline electron candidates are reconstructed from an isolated electromagnetic calorimeter energy deposit matched to an ID track [109] and are required to possess $p_{\mathrm{T}} > 7\,\mathrm{GeV}$ and $|\eta| < 2.47$, and to satisfy the *Loose* likelihood-based identification criteria described in refs. [109, 110]. High-purity electron candidates are also required to possess $|d_0^{\mathrm{BL}}|/\sigma(d_0^{\mathrm{BL}}) < 5$ and $|z_0 \sin(\theta)| < 0.5\,\mathrm{mm}$, and to satisfy *Tight* isolation requirements [109, 110].

High-purity muon and electron candidates used to estimate backgrounds in this analysis are required to possess $p_{\mathrm{T}} > 20\,\mathrm{GeV}$ in order to reduce the impact of misidentified or non-prompt leptons. In addition, when using events selected with single-lepton triggers, the leading lepton is required to possess $p_{\mathrm{T}} > 27\,\mathrm{GeV}$ in order to ensure that events are selected in the trigger plateau.

After the selections described above, a procedure is applied to remove non-isolated leptons and avoid double counting of tracks and energy depositions associated with overlapping reconstructed jets, electrons and muons. The procedure applies the following actions to the event. First, baseline electrons are discarded if they share an ID track with a baseline muon. Next, any jet with $|\eta| < 2.8$ lying within a distance $\Delta R \equiv \sqrt{(\Delta y)^2 + (\Delta\phi)^2} = 0.2$ of a baseline electron is discarded and the electron is retained. Similarly, any jet with $|\eta| < 2.8$ satisfying $N_{\mathrm{trk}} < 3$ (where N_{trk} refers to the number of tracks with $p_{\mathrm{T}} > 500\,\mathrm{MeV}$ that are associated with the jet) within $\Delta R \equiv \sqrt{(\Delta y)^2 + (\Delta\phi)^2} = 0.2$ of a baseline muon is discarded and the muon is retained. Finally, baseline electrons or muons lying within a distance $\Delta R = \min(0.4, 0.04 + 10\,\mathrm{GeV}/p_{\mathrm{T}}^{e/\mu})$ of a remaining jet are discarded.

Multiplicative scale factors are applied to simulated events to account for differences between data and simulation for the lepton trigger, reconstruction, identification and isolation efficiencies, and for the jet momentum scales and energy resolutions. Similar corrections are also applied to the probability of mis-tagging jets originating from the hard pp scattering as pile-up jets with the JVT discriminant.

The missing transverse momentum $\mathbf{p}_{\mathrm{T}}^{\mathrm{miss}}$, whose magnitude is referred to as $E_{\mathrm{T}}^{\mathrm{miss}}$, is defined as the negative vector sum of the p_{T} of all selected and calibrated physics objects (electrons, muons, photons and jets) in the event, with an extra term added to account for energy in the event that is not associated with any of these objects [111]. This last 'soft term' contribution is calculated from the ID tracks with $p_{\mathrm{T}} > 500\,\mathrm{MeV}$ associated with the primary vertex, thus ensuring that it is robust against pile-up contamination [111, 112]. Photons contributing to the $\mathbf{p}_{\mathrm{T}}^{\mathrm{miss}}$ calculation are required to satisfy $p_{\mathrm{T}} > 25\,\mathrm{GeV}$ and

JHEP05(2021)093

$|\eta| < 2.37$ (excluding the transition region $1.37 < |\eta| < 1.52$ between the barrel and endcap EM calorimeters), to pass photon shower shape and electron rejection criteria, and to be isolated [109, 113].

5 Analysis strategy

In total, four sets of SRs are defined to target bottom squark pair-production or generic WIMP production in association with b-jets and are labelled SRX with X = A to D. Each set of signal regions targets different values of $\Delta m(\tilde{b}_1, \tilde{\chi}_1^0)$, the mass separation between the $\tilde{b}_1$ and $\tilde{\chi}_1^0$, or low and high dark matter mediator masses. The event selections defined for these regions all require the absence of baseline leptons, and exploit different techniques to improve the sensitivity to the target signal models. SRA targets large values of $\Delta m(\tilde{b}_1, \tilde{\chi}_1^0)$, and its definition resembles that used in refs. [42, 43, 114–116]. SRB, whose selection is mutually exclusive with that of SRA, is designed to be optimal for $50\,\text{GeV} < \Delta m(\tilde{b}_1, \tilde{\chi}_1^0) < 200\,\text{GeV}$, and uses a boosted decision tree (BDT) [117] as the final discriminant. SRC targets signals with $\Delta m(\tilde{b}_1, \tilde{\chi}_1^0) < 50\,\text{GeV}$, and exploits the information from the TC-LVT algorithm about the presence of vertices associated with low-p_T b-hadrons produced by the bottom squark decays. When deriving mass exclusion limits on bottom squarks or leptoquarks, SRA and SRB are statistically combined, and the analysis yielding the better of the expected CL_S values [118] from the combined SRA/SRB and SRC is used for each signal point. Finally, SRD is optimised to target the dark matter models with scalar or pseudoscalar mediators by making use of a BDT.

For all signal regions, the SM background estimation is performed with a likelihood fit [119] where the normalisation factors of the MC datasets corresponding to the SM processes expected to contribute the most to the event yields in the SRs (Z + jets for all signal regions, W+ jets and $t\bar{t}$ for SRC) are left free to float. To aid their determination, dedicated control regions (CR) select events containing either one or two leptons, and having kinematic properties similar to events in the signal regions, but with negligible expected signal contributions. The quality of the background estimation is verified in dedicated validation regions (VR), designed to select events as similar as possible to those populating the SRs, while keeping signal contributions low. The likelihood is built as the product of Poissonian terms for each CR and, when assessing the discovery and exclusion sensitivity to new phenomena, SR bins. The effect of systematic uncertainties on the Poissonian expectation values is included through nuisance parameters assumed to have Gaussian probability distributions, as described in section 6.

5.1 Discriminating variables

Several kinematic variables built from the physics objects defined in the previous section are used to discriminate new physics from known SM background events. Variables which are used in many SRs are described here, while SR-specific variables are described in the corresponding SR sections below. Wherever necessary, final-state objects are labelled following a descending p_T ordering.

JHEP05(2021)093

- $\min[\Delta\phi(\mathbf{p}^{\text{jet}}_{1-n}, \mathbf{p}^{\text{miss}}_{\text{T}})]$: the minimum $\Delta\phi$ between any of the leading n jets and $\mathbf{p}^{\text{miss}}_{\text{T}}$. The background from multijet processes is characterised by small values of this variable.

- $H_{\text{T;3}}$: it is defined as the scalar sum of the p_{T} of all jets excluding the leading two:

$$H_{\text{T;3}} = \sum_{i \geq 3} (p^{\text{jet}}_{\text{T}})_i.$$

  The variable is used to reject events with extra-jet activity in signal regions targeting models characterised by small mass-splitting between the bottom squark and the neutralino.

- m_{eff}: it is defined as the scalar sum of the p_{T} of the jets and the $E^{\text{miss}}_{\text{T}}$, i.e.:

$$m_{\text{eff}} = \sum_{i} (p^{\text{jet}}_{\text{T}})_i + E^{\text{miss}}_{\text{T}}.$$

  The m_{eff} observable is correlated with the mass of the directly pair-produced SUSY particles and is employed as a discriminating variable, as well as in the computation of other composite observables.

- $\mathcal{S}$: the global $E^{\text{miss}}_{\text{T}}$ significance, calculated including parameterisations of the resolutions of all selected objects [120]. It is defined as follows:

$$\mathcal{S} = \sqrt{\frac{|\mathbf{p}^{\text{miss}}_{\text{T}}|^2}{\sigma^2_{\text{L}}(1-\rho^2_{\text{LT}})}}.$$

  Here σ_{L} is the total momentum resolution after being rotated into the longitudinal (parallel to the $\mathbf{p}^{\text{miss}}_{\text{T}}$) plane. The total momentum resolution of all jets and leptons, at a given p_{T} and $|\eta|$, is determined from parameterised Monte Carlo simulation in which the resolution measured in data is modelled well. The quantity ρ_{LT} is a correlation factor between the longitudinal and transverse momentum resolution (again with respect to the $\mathbf{p}^{\text{miss}}_{\text{T}}$) of each jet or lepton. The significance $\mathcal{S}$ is used to discriminate between events where the $E^{\text{miss}}_{\text{T}}$ arises from invisible particles in the final state and events where the $E^{\text{miss}}_{\text{T}}$ arises from poorly measured particles (and jets).

- m_{jj}: the invariant mass of the two leading jets. In events where at least one of the leading jets is b-tagged, this variable helps to reduce the contamination from $t\bar{t}$ events. It is referred to as m_{bb} when the two leading b-tagged jets are considered.

- $m_{\text{T}}(\mathbf{p}^{\ell}_{\text{T}}, \mathbf{p}^{\text{miss}}_{\text{T}})$: the transverse mass of the lepton and the missing transverse momentum is defined as:

$$m_{\text{T}}(\mathbf{p}^{\ell}_{\text{T}}, \mathbf{p}^{\text{miss}}_{\text{T}}) = \sqrt{2p^{\ell}_{\text{T}}E^{\text{miss}}_{\text{T}} - 2\boldsymbol{p}^{\ell}_{\text{T}} \cdot \mathbf{p}^{\text{miss}}_{\text{T}}}$$

  and is used in the CRs to suppress the contribution from fake and non-prompt leptons, which are normally characterised by low $m_{\text{T}}(\mathbf{p}^{\ell}_{\text{T}}, \mathbf{p}^{\text{miss}}_{\text{T}})$ values in multijet production events.

JHEP05(2021)093

- m_{CT}: the contransverse mass [121] is the main discriminating variable in the SRA signal regions. It is used to measure the masses of pair-produced heavy particles decaying semi-invisibly. For identical decays of two heavy particles (e.g. the bottom squarks decaying exclusively as $\tilde{b}_1 \to b\tilde{\chi}^0$) into two visible particles v_1 and v_2 (the bottom quarks), and two invisible particles X_1 and X_2 (the $\tilde{\chi}^0$ for the signal), m_{CT} is defined as

$$m^2_{\mathrm{CT}}(v_1,\ v_2) = [E_{\mathrm{T}}(v_1) + E_{\mathrm{T}}(v_2)]^2 - [\mathbf{p}_{\mathrm{T}}(v_1) - \mathbf{p}_{\mathrm{T}}(v_2)]^2,$$

  with $E_{\mathrm{T}} = \sqrt{p^2_{\mathrm{T}} + m^2}$, and it has a kinematic endpoint at $m^{\mathrm{max}}_{\mathrm{CT}} = (m_I^2 - m_X^2)/m_I$, where I is the initially pair-produced particle. This variable is extremely effective in suppressing the top quark pair production background ($I = t, X = W$), for which the endpoint is at 135 GeV.

- $m^{\mathrm{min}}_{\mathrm{T}}(\mathrm{jet}_{1-4}, \mathbf{p}^{\mathrm{miss}}_{\mathrm{T}})$: this is the minimum of the transverse masses calculated using any of the leading four jets and the $\mathbf{p}^{\mathrm{miss}}_{\mathrm{T}}$ in the event. For signal scenarios with low values of $m^{\mathrm{max}}_{\mathrm{CT}}$, this kinematic variable is an alternative discriminating variable to reduce the $t\bar{t}$ background.

5.2 SRA definition

SRA targets bottom squark pair production with large values of $\Delta m(\tilde{b}_1, \tilde{\chi}^0_1)$. The selection criteria are summarised in table 2. Only events with $E^{\mathrm{miss}}_{\mathrm{T}} > 250\,\mathrm{GeV}$ are retained to ensure full efficiency of the online trigger selection and comply with the expected signal topology. To discriminate against multijet production, events where $\mathbf{p}^{\mathrm{miss}}_{\mathrm{T}}$ originates from the mismeasurement of a jet are suppressed with selections on $\min[\Delta\phi(\mathbf{p}^{\mathrm{jet}}_{1-4}, \mathbf{p}^{\mathrm{miss}}_{\mathrm{T}})]$ and $E^{\mathrm{miss}}_{\mathrm{T}}/m_{\mathrm{eff}}$. The final state is expected to contain two b-jets from the two bottom squark decays. A veto on large hadronic activity (implemented by rejecting events with a fourth jet of significant p_{T}) is imposed to suppress mostly events from SM $t\bar{t}$ production. SM $W+$jets and $Z+$jets production, where b-jets are produced mainly via gluon splitting, is suppressed by a selection on m_{bb}. Finally, selections on m_{eff} and m_{CT} are applied to maximise the sensitivity to the signal. When excluding specific models of bottom squark production, a two-dimensional binning in m_{CT} and m_{eff} is applied. Five mutually exclusive regions ($m_{\mathrm{CT}} \in [250, 350), [350, 450), [450, 550), [550, 650)$ and $[650, \infty)$, with all units in GeV) denoted by SRAmctX, where X is the bin lower bound, are used. SRAmct250 is subdivided into five bins of m_{eff}, starting from $m_{\mathrm{eff}} > 500\,\mathrm{GeV}$ and increasing in steps of 200 GeV, with the last bin including all events with $m_{\mathrm{eff}} > 1300\,\mathrm{GeV}$. SRAmct350 and SRAmct450 are both defined with two bins of m_{eff} ($[0.5\,\mathrm{TeV}, 1\,\mathrm{TeV}), [1\,\mathrm{TeV}, \infty)$ and $[1\,\mathrm{TeV}, 1.5\,\mathrm{TeV}), [1.5\,\mathrm{TeV}, \infty)$ respectively). Due to the relatively small number of events selected by the highest two m_{CT} bins, a single selection $m_{\mathrm{eff}} > 1.0\,(1.5)\,\mathrm{TeV}$ is applied in SRAmct550 (SRAmct650) respectively. When assessing the model-independent discovery significance against the background-only hypothesis (see section 7), five discovery regions, named SRAmctXi are defined by removing any binning in m_{eff}.

JHEP05(2021)093

Variable		SRA	CRzA	$\text{VR}_{\text{A1}}^{m_{\text{CT}}}$	$\text{VR}_{\text{A1}}^{m_{bb}}$	$\text{VR}_{\text{A2}}^{m_{\text{CT}}}$	$\text{VR}_{\text{A2}}^{m_{bb}}$
Number of baseline leptons		0	2	0			
Number of high-purity leptons		—	2 SFOS	—			
$p_{\text{T}}(\ell_1)$	[GeV]	—	> 27	—			
$p_{\text{T}}(\ell_2)$	[GeV]	—	> 20	—			
$m_{\text{T}}(\mathbf{p}_{\text{T}}^{\ell}, \mathbf{p}_{\text{T}}^{\text{miss}})$	[GeV]	—	> 20	—			
$m_{\ell\ell}$	[GeV]	—	$[81, 101]$	—			
Number of jets		$\in [2, 4]$					
Number of b-tagged jets		2					
j_1 and j_2 b-tagged		✓					
$p_{\text{T}}(j_1)$	[GeV]	> 150					
$p_{\text{T}}(j_2)$	[GeV]	> 50					
$p_{\text{T}}(j_4)$	[GeV]	< 50					
$\min[\Delta\phi(\mathbf{p}_{1-4}^{\text{jet}}, \mathbf{p}_{\text{T}}^{\text{miss}})]$	[rad]	> 0.4					
$E_{\text{T}}^{\text{miss}}$	[GeV]	> 250	< 100	> 250			
$\tilde{E}_{\text{T}}^{\text{miss}}$	[GeV]	—	> 250	—			
$E_{\text{T}}^{\text{miss}}/m_{\text{eff}}$		> 0.25	—	—			
$\tilde{E}_{\text{T}}^{\text{miss}}/m_{\text{eff}}$		—	> 0.25	—			
m_{bb}	[GeV]	> 200		< 200	> 200	< 200	> 200
m_{CT}	[GeV]	> 250		> 250	$[150, 250]$	> 250	$[150, 250]$
m_{eff}	[GeV]	> 500		$[500, 1500]$		> 1500	

Table 2. SRA signal, control and validation region definitions. Pink cells for the control and validation regions' columns indicate which selections ensure that the regions are orthogonal to the SR.

5.3 SRB definition

If $\Delta m(\tilde{b}_1, \tilde{\chi}_1^0) < 200\,\text{GeV}$, selections based on the m_{CT} and m_{bb} variables are no longer effective and a multivariate approach is preferred to separate the signal from SM production processes. A BDT is implemented by making use of the `XGBoost` (XGB) framework [117]. The training procedure used events that pass the selection specified in table 3 (with the exception of the BDT output score) and are classified in four different categories: three corresponding to the main backgrounds processes ($t\bar{t}$, $Z+$jets, $W+$jets production), and one grouping together semi-compressed signal samples ($\Delta m(\tilde{b}_1, \tilde{\chi}_1^0) \leq 200\,\text{GeV}$, where the event selection suppresses the acceptance for samples with $\Delta m(\tilde{b}_1, \tilde{\chi}_1^0) \leq 30\,\text{GeV}$), for scalar bottom squark masses $m_{\tilde{b}_1} < 800\,\text{GeV}$. A *one vs. rest* multi-classification procedure was used: for each classifier, the class is fitted against all the other classes producing output scores containing the predicted probability of an event being in each class. The output score w_{XGB} denotes the signal classifier output score and is used in the definition of the signal region. The rotational invariance of event topologies in the transverse plane is exploited by rotating the azimuthal angles of all final-state objects so that $E_{\text{T}}^{\text{miss}}$ has $\phi(\mathbf{p}_{\text{T}}^{\text{miss}}) = 0$. The variables used in the training are the momentum vectors of the jets, the b-tagging information, and other event-level variables (m_{eff}, $\mathcal{S}$, m_{CT}, $m_{\text{T}}^{\min}(\text{jet}_{1-4}, \mathbf{p}_{\text{T}}^{\text{miss}})$

JHEP05(2021)093

Variable		SRB	CRzB	VRzB
Number of baseline leptons		0	2	
Number of high-purity leptons		—	2 SFOS	
$p_{\mathrm{T}}(\ell_1)$	[GeV]	—	> 27	
$p_{\mathrm{T}}(\ell_2)$	[GeV]	—	> 20	
$m_{\ell\ell}$	[GeV]	—	$[76, 106]$	
$m_{\mathrm{T}}(\mathbf{p}_{\mathrm{T}}^{\ell}, \mathbf{p}_{\mathrm{T}}^{\mathrm{miss}})$	[GeV]	—	> 20	
Number of jets		$\in [2, 4]$		
Number of b-tagged jets		2		
$p_{\mathrm{T}}(j_1)$	[GeV]	> 100		
$p_{\mathrm{T}}(j_2)$	[GeV]	> 50		
$\min[\Delta\phi(\mathbf{p}_{1-4}^{\mathrm{jet}}, \mathbf{p}_{\mathrm{T}}^{\mathrm{miss}})]$	[rad]	> 0.4		
j_1 not b-tagged		—	✓	—
$E_{\mathrm{T}}^{\mathrm{miss}}$	[GeV]	> 250	< 100	
$\tilde{E}_{\mathrm{T}}^{\mathrm{miss}}$	[GeV]	—	> 250	
m_{CT}	[GeV]	< 250		
w_{XGB}		> 0.85	$[0.3, 0.63]$	> 0.63

Table 3. SRB signal, control and validation region definitions. Pink cells for the control and validation regions' columns indicate which selections ensure that the regions are orthogonal to the SR.

and $\Delta R(b_1, b_2)$). The highest-ranked variables after training are $m_{\mathrm{T}}^{\mathrm{min}}(\mathrm{jet}_{1-4}, \mathbf{p}_{\mathrm{T}}^{\mathrm{miss}})$ and the transverse momenta of the first three jets in the event.

The full selection of SRB is defined in table 3. An upper bound on m_{CT} ensures that the selection is orthogonal to SRA. When assessing the exclusion sensitivity for the signal-plus-background hypothesis for specific BSM models, four w_{XGB} bins are used in the likelihood fit ($[0.75, 0.80), [0.80, 0.85), [0.85, 0.90), [0.90, 1]$).

5.4 SRC definition

SRC targets events where a bottom squark pair is produced recoiling against a high-p_{T} initial-state-radiation (ISR) jet and $\Delta m(\tilde{b}_1, \tilde{\chi}_1^0) < 50\,\mathrm{GeV}$. In the boosted bottom squark decay, the boost is mostly transferred to $\tilde{\chi}_1^0$ because of its mass. It is because of such boost that the $E_{\mathrm{T}}^{\mathrm{miss}}$ satisfies the trigger requirements, while the bottom quarks are instead expected to have low p_{T}. Three mutually exclusive signal regions, based on the number of b-tagged jets and TC-LVT-identified vertices (N_{vtx}), are defined: SRC-2b, two b-jets; SRC-1b1v, one b-jet and at least one TC-LVT vertex; and SRC-0b1v, no b-jets and at least one TC-LVT vertex. The three regions offer complementary sensitivity depending on $\Delta m(\tilde{b}_1, \tilde{\chi}_1^0)$, and are statistically combined when stating the sensitivity for exclusion of bottom squark pair production models. They all exploit the topological and kinematic features of the signal by requiring large $E_{\mathrm{T}}^{\mathrm{miss}}$ and a high-p_{T}, non-b-tagged leading jet, and vetoing on additional hadronic activity by imposing an upper bound on $H_{\mathrm{T;3}}$. The following variables are used to better extract the signal from the SM background:

JHEP05(2021)093

Variable		SRC-2b	SRC-1b1v	SRC-0b1v	VRC-2b	VRC-1b1v	VRC-0b1v
Number of jets		$\in [2,5]$					
j_1 not b-tagged		✓					
Number of baseline leptons		0					
Number of b-tagged jets		≥ 2	1	0	≥ 2	1	0
N_{vtx}		≥ 0	≥ 1	≥ 1	≥ 0	≥ 1	≥ 1
m_{vtx}	[GeV]	—	> 0.6	> 1.5	—	> 0.6	> 1.5
$p_{\text{T}}^{\text{vtx}}$	[GeV]	—	> 3	> 5	—	> 3	> 5
$p_{\text{T}}(j_1)$	[GeV]	> 500	> 400	> 400	< 500	> 400	> 400
$E_{\text{T}}^{\text{miss}}$	[GeV]	> 500	> 400	> 400	< 500	> 400	> 400
$H_{\text{T;3}}$	[GeV]	—	< 80	< 80	—	< 80	< 80
$\mathcal{A}$		> 0.80	> 0.86	—	$[0.8, 0.9]$	> 0.86	—
m_{jj}	[GeV]	> 250	> 250	—	$[150, 250]$	> 250	—
$\Delta\phi(j_1, b_1)$	[rad]	—	> 2.2	—	—	< 2.2	—
$\Delta\phi(j_1, \text{vtx})$	[rad]	—	–	> 2.2	—	–	< 2.2
$\lvert\eta_{\text{vtx}}\rvert$		—	< 1.2	< 1.2	—	> 1.2	> 1.2

Table 4. SRC signal and validation region definitions. Pink cells for the validation regions' columns indicate which selections ensure that they are orthogonal to the corresponding SR.

- The bottom quarks coming from the bottom squark decay are expected to be produced centrally in pseudorapidity, angularly close to each other and nearly back-to-back to the ISR jet. This is exploited in SRC-1b1v and SRC-0b1v with selections on the angular separation in the transverse plane between the leading jet and the b-jet or TC-LVT vertex, and on the pseudorapidity of the TC-LVT vertex, η_{vtx}.
- The p_{T} of the leading ISR jet is expected to be significantly higher than that of the second jet, expected to come from the bottom squark decay. Therefore the variable

$$\mathcal{A} = \frac{p_{\text{T}}(j_1) - p_{\text{T}}(j_2)}{p_{\text{T}}(j_1) + p_{\text{T}}(j_2)}$$

  is expected to take values close to one for the signal, while it is expected to have a wider distribution for the background. This variable is not used in SRC-0b1v, where a jet coming from the bottom squark decay cannot be identified.
- The vertex mass (m_{vtx}) and p_{T} ($p_{\text{T}}^{\text{vtx}}$) are useful in rejecting events where the vertex is due to a c-hadron decay or to a random track crossing. For these *fake* vertices the values of both variables tend to be lower than for vertices originating from b-hadron decays.

The full list of selections applied to these variables and to other variables introduced in section 5.1 is shown in table 4. To further enhance the exclusion sensitivity, two different bins in $E_{\text{T}}^{\text{miss}}$ are defined ($E_{\text{T}}^{\text{miss}} \in [500\,\text{GeV}, 650\,\text{GeV}), [650\,\text{GeV}, \infty)$ for SRC-2b and $E_{\text{T}}^{\text{miss}} \in [400\,\text{GeV}, 600\,\text{GeV}), [600\,\text{GeV}, \infty)$ for SRC-1b1v and SRC-0b1v).

JHEP05(2021)093

5.5 SRD definition

Two signal regions target low- and high-mediator-mass dark matter signals, and are named SRD-low and SRD-high, respectively: SRD-low is optimised for mediator masses from 10 to 100 GeV, while SRD-high is optimised for mediator masses from 200 to 500 GeV. A common preselection is applied including the requirement of two b-jets in the final state. The thresholds for the missing transverse momentum and the p_{T} of the leading jet are kept as low as possible via a two-dimensional requirement selecting events on the trigger plateau, i.e. $(p_{\mathrm{T}}(j_1) - 20\,\mathrm{GeV})(E_{\mathrm{T}}^{\mathrm{miss}} - 160\,\mathrm{GeV}) > 5000\,\mathrm{GeV}^2$. Then BDTs are trained to discriminate between the three most relevant background processes (top pair production, $W+$jets, $Z+$jets) and two sets of kinematically similar signal models which are characterised by either low or high mediator mass. This results in six BDT discriminants, denoted by $w_{\mathrm{Y}}^{\mathrm{X}}$, where X and Y are the background process and signal mass range used in the training, respectively. The BDT discriminants have ranges of $[-1, 1]$ with the more positive values being more signal-like. In addition to some of the variables listed in section 5.1, the following variables are used specifically in SRD:

- H_{T}: the scalar sum of the jet transverse momenta. The ratio of the leading jet p_{T} to H_{T} is used in the signal region selection.
- δ^+, δ^-: angular variables that exploit the topology of the event [44]. They are defined as two linear combinations of $\min[\Delta\phi(\mathbf{p}_{1-3}^{\mathrm{jet}}, \mathbf{p}_{\mathrm{T}}^{\mathrm{miss}})]$ and the azimuthal separation between the b-jets, $\Delta\phi_{bb}$.

$$\delta^- = \min[\Delta\phi(\mathbf{p}_{1-3}^{\mathrm{jet}}, \mathbf{p}_{\mathrm{T}}^{\mathrm{miss}})] - \Delta\phi_{bb},$$
$$\delta^+ = |\min[\Delta\phi(\mathbf{p}_{1-3}^{\mathrm{jet}}, \mathbf{p}_{\mathrm{T}}^{\mathrm{miss}})] + \Delta\phi_{bb} - \pi|.$$

These variables are used in the training of the different BDTs together with the p_{T} of the leading b-jet and of the second and third jets in the event, $E_{\mathrm{T}}^{\mathrm{miss}}$, $\mathcal{S}$, $\min[\Delta\phi(\mathbf{p}_{1-3}^{\mathrm{jet}}, \mathbf{p}_{\mathrm{T}}^{\mathrm{miss}})]$, and m_{CT} computed using the two leading jets. The most discriminating variables are $\min[\Delta\phi(\mathbf{p}_{1-3}^{\mathrm{jet}}, \mathbf{p}_{\mathrm{T}}^{\mathrm{miss}})]$ and the ratio of the leading jet p_{T} to H_{T}. The signal region selections are detailed in table 5. A final discriminating variable $\cos\theta_{bb}^*$ [122] is considered: it is defined as

$$\cos\theta_{bb}^* = \left|\tanh\frac{\Delta\eta\,(b_1, b_2)}{2}\right|.$$

When excluding models of DM production, the SRDs are further divided into five equal bins of width 0.2 in the $[0, 1]$ range of $\cos\theta_{bb}^*$. When assessing the model-independent discovery significance against the background-only hypothesis, a single bin in $\cos\theta_{bb}^*$ defined by $\cos\theta_{bb}^* > 0.6\,(0.8)$ is used in SRD-low (SRD-high).

5.6 Control and validation region definition

Event selections kinematically similar to those of the signal regions are defined for the control regions, which are characterised by negligible expected signal contributions for the BSM models considered. Contrary to the SRs, such CRs rely on the presence of either one or two same-flavour opposite-sign (SFOS) high-purity electrons or muons (generically

JHEP05(2021)093

Variable		SRD-low	SRD-high	CRzD-low	CRzD-high	VRzD-low	VRzD-high
Trigger plateau		$(p_{\mathrm{T}}(j_1) - 20\,\mathrm{GeV})(E_{\mathrm{T}}^{\mathrm{miss}} - 160\,\mathrm{GeV}) > 5000\,\mathrm{GeV}^2$					
N_{jets}		2–3					
$N_{b\text{-jets}}$		≥ 2					
$p_{\mathrm{T}}(j_1)$	[GeV]	> 100					
$p_{\mathrm{T}}(j_2)$	[GeV]	> 50					
$\min[\Delta\phi(\mathbf{p}_{1-3}^{\mathrm{jet}}, \mathbf{p}_{\mathrm{T}}^{\mathrm{miss}})]$	[rad]	> 0.4					
$\mathcal{S}$		> 7					
$p_{\mathrm{T}}(j_1)/H_{\mathrm{T}}$		> 0.7					
Number of baseline leptons		0		2		0	
Number of high-purity leptons		—		2 SFOS		—	
$p_{\mathrm{T}}(\ell_1)$	[GeV]	—		> 27		—	
$p_{\mathrm{T}}(\ell_2)$	[GeV]	—		> 20		—	
$m_{\mathrm{T}}(\mathbf{p}_{\mathrm{T}}^{\ell}, \mathbf{p}_{\mathrm{T}}^{\mathrm{miss}})$	[GeV]	—		> 20		—	
$m_{\ell\ell}$	[GeV]	—		$[81, 101]$		—	
$\tilde{E}_{\mathrm{T}}^{\mathrm{miss}}$	[GeV]	—		> 180		—	
$E_{\mathrm{T}}^{\mathrm{miss}}$	[GeV]	> 180		< 100		> 180	
$w_{\text{D-low}}^{tt}$		> 0	—	—		> 0	—
$w_{\text{D-low}}^{Z}$		> 0	—	> 0	—	$[-0.2, 0]$	—
$w_{\text{D-low}}^{W}$		> 0	—	—		> 0	—
$w_{\text{D-high}}^{tt}$		—	> 0	—		—	> 0
$w_{\text{D-high}}^{Z}$		—	> -0.1	—	> -0.1	—	$[-0.3, -0.1]$
$w_{\text{D-high}}^{W}$		—	> -0.05	—		—	> -0.05

Table 5. SRD signal, control and validation region definitions. Pink cells for the control and validation regions' columns indicate which selections ensure that they are orthogonal to the corresponding SR.

denoted by ℓ), and are defined such that their event yield is dominated by one specific SM production process. They are part of the likelihood fit, where they are key to determining the value of the free-floating normalisation parameter associated with the MC prediction of the dominant background process.

The SM background yield is dominated in most signal regions by $Z+\text{jets}$ production followed by $Z \to \nu\bar{\nu}$. For each signal region, a corresponding control region (CRz) with two SFOS leptons is defined, with an invariant mass of the lepton pair close the Z boson mass: the kinematic properties of the events populating such a control region are expected to be very similar to those of events in the signal region. The full definition of the control region selection needs to take into account the lower branching ratio of $Z \to \ell\ell$ relative to $Z \to \nu\bar{\nu}$: the selection is therefore close, but not identical, to that of the signal region. After having rejected events with high $E_{\mathrm{T}}^{\mathrm{miss}}$ values to suppress contributions from dileptonic $t\bar{t}$ production, the p_{T} of the leptons is added vectorially to the $\mathbf{p}_{\mathrm{T}}^{\mathrm{miss}}$ to mimic the expected missing transverse momentum spectrum of $Z \to \nu\bar{\nu}$ events, and is denoted in the following by $\tilde{E}_{\mathrm{T}}^{\mathrm{miss}}$. All variables constructed from $E_{\mathrm{T}}^{\mathrm{miss}}$ are recomputed using $\tilde{E}_{\mathrm{T}}^{\mathrm{miss}}$ instead, including the BDT scores used in regions B and D. The selections corresponding to the control regions associated with SRA and SRB, named CRzA and CRzB, are shown in tables 2 and 3, respectively. Those corresponding to the control regions associated with SRD-low

JHEP05(2021)093

Variable		CRtC	CRwC-1b1v	CRwC-0b1v	CRzC-2b	CRzC-1b1v	CRzC-0b1v
j_1 not b-tagged		✓					
Number of high-purity leptons		1			2 SFOS		
$H_{\mathrm{T};3}$	[GeV]	< 80					
$p_{\mathrm{T}}(j_1)$	[GeV]	> 400			> 300	> 400	
$m_{\mathrm{T}}(\mathbf{p}_{\mathrm{T}}^{\ell}, \mathbf{p}_{\mathrm{T}}^{\mathrm{miss}})$	[GeV]	$[20, 120]$			—		
$m_{\ell\ell}$	[GeV]	—			$[81, 101]$		
$E_{\mathrm{T}}^{\mathrm{miss}}$	[GeV]	> 400			< 100		
$\tilde{E}_{\mathrm{T}}^{\mathrm{miss}}$	[GeV]	—			> 250	> 400	
$\mathcal{A}$		> 0.5	> 0.8	—	> 0.5	> 0.8	—
m_{jj}	[GeV]	> 250	> 250	—	—	> 250	—
$N_{b\text{-jets}}$		≥ 2	1	0	≥ 2	1	0
N_{vtx}		—	≥ 1	≥ 1	—	≥ 1	≥ 1
m_{vtx}	[GeV]	—	> 0.6	> 1.5	—	> 0.6	> 1.5
$p_{\mathrm{T}}^{\mathrm{vtx}}$	[GeV]	—	> 3	> 5	—	> 3	> 5

Table 6. SRC control region definitions. Pink cells for the control regions' columns indicate which selections ensure that they are orthogonal to the corresponding SR.

and SRD-high, named CRzD-low and CRzD-high, are shown in table 5. In the case of SRC, one $Z+$jets control region is defined for each of SRC-2b, SRC-1b1v and SRC-0b1v: they are named CRzC-2b, CRzC-1b1v and CRzC-0b1v respectively, and their selection is shown in table 6.

The production of $W+$jets and, to a lesser extent, top quarks, also results in important backgrounds in SRC. A set of control regions (CRt and CRw) is defined, all containing exactly one high-purity lepton in the final state. The zero-lepton signals considered for the signal region optimisation do not contaminate the one-lepton control regions. However, potential signal contributions from possible related BSM signal production (e.g. top squark pairs) or from third-generation leptoquarks are rejected by imposing an upper bound on the transverse mass of the lepton and the missing transverse momentum, $m_{\mathrm{T}}(\mathbf{p}_{\mathrm{T}}^{\ell}, \mathbf{p}_{\mathrm{T}}^{\mathrm{miss}})$.

A common top control region containing two b-tagged jets and no TC-LVT vertex, named CRtC, and two $W+$jets control regions containing at least one TC-LVT vertex and, respectively, one (CRwC-1b1v) and no (CRwC-0b1v) b-tagged jets are defined and summarised in table 6. The definition of a $W+$jets control region containing two b-tagged jets was considered, but it was found too difficult to obtain a satisfactory $W+$jets purity because of contamination from top quark production.

Finally, a series of validation regions is defined, with the purpose of evaluating the quality of the background estimation after the likelihood fit. They are characterised by an expected signal contamination below 10%, and they are obtained by inverting one or more signal region variable selections. They are defined in tables 2, 3, 4 and 5

6 Systematic uncertainties

The effects of several sources of systematic uncertainty on the signal and background estimates are introduced in the likelihood fit through nuisance parameters that affect the

JHEP05(2021)093

expectation values of the Poissonian terms for each CR and SR bin. Each nuisance parameter's probability density function is described by a Gaussian distribution whose standard deviation corresponds to a specific experimental or theoretical modelling uncertainty. The preferred value of each nuisance parameter is determined as part of the likelihood fit. The fits performed do not significantly alter or constrain the nuisance parameter values relative to the fit input.

Jet energy scale and resolution uncertainties are derived as a function of the jet p_{T} and η, jet flavour, and pile-up conditions, using a combination of data and simulated events through measurements of jet response asymmetry for several processes, as detailed in refs. [123, 124]. The impact of uncertainties on the efficiencies and mis-tag rates of the b-tagging algorithm is estimated by varying, as a function of p_{T}, η and jet flavour, the scale factors used to correct the MC simulation, within a range reflecting the uncertainty in their measurement [104]. Similarly, the impact of the uncertainty on the MC modelling of the efficiency and fake rate for the TC-LVT vertex reconstruction is estimated by varying the corresponding scale factors within the uncertainty associated with their determination (about 6% for the efficiency and 30% for the fake rate). Uncertainties connected with the lepton reconstruction and identification are included in the fit, and they are found to have a negligible impact. All uncertainties in the final-state object reconstruction are propagated to the reconstruction of the $E_{\mathrm{T}}^{\mathrm{miss}}$, including an additional one taking into account uncertainties in the scale and resolution of the soft term.

Uncertainties in the modelling of the SM background processes from MC simulation are taken into account. They are assumed to be fully correlated across signal regions, but uncorrelated between different processes. An alternative correlation model, where the uncertainties are assumed to be uncorrelated across signal regions, leads to a small increase in the final yield uncertainty, but to no significant change in the mass and cross-section limits obtained.

Several contributions to the uncertainty in the theoretical modelling of $t\bar{t}$ and single top production are considered. The uncertainty due the choice of hard-scattering generator and matching scheme is evaluated by comparing the nominal sample with a sample generated with MadGraph5_aMC@NLO and a shower starting scale $\mu_{\mathrm{q}} = H_{\mathrm{T}}^{\mathrm{gen}}/2$. The uncertainty due to the choice of parton shower and hadronisation model is evaluated by a comparison with a sample generated with Powheg-Box interfaced to Herwig 7 [125, 126], using the H7UE set of tuned parameters [126]. Variations of the renormalisation and factorisation scales, the initial- and final-state radiation parameters and PDF sets are also considered [127]. Uncertainties on the interference between the single top Wt and $t\bar{t}$ production have negligible impact on the analysis results and are not included.

Uncertainties in the modelling of $Z+$jets and $W+$jets [128] are evaluated by using 7-point variations of the renormalisation and factorisation scales by factors of 0.5 and 2. The matching scale between the matrix element and parton shower calculation, and the resummation scale for soft gluon emission, are also varied by factors of 0.5 and 2. As no Monte Carlo generator has been found to accurately describe $Z + b\bar{b}$ production in all observables [129], nor are these discrepancies accounted for by scale variations, an uncertainty due to the choice of generator is evaluated by comparing the nominal samples

JHEP05(2021)093

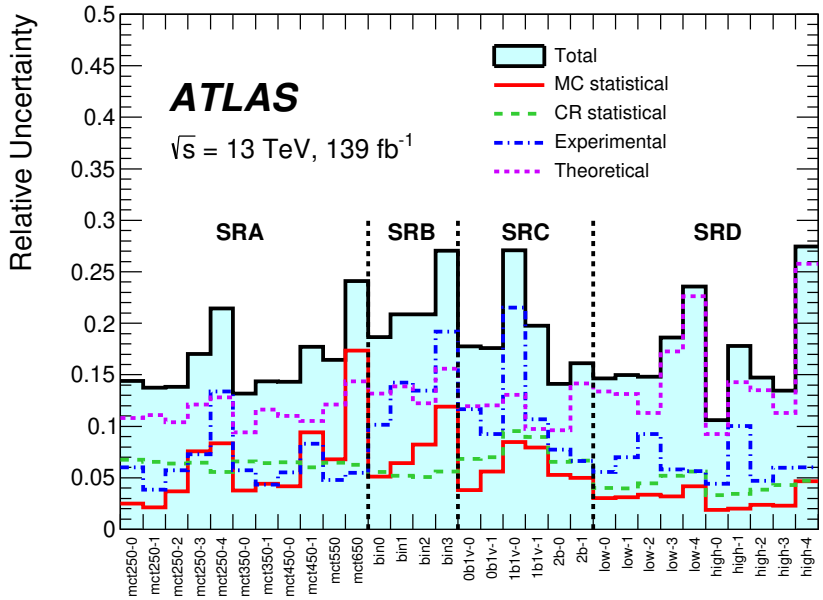

Figure 2. Summary of the post-fit relative systematic uncertainties of the various signal region yields, also split by component.

with those produced using aMC@NLO 2.3.3 + Pythia. After constraints from the control regions these variations are found to be relevant only in SRD, where modelling uncertainties dominate the systematic effect on the shape of the $\cos\theta^*_{bb}$ distribution.

The impact of the most relevant background systematic uncertainties in the different signal regions is shown in figure 2. Modelling uncertainties of the $Z+$jets process dominate the signal regions' uncertainties, while the most important experimental uncertainties are those related to the jet energy scale.

7 Results and interpretation

Different likelihood fits are run when assessing the accuracy of the SM background determination (*background-only* fit), when computing the p-value of the SM-only hypothesis (*model-independent* fit) and when evaluating the confidence level for excluding a specific BSM hypothesis (*model-dependent* fit) [119].

In the background-only fit, only the control regions are used in the likelihood, and the predicted post-fit level of background is compared with the observed yields in the corresponding VRs and SRs. Three distinct fits are run for the combination of SRA and SRB, for SRC and for SRD. In the SRA/SRB and SRD fits, only the normalisation of the $Z+$jets MC background prediction is left free to float. For SRC, a combined fit is run including SRC-2b, SRC-1b1v and SRC-0b1v: one common normalisation factor is applied to the $t\bar{t}$ and single-top contributions; one normalisation factor is applied to the $W+$jets MC predictions in all regions with one or more b-tagged jets, while an independent one is

JHEP05(2021)093

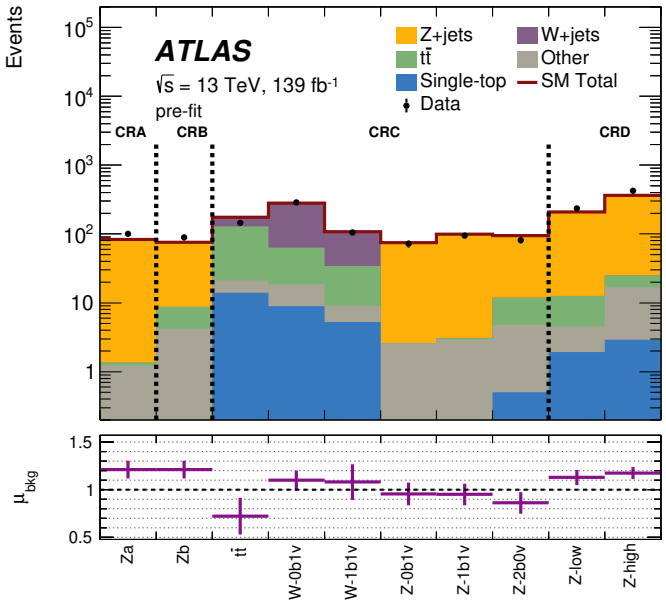

Figure 3. Comparison between observed and pre-fit predicted background yields for the control regions. In the ratio plot, μ_{bkg} represents the value (with uncertainty) of the free-floating normalisation parameter for the dominant background process in each region obtained with the background-only fit. The "Other" category includes contributions from diboson and $t\bar{t}+W/Z/H$ production.

applied to those with no b-tagged jets; and, finally, three independent normalisation factors are applied to the $Z+$jets MC predictions depending on the number of b-tagged jets.

The background-only pre-fit event yields are compared with the observation for all CRs in figure 3, while figure 4 shows the background-only post-fit prediction compared with the observation for the VRs. Agreement is observed in the validation regions. Distributions of relevant variables in the validation regions were inspected in detail, and were found to be consistent with the post-fit predictions. The corresponding SR yield comparison is shown in figure 5. The largest background contribution in all SRs arises from $Z+$jets production, while $W+$jets and top quark production contributions are minor, except in SRC. Other background sources are $t\bar{t}+W/Z$, $t\bar{t}+H$, and diboson production. Multijet production was found to be negligible in every region considered. No significant deviation from the background-only prediction is observed in any of the signal regions. An excess of about one standard deviation, covered by the largely correlated systematic uncertainty, is observed in the SRD-low bins. Figures 6 and 7 show comparisons between the observed data and the post-fit background predictions for relevant kinematic distributions for the SRs.

The model-independent fit includes also the signal regions of tables 2, 3, 4 and 5 in the likelihood as additional constraining bins. To maximise the model-independent sensitivity to new phenomena, no additional binning of m_{eff} (for SRA), w_{XGB} (for SRB), $E_{\text{T}}^{\text{miss}}$ (SRC) or $\cos\theta^{*}_{bb}$ (in SRD) is considered. In the case of SRA, an additional selection on m_{CT} is added with respect to table 2, corresponding to the SRAmctXi selections described

JHEP05(2021)093

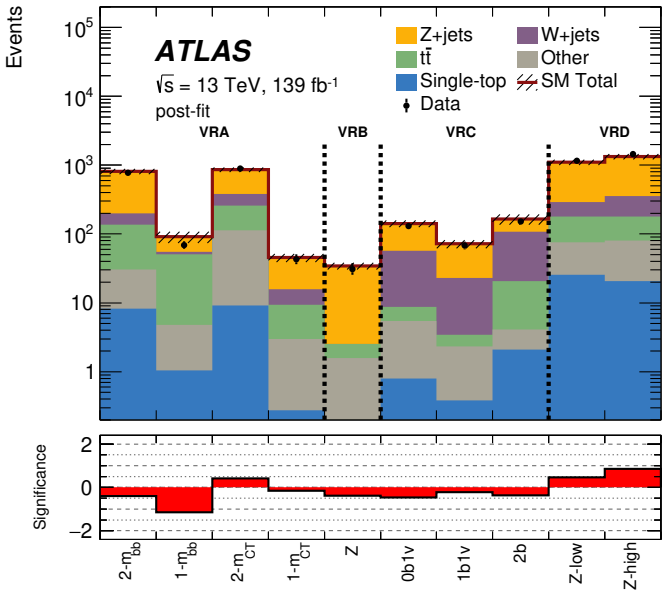

Figure 4. Comparison between observed and post-fit predicted background yields for the validation regions. The ratio plot represents the statistical significance [130] of the discrepancy between the observed and predicted value. The "Other" category includes contributions from diboson and $t\bar{t} + W/Z/H$ production. The shaded band represents the total uncertainty of the background prediction.

in section 5.2. A profile-likelihood-ratio statistic [131], where a signal of intensity μ_{sig} is assumed to contribute to the signal region only, is used to assess the p-value of the background-only hypothesis (corresponding to $\mu_{\text{sig}} = 0$) and to extract S^{95}_{exp} and S^{95}_{obs}, i.e. the expected and observed 95% confidence level (CL) limits on μ_{sig} using the CL_S prescription. The limit S^{95}_{obs} is also converted to a limit on the visible cross-section σ_{vis} by dividing by the total integrated luminosity. The results are summarised in table 7.

Finally, the model-dependent fit includes the contributions of specific BSM models to all control and signal regions and considers the full binning defined in sections 5.2, 5.3, 5.4 and 5.5, to determine 95% CL exclusion limits on BSM particle masses and, where relevant, couplings.

The exclusion reach for the bottom squark pair production model is obtained by comparing, for each value of the bottom squark and neutralino masses, the expected CL_S value of the combined SRC fit and that of a combined fit to SRA and SRB: the one yielding the smaller expected CL_S value is chosen to evaluate the expected and observed CL_S. The result is shown in figure 8. A deviation of the observed limit from the expected one is observed at $\left(m_{\tilde{b}_1}, m_{\tilde{\chi}^0_1}\right)$ of about (1150 GeV, 700 GeV) in figure 8a: it is due to a small deficit of events relative to the background prediction in SRAmct350, SRAmct450 and SRAmct550, where the signal contributions from models in this region of the parameter space is found to be significant. The small excess of observed events in SRC-2b is instead responsible for the weaker than expected limit for a broad range of values around $m_{\tilde{b}_1} = 700\,\text{GeV}$ and

JHEP05(2021)093

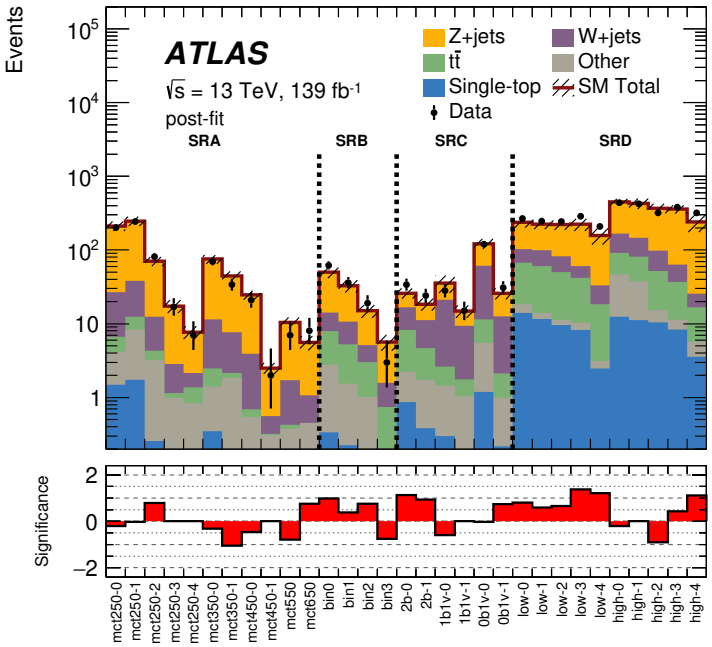

Figure 5. Comparison between observed and background-only post-fit predicted background yields for the signal regions. The ratio plot represents the statistical significance of the discrepancy between the observed and predicted value. The "Other" category includes contributions from diboson and $t\bar{t} + W/Z/H$ production. The shaded band represents the total uncertainty of the background prediction. Where present, the last digit in the signal region name labels the bins of m_{eff} for SRA, w_{XGB} for SRB, $E_{\text{T}}^{\text{miss}}$ for SRC and $\cos\theta_{bb}^{*}$ for SRD.

$m_{\tilde{\chi}_1^0} > 20\,\text{GeV}$ in figure 8b. Finally, the transition between regions where SRA, SRB or SRC dominate the sensitivity is responsible for the wiggles in the expected and observed limits for $650\,\text{GeV} < m_{\tilde{b}_1} < 850\,\text{GeV}$ in figure 8a.

Bottom squark masses up to 1270 GeV are excluded for massless $\tilde{\chi}_1^0$. SRC dominates the expected sensitivity up to $\Delta m(\tilde{b}_1, \tilde{\chi}_1^0) \sim 70\,\text{GeV}$. The use of the TC-LVT algorithm largely contributed to the sensitivity for small $\Delta m(\tilde{b}_1, \tilde{\chi}_1^0)$, allowing the exclusion of bottom squark masses up to 660 GeV for $\Delta m(\tilde{b}_1, \tilde{\chi}_1^0) = 10\,\text{GeV}$: for example, the minimum expected exclusion value of $\Delta m(\tilde{b}_1, \tilde{\chi}_1^0)$ for $m_{\tilde{b}_1} = 600\,\text{GeV}$ using SRC-2b alone would be about 25 GeV.

The combined fit to SRA and SRB is also used to set limits on the model where pairs of scalar third-generation down-type leptoquarks are produced. Limits at 95% CL are set on the branching ratio $\mathcal{B}\left(\text{LQ}_3^d \to t\tau\right) = 1 - \mathcal{B}\left(\text{LQ}_3^d \to b\nu_\tau\right)$ as a function of the leptoquark mass. The result is shown in figure 9. LQ_3^d masses up to 1260 GeV are excluded for $\mathcal{B}\left(\text{LQ}_3^d \to t\tau\right) = 0$, while the limit decreases to 400 GeV if $\mathcal{B}\left(\text{LQ}_3^d \to t\tau\right) = 95\%$. The same event deficit in SRAmct350, SRAmct450 and SRAmct550 already discussed in relation to figure 8a is responsible for the discrepancy between the observed and expected limit for leptoquark masses around 700 GeV.

JHEP05(2021)093

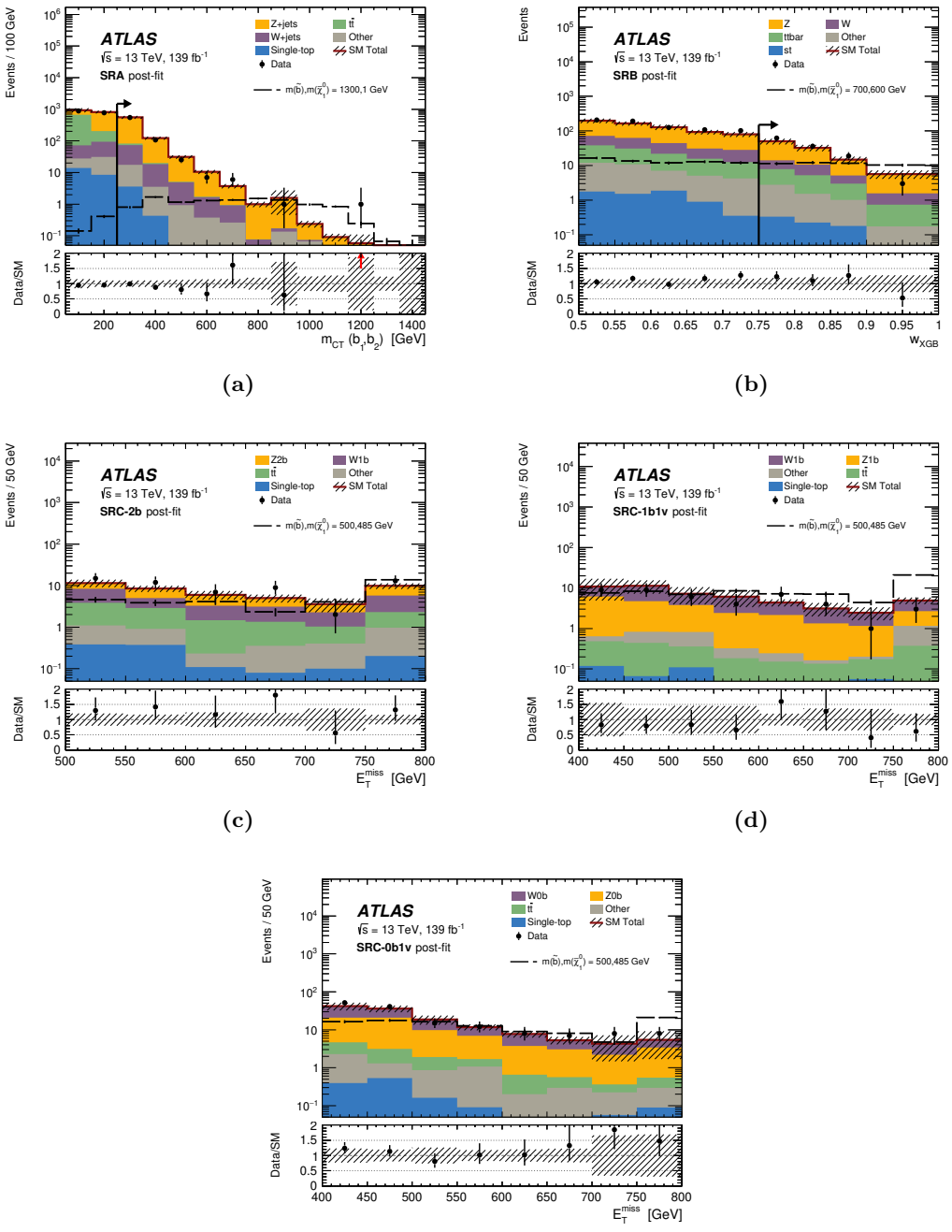

Figure 6. Post-fit distribution of (a) m_{CT} in SRA; (b) w_{XGB} in SRB; and $E_{\mathrm{T}}^{\mathrm{miss}}$ in (c) SRC-2b, (d) SRC-1b1v, (e) SRC-0b1v. Where relevant, the signal region selection is indicated by a black arrow. In each of (a)–(e) the lower plot shows the ratios of the observed yields to the post-fit predicted background yields, with a red arrow indicating when a ratio value is outside the displayed interval. The "Other" category includes contributions from diboson, and $t\bar{t} + W/Z/H$ production. The shaded band represents the total uncertainty of the background prediction. The last bin includes overflow events.

JHEP05(2021)093

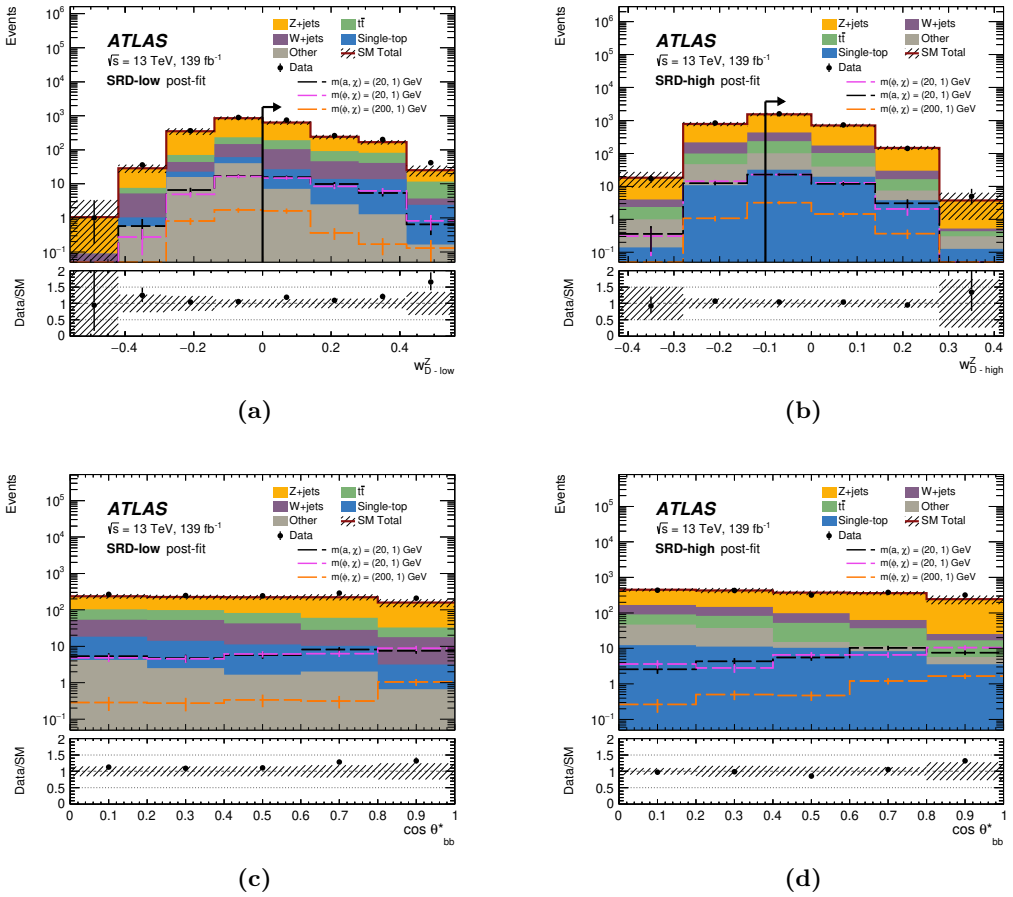

Figure 7. Post-fit distribution of (a) $w^{Z}_{\text{D-low}}$ and (c) $\cos\theta^{*}_{bb}$ in SRD-low and (b) $w^{Z}_{\text{D-high}}$ and (d) $\cos\theta^{*}_{bb}$ in SRD-high. Where relevant, the signal region selection is indicated by a black arrow. In each of (a)–(d) the lower plot shows the ratios of the observed yields to the post-fit predicted background yields. The "Other" category includes contributions from diboson and $t\bar{t}+W/Z/H$ production. The shaded band represents the total uncertainty of the background prediction. The last bin includes the overflow events.

Finally, exclusion limits are set on DM production models with scalar or pseudoscalar mediators in figure 10. The limits are obtained by taking for each point the signal region (either SRD-low or SRD-high) that yields the better expected CL_S value. Limits on the cross-section are provided for a χ mass of 1 GeV and unity coupling of the mediator to the dark matter particles, separately for scenarios with a scalar or a pseudoscalar mediator. In both cases, cross-sections exceeding between 5 and 300 times the predicted rate for mediators with masses between 10 and 500 GeV are excluded.

8 Conclusions

The result of a search for an excess of events containing large missing transverse momentum and at least one jet or decay vertex originating from the hadronisation and fragmentation of

JHEP05(2021)093

Signal channel	Obs.	SM exp.	$\langle\epsilon\sigma\rangle^{95}_{\text{obs}}$ [fb]	S^{95}_{obs}	S^{95}_{exp}	CL_B	$p(s=0)$ (Z)
SRAmct250i	552	555 ± 75	0.94	131	133^{+47}_{-35}	0.48	0.49 (0.03)
SRAmct350i	104	120 ± 16	0.17	24	32^{+8}_{-9}	0.19	0.5 (0)
SRAmct450i	23	27.1 ± 3.8	0.06	8.7	$12.3^{+5.5}_{-3.7}$	0.17	0.5 (0)
SRAmct550i	7	10.4 ± 1.7	0.04	5.6	$8.1^{+3.9}_{-2.3}$	0.14	0.5 (0)
SRAmct650i	8	5.6 ± 1.4	0.06	8.5	$6.7^{+3.4}_{-2.0}$	0.73	0.24 (0.72)
SRB	22	20.6 ± 4.6	0.11	15.3	$14.8^{+5.2}_{-3.2}$	0.54	0.40 (0.26)
SRC-2b	58	44.4 ± 5.8	0.22	30.3	$20.7^{+8.1}_{-5.6}$	0.88	0.09 (1.33)
SRC-1b1v	43	51 ± 10	0.13	17.6	$21.2^{+8.2}_{-5.8}$	0.28	0.5 (0)
SRC-0b1v	151	148 ± 25	0.37	51	50^{+18}_{-13}	0.54	0.48 (0.2)
SRD-low	497	381 ± 76	1.8	250	155^{+65}_{-60}	0.91	0.07 (1.48)
SRD-high	320	242 ± 66	1.4	195	140^{+48}_{-44}	0.82	0.13 (1.13)

Table 7. Left to right: SM expectation from background-only fit for the model-independent regions, 95% CL upper limits on the visible cross-section ($\langle\epsilon\sigma\rangle^{95}_{\text{obs}}$), on the observed ($S^{95}_{\text{obs}}$) and expected ($S^{95}_{\text{exp}}$) number of signal events. The last two columns indicate the CL_B value, i.e. the confidence level observed for the background-only hypothesis, and the discovery p-value ($p(s=0)$) capped at a value of 0.5.

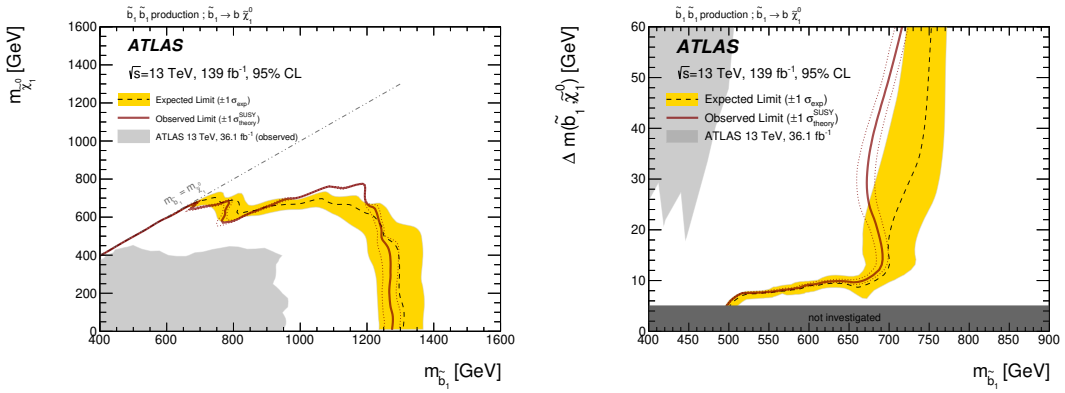

(a) **(b)**

Figure 8. Exclusion limits at 95% CL on the masses of the $\tilde{b}_1$ and $\tilde{\chi}^0_1$ displayed in the (a) $\left(m_{\tilde{b}_1}, m_{\tilde{\chi}^0_1}\right)$ and (b) $\left(m_{\tilde{b}_1}, \Delta m(\tilde{b}_1, \tilde{\chi}^0_1)\right)$ planes. The dashed line and the shaded band are the expected limit and its $\pm 1\sigma$ uncertainty, respectively. The thick solid line is the observed limit for the central value of the signal cross-section. The expected and observed limits do not include the effect of the theoretical uncertainties in the signal cross-section. The dotted lines show the effect on the observed limit of varying the signal cross-section by $\pm 1\sigma$ of the theoretical uncertainty. Regions excluded by previous analyses are shaded in light grey, while the region with $\Delta m(\tilde{b}_1, \tilde{\chi}^0_1) < 5\,\text{GeV}$, not investigated in this analysis, is shaded in dark grey.

JHEP05(2021)093

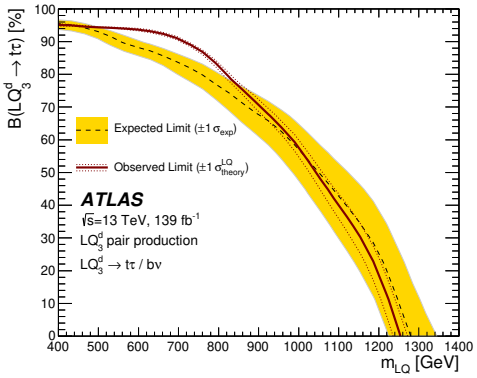

Figure 9. Exclusion limits at 95% CL on $\mathcal{B}\left(\mathrm{LQ}_3^d \to t\tau\right)$ as a function of the LQ_3^d mass for a model of LQ_3^d pair production. The dashed line and the shaded band are the expected limit and its $\pm 1\sigma$ uncertainty, respectively. The thick solid line is the observed limit for the central value of the signal cross-section.

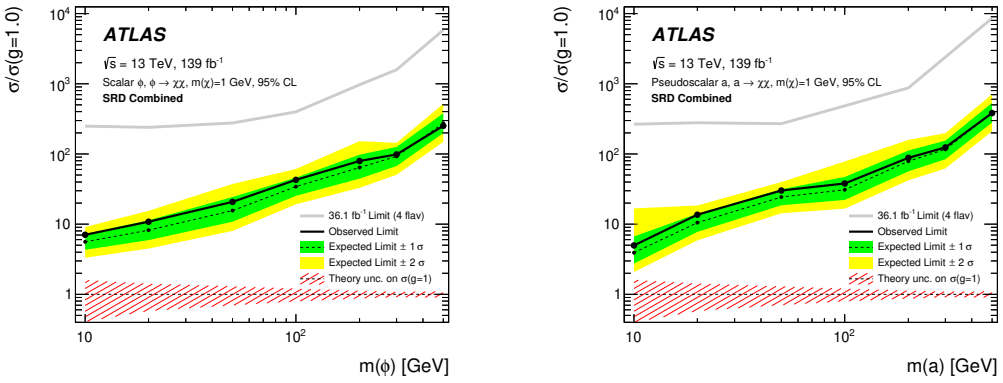

(a) **(b)**

Figure 10. 95% CL limits on the cross-section for the models of dark matter production mediated by a (a) scalar or (b) pseudoscalar mediator. The dashed line and the shaded band are the expected limit and its $\pm 1\sigma$ and $\pm 2\sigma$ uncertainties, respectively. The thick solid line is the observed limit for the central value of the signal cross-section. The grey line shows the limit from previous results [44]. The hatched red band shows the uncertainty of the model cross-section.

a b-quark is reported. The analysis uses $139\,\mathrm{fb}^{-1}$ of pp collisions at $\sqrt{s} = 13\,\mathrm{TeV}$ collected by the ATLAS experiment at the LHC between 2015 and 2018. No excess above the Standard Model prediction is observed for any of the signal regions considered. Limits on the visible cross-section of a generic BSM contribution in the signal regions have been set and range from 0.04 fb to 1.8 fb, depending on the signal region. The results are also used to set exclusion limits on specific BSM scenarios. In R-parity-conserving SUSY scenarios where bottom squarks decay into a b-quark and the lightest neutralino, the results are used to derive 95% CL exclusion limits as a function of the $\tilde{b}_1$ and $\tilde{\chi}_1^0$ masses. Bottom squark masses up to 1270 GeV are excluded for massless $\tilde{\chi}_1^0$, while the use of dedicated techniques to identify the secondary vertex from a low-p_{T} b-hadron allows the exclusion of bottom squark

JHEP05(2021)093

masses up to 660 GeV for $\Delta m(\tilde{b}_1, \tilde{\chi}_1^0) = 10$ GeV. The search is also interpreted to exclude pair-produced LQ_3^d with masses up to 1260 GeV (400 GeV) for $\mathcal{B}\left(\mathrm{LQ}_3^d \to t\tau\right) = 0$ (95%). In scenarios where dark matter particles with a mass of 1 GeV are produced via a scalar or pseudoscalar mediator in association with b-quarks, cross-sections exceeding between 5 and 300 times the predicted rate for mediators with masses between 10 and 500 GeV and unitary coupling to the dark matter particles are excluded. All these limits extend substantially beyond the region of parameter space excluded by similar searches with the ATLAS detector using 36.1 fb^{-1} of pp collisions. This is due to several improvements in the analysis in addition to the increase in integrated luminosity; in particular the use of multivariate techniques and the TC-LVT algorithm which provide enhanced sensitivity to models with small $\Delta m(\tilde{b}_1, \tilde{\chi}_1^0)$.

Acknowledgments

We thank CERN for the very successful operation of the LHC, as well as the support staff from our institutions without whom ATLAS could not be operated efficiently.

We acknowledge the support of ANPCyT, Argentina; YerPhI, Armenia; ARC, Australia; BMWFW and FWF, Austria; ANAS, Azerbaijan; SSTC, Belarus; CNPq and FAPESP, Brazil; NSERC, NRC and CFI, Canada; CERN; ANID, Chile; CAS, MOST and NSFC, China; COLCIENCIAS, Colombia; MSMT CR, MPO CR and VSC CR, Czech Republic; DNRF and DNSRC, Denmark; IN2P3-CNRS and CEA-DRF/IRFU, France; SRNSFG, Georgia; BMBF, HGF and MPG, Germany; GSRT, Greece; RGC and Hong Kong SAR, China; ISF and Benoziyo Center, Israel; INFN, Italy; MEXT and JSPS, Japan; CNRST, Morocco; NWO, Netherlands; RCN, Norway; MNiSW and NCN, Poland; FCT, Portugal; MNE/IFA, Romania; JINR; MES of Russia and NRC KI, Russian Federation; MESTD, Serbia; MSSR, Slovakia; ARRS and MIZŠ, Slovenia; DST/NRF, South Africa; MICINN, Spain; SRC and Wallenberg Foundation, Sweden; SERI, SNSF and Cantons of Bern and Geneva, Switzerland; MOST, Taiwan; TAEK, Turkey; STFC, U.K.; DOE and NSF, U.S.A.. In addition, individual groups and members have received support from BCKDF, CANARIE, Compute Canada, CRC and IVADO, Canada; Beijing Municipal Science & Technology Commission, China; COST, ERC, ERDF, Horizon 2020 and Marie Skłodowska-Curie Actions, European Union; Investissements d'Avenir Labex, Investissements d'Avenir Idex and ANR, France; DFG and AvH Foundation, Germany; Herakleitos, Thales and Aristeia programmes co-financed by EU-ESF and the Greek NSRF, Greece; BSF-NSF and GIF, Israel; La Caixa Banking Foundation, CERCA Programme Generalitat de Catalunya and PROMETEO and GenT Programmes Generalitat Valenciana, Spain; Göran Gustafssons Stiftelse, Sweden; The Royal Society and Leverhulme Trust, U.K..

The crucial computing support from all WLCG partners is acknowledged gratefully, in particular from CERN, the ATLAS Tier-1 facilities at TRIUMF (Canada), NDGF (Denmark, Norway, Sweden), CC-IN2P3 (France), KIT/GridKA (Germany), INFN-CNAF (Italy), NL-T1 (Netherlands), PIC (Spain), ASGC (Taiwan), RAL (U.K.) and BNL (U.S.A.), the Tier-2 facilities worldwide and large non-WLCG resource providers. Major contributors of computing resources are listed in ref. [132].

JHEP05(2021)093

Open Access. This article is distributed under the terms of the Creative Commons Attribution License (CC-BY 4.0), which permits any use, distribution and reproduction in any medium, provided the original author(s) and source are credited.

References

[1] WMAP collaboration, *Nine-Year Wilkinson Microwave Anisotropy Probe (WMAP) Observations: Cosmological Parameter Results*, *Astrophys. J. Suppl.* **208** (2013) 19 [arXiv:1212.5226] [INSPIRE].

[2] PLANCK collaboration, *Planck 2018 results. I. Overview and the cosmological legacy of Planck*, *Astron. Astrophys.* **641** (2020) A1 [arXiv:1807.06205] [INSPIRE].

[3] V. Trimble, *Existence and Nature of Dark Matter in the Universe*, *Ann. Rev. Astron. Astrophys.* **25** (1987) 425 [INSPIRE].

[4] G. Bertone, D. Hooper and J. Silk, *Particle dark matter: Evidence, candidates and constraints*, *Phys. Rept.* **405** (2005) 279 [hep-ph/0404175] [INSPIRE].

[5] J.L. Feng, *Dark Matter Candidates from Particle Physics and Methods of Detection*, *Ann. Rev. Astron. Astrophys.* **48** (2010) 495 [arXiv:1003.0904] [INSPIRE].

[6] H. Goldberg, *Constraint on the Photino Mass from Cosmology*, *Phys. Rev. Lett.* **50** (1983) 1419 [*Erratum ibid.* **103** (2009) 099905] [INSPIRE].

[7] J.R. Ellis, J.S. Hagelin, D.V. Nanopoulos, K.A. Olive and M. Srednicki, *Supersymmetric Relics from the Big Bang*, *Nucl. Phys. B* **238** (1984) 453 [INSPIRE].

[8] G.R. Farrar and P. Fayet, *Phenomenology of the Production, Decay, and Detection of New Hadronic States Associated with Supersymmetry*, *Phys. Lett. B* **76** (1978) 575 [INSPIRE].

[9] Y.A. Golfand and E.P. Likhtman, *Extension of the Algebra of Poincaré Group Generators and Violation of p Invariance*, *JETP Lett.* **13** (1971) 323 [*Pisma Zh. Eksp. Teor. Fiz.* **13** (1971) 452] [INSPIRE].

[10] D.V. Volkov and V.P. Akulov, *Is the Neutrino a Goldstone Particle?*, *Phys. Lett. B* **46** (1973) 109 [INSPIRE].

[11] J. Wess and B. Zumino, *Supergauge Transformations in Four-Dimensions*, *Nucl. Phys. B* **70** (1974) 39 [INSPIRE].

[12] J. Wess and B. Zumino, *Supergauge Invariant Extension of Quantum Electrodynamics*, *Nucl. Phys. B* **78** (1974) 1 [INSPIRE].

[13] S. Ferrara and B. Zumino, *Supergauge invariant Yang-Mills theories*, *Nucl. Phys. B* **79** (1974) 413 [INSPIRE].

[14] A. Salam and J.A. Strathdee, *Supersymmetry and Nonabelian Gauges*, *Phys. Lett. B* **51** (1974) 353 [INSPIRE].

[15] N. Sakai, *Naturalness in Supersymmetric Guts*, *Z. Phys. C* **11** (1981) 153 [INSPIRE].

[16] S. Dimopoulos, S. Raby and F. Wilczek, *Supersymmetry and the Scale of Unification*, *Phys. Rev. D* **24** (1981) 1681 [INSPIRE].

[17] L.E. Ibáñez and G.G. Ross, *Low-Energy Predictions in Supersymmetric Grand Unified Theories*, *Phys. Lett. B* **105** (1981) 439 [INSPIRE].

[18] S. Dimopoulos and H. Georgi, *Softly broken supersymmetry and* SU(5), *Nucl. Phys. B* **193** (1981) 150 [INSPIRE].

JHEP05(2021)093

[19] R. Barbieri and G.F. Giudice, *Upper Bounds on Supersymmetric Particle Masses*, *Nucl. Phys. B* **306** (1988) 63 [INSPIRE].

[20] B. de Carlos and J.A. Casas, *One loop analysis of the electroweak breaking in supersymmetric models and the fine tuning problem*, *Phys. Lett. B* **309** (1993) 320 [hep-ph/9303291] [INSPIRE].

[21] L. Evans and P. Bryant, *LHC Machine*, 2008 *JINST* **3** S08001 [INSPIRE].

[22] G. Steigman and M.S. Turner, *Cosmological Constraints on the Properties of Weakly Interacting Massive Particles*, *Nucl. Phys. B* **253** (1985) 375 [INSPIRE].

[23] E.W. Kolb and M.S. Turner, *The Early Universe*, *Front. Phys.* **69** (1990) 1 [INSPIRE].

[24] P.J. Fox and E. Poppitz, *Leptophilic Dark Matter*, *Phys. Rev. D* **79** (2009) 083528 [arXiv:0811.0399] [INSPIRE].

[25] S. Cassel, D.M. Ghilencea and G.G. Ross, *Electroweak and Dark Matter Constraints on a Z' in Models with a Hidden Valley*, *Nucl. Phys. B* **827** (2010) 256 [arXiv:0903.1118] [INSPIRE].

[26] Y. Bai, P.J. Fox and R. Harnik, *The Tevatron at the Frontier of Dark Matter Direct Detection*, *JHEP* **12** (2010) 048 [arXiv:1005.3797] [INSPIRE].

[27] J. Abdallah et al., *Simplified Models for Dark Matter Searches at the LHC*, *Phys. Dark Univ.* **9–10** (2015) 8 [arXiv:1506.03116] [INSPIRE].

[28] D. Abercrombie et al., *Dark Matter Benchmark Models for Early LHC Run-2 Searches: Report of the ATLAS/CMS Dark Matter Forum*, *Phys. Dark Univ.* **27** (2020) 100371 [arXiv:1507.00966] [INSPIRE].

[29] T. Abe et al., *LHC Dark Matter Working Group: Next-generation spin-0 dark matter models*, *Phys. Dark Univ.* **27** (2020) 100351 [arXiv:1810.09420] [INSPIRE].

[30] M.R. Buckley, D. Feld and D. Goncalves, *Scalar Simplified Models for Dark Matter*, *Phys. Rev. D* **91** (2015) 015017 [arXiv:1410.6497] [INSPIRE].

[31] U. Haisch and E. Re, *Simplified dark matter top-quark interactions at the LHC*, *JHEP* **06** (2015) 078 [arXiv:1503.00691] [INSPIRE].

[32] A. Boveia et al., *Recommendations on presenting LHC searches for missing transverse energy signals using simplified s-channel models of dark matter*, *Phys. Dark Univ.* **27** (2020) 100365 [arXiv:1603.04156] [INSPIRE].

[33] A. Albert et al., *Recommendations of the LHC Dark Matter Working Group: Comparing LHC searches for dark matter mediators in visible and invisible decay channels and calculations of the thermal relic density*, *Phys. Dark Univ.* **26** (2019) 100377 [arXiv:1703.05703] [INSPIRE].

[34] S. Dimopoulos and L. Susskind, *Mass Without Scalars*, *Nucl. Phys. B* **155** (1979) 237 [INSPIRE].

[35] S. Dimopoulos, *Technicolored Signatures*, *Nucl. Phys. B* **168** (1980) 69 [INSPIRE].

[36] E. Eichten and K.D. Lane, *Dynamical Breaking of Weak Interaction Symmetries*, *Phys. Lett. B* **90** (1980) 125 [INSPIRE].

[37] V.D. Angelopoulos, J.R. Ellis, H. Kowalski, D.V. Nanopoulos, N.D. Tracas and F. Zwirner, *Search for New Quarks Suggested by the Superstring*, *Nucl. Phys. B* **292** (1987) 59 [INSPIRE].

JHEP05(2021)093

[38] W. Buchmüller and D. Wyler, *Constraints on* SU(5) *Type Leptoquarks*, *Phys. Lett. B* **177** (1986) 377 [INSPIRE].

[39] J.C. Pati and A. Salam, *Lepton Number as the Fourth Color*, *Phys. Rev. D* **10** (1974) 275 [*Erratum ibid.* **11** (1975) 703] [INSPIRE].

[40] H. Georgi and S.L. Glashow, *Unity of All Elementary Particle Forces*, *Phys. Rev. Lett.* **32** (1974) 438 [INSPIRE].

[41] W. Buchmüller, R. Rückl and D. Wyler, *Leptoquarks in Lepton-Quark Collisions*, *Phys. Lett. B* **191** (1987) 442 [*Erratum ibid.* **448** (1999) 320] [INSPIRE].

[42] ATLAS collaboration, *ATLAS Run 1 searches for direct pair production of third-generation squarks at the Large Hadron Collider*, *Eur. Phys. J. C* **75** (2015) 510 [*Erratum ibid.* **76** (2016) 153] [arXiv:1506.08616] [INSPIRE].

[43] ATLAS collaboration, *Search for supersymmetry in events with b-tagged jets and missing transverse momentum in pp collisions at* $\sqrt{s} = 13$ *TeV with the ATLAS detector*, *JHEP* **11** (2017) 195 [arXiv:1708.09266] [INSPIRE].

[44] ATLAS collaboration, *Search for dark matter produced in association with bottom or top quarks in* $\sqrt{s} = 13$ *TeV pp collisions with the ATLAS detector*, *Eur. Phys. J. C* **78** (2018) 18 [arXiv:1710.11412] [INSPIRE].

[45] ATLAS collaboration, *Searches for third-generation scalar leptoquarks in* $\sqrt{s} = 13$ *TeV pp collisions with the ATLAS detector*, *JHEP* **06** (2019) 144 [arXiv:1902.08103] [INSPIRE].

[46] CMS collaboration, *Searches for physics beyond the standard model with the* M_{T2} *variable in hadronic final states with and without disappearing tracks in proton-proton collisions at* $\sqrt{s} = 13$ *TeV*, *Eur. Phys. J. C* **80** (2020) 3 [arXiv:1909.03460] [INSPIRE].

[47] CMS collaboration, *Search for supersymmetry in proton-proton collisions at* 13 *TeV in final states with jets and missing transverse momentum*, *JHEP* **10** (2019) 244 [arXiv:1908.04722] [INSPIRE].

[48] ATLAS collaboration, *The ATLAS Experiment at the CERN Large Hadron Collider*, 2008 *JINST* **3** S08003 [INSPIRE].

[49] ATLAS collaboration, *ATLAS Insertable B-Layer Technical Design Report*, ATLAS-TDR-19 (2010) [INSPIRE].

[50] ATLAS IBL collaboration, *Production and Integration of the ATLAS Insertable B-Layer*, 2018 *JINST* **13** T05008 [arXiv:1803.00844] [INSPIRE].

[51] ATLAS collaboration, *ATLAS data quality operations and performance for 2015–2018 data-taking*, 2020 *JINST* **15** P04003 [arXiv:1911.04632] [INSPIRE].

[52] ATLAS collaboration, *Luminosity determination in pp collisions at* $\sqrt{s} = 13$ *TeV using the ATLAS detector at the LHC*, ATLAS-CONF-2019-021 (2019).

[53] G. Avoni et al., *The new LUCID-2 detector for luminosity measurement and monitoring in ATLAS*, 2018 *JINST* **13** P07017 [INSPIRE].

[54] ATLAS collaboration, *Performance of the ATLAS Trigger System in 2015*, *Eur. Phys. J. C* **77** (2017) 317 [arXiv:1611.09661] [INSPIRE].

[55] ATLAS collaboration, *Performance of the missing transverse momentum triggers for the ATLAS detector during Run-2 data taking*, *JHEP* **08** (2020) 080 [arXiv:2005.09554] [INSPIRE].

JHEP05(2021)093

[56] ATLAS collaboration, *Performance of the ATLAS muon triggers in Run 2*, 2020 *JINST* **15** P09015 [arXiv:2004.13447] [INSPIRE].

[57] ATLAS collaboration, *Performance of electron and photon triggers in ATLAS during LHC Run 2*, *Eur. Phys. J. C* **80** (2020) 47 [arXiv:1909.00761] [INSPIRE].

[58] J. Alwall et al., *The automated computation of tree-level and next-to-leading order differential cross sections, and their matching to parton shower simulations*, *JHEP* **07** (2014) 079 [arXiv:1405.0301] [INSPIRE].

[59] NNPDF collaboration, *Parton distributions with LHC data*, *Nucl. Phys. B* **867** (2013) 244 [arXiv:1207.1303] [INSPIRE].

[60] T. Mandal, S. Mitra and S. Seth, *Pair Production of Scalar Leptoquarks at the LHC to NLO Parton Shower Accuracy*, *Phys. Rev. D* **93** (2016) 035018 [arXiv:1506.07369] [INSPIRE].

[61] M. Krämer, T. Plehn, M. Spira and P.M. Zerwas, *Pair production of scalar leptoquarks at the CERN LHC*, *Phys. Rev. D* **71** (2005) 057503 [hep-ph/0411038] [INSPIRE].

[62] M. Krämer, T. Plehn, M. Spira and P.M. Zerwas, *Pair production of scalar leptoquarks at the Tevatron*, *Phys. Rev. Lett.* **79** (1997) 341 [hep-ph/9704322] [INSPIRE].

[63] NNPDF collaboration, *Parton distributions for the LHC Run II*, *JHEP* **04** (2015) 040 [arXiv:1410.8849] [INSPIRE].

[64] T. Sjöstrand et al., *An introduction to PYTHIA 8.2*, *Comput. Phys. Commun.* **191** (2015) 159 [arXiv:1410.3012] [INSPIRE].

[65] L. Lönnblad and S. Prestel, *Merging Multi-leg NLO Matrix Elements with Parton Showers*, *JHEP* **03** (2013) 166 [arXiv:1211.7278] [INSPIRE].

[66] W. Beenakker, C. Borschensky, M. Krämer, A. Kulesza and E. Laenen, *NNLL-fast: predictions for coloured supersymmetric particle production at the LHC with threshold and Coulomb resummation*, *JHEP* **12** (2016) 133 [arXiv:1607.07741] [INSPIRE].

[67] W. Beenakker, M. Krämer, T. Plehn, M. Spira and P.M. Zerwas, *Stop production at hadron colliders*, *Nucl. Phys. B* **515** (1998) 3 [hep-ph/9710451] [INSPIRE].

[68] W. Beenakker, S. Brensing, M. Krämer, A. Kulesza, E. Laenen and I. Niessen, *Supersymmetric top and bottom squark production at hadron colliders*, *JHEP* **08** (2010) 098 [arXiv:1006.4771] [INSPIRE].

[69] W. Beenakker, C. Borschensky, R. Heger, M. Krämer, A. Kulesza and E. Laenen, *NNLL resummation for stop pair-production at the LHC*, *JHEP* **05** (2016) 153 [arXiv:1601.02954] [INSPIRE].

[70] J. Butterworth et al., *PDF4LHC recommendations for LHC Run II*, *J. Phys. G* **43** (2016) 023001 [arXiv:1510.03865] [INSPIRE].

[71] C. Borschensky, B. Fuks, A. Kulesza and D. Schwartländer, *Scalar leptoquark pair production at hadron colliders*, *Phys. Rev. D* **101** (2020) 115017 [arXiv:2002.08971] [INSPIRE].

[72] Y. Afik et al., *$DM + b\bar{b}$ simulations with DMSimp: an update*, in proceedings of the *Dark Matter at the LHC 2018: Experimental and theoretical workshop (DM@LHC 2018)*, Heidelberg, Germany, 3–6 April 2018, arXiv:1811.08002 [INSPIRE].

[73] T. Gleisberg et al., *Event generation with SHERPA 1.1*, *JHEP* **02** (2009) 007 [arXiv:0811.4622] [INSPIRE].

JHEP05(2021)093

[74] S. Catani, L. Cieri, G. Ferrera, D. de Florian and M. Grazzini, *Vector boson production at hadron colliders: a fully exclusive QCD calculation at NNLO*, *Phys. Rev. Lett.* **103** (2009) 082001 [arXiv:0903.2120] [INSPIRE].

[75] S. Alioli, P. Nason, C. Oleari and E. Re, *A general framework for implementing NLO calculations in shower Monte Carlo programs: the POWHEG BOX*, *JHEP* **06** (2010) 043 [arXiv:1002.2581] [INSPIRE].

[76] M. Czakon, P. Fiedler and A. Mitov, *Total Top-Quark Pair-Production Cross Section at Hadron Colliders Through $O(\alpha_S^4)$*, *Phys. Rev. Lett.* **110** (2013) 252004 [arXiv:1303.6254] [INSPIRE].

[77] M. Czakon and A. Mitov, *NNLO corrections to top pair production at hadron colliders: the quark-gluon reaction*, *JHEP* **01** (2013) 080 [arXiv:1210.6832] [INSPIRE].

[78] M. Czakon and A. Mitov, *NNLO corrections to top-pair production at hadron colliders: the all-fermionic scattering channels*, *JHEP* **12** (2012) 054 [arXiv:1207.0236] [INSPIRE].

[79] P. Bärnreuther, M. Czakon and A. Mitov, *Percent Level Precision Physics at the Tevatron: First Genuine NNLO QCD Corrections to $q\bar{q} \to t\bar{t} + X$*, *Phys. Rev. Lett.* **109** (2012) 132001 [arXiv:1204.5201] [INSPIRE].

[80] M. Cacciari, M. Czakon, M. Mangano, A. Mitov and P. Nason, *Top-pair production at hadron colliders with next-to-next-to-leading logarithmic soft-gluon resummation*, *Phys. Lett. B* **710** (2012) 612 [arXiv:1111.5869] [INSPIRE].

[81] M. Czakon and A. Mitov, *Top++: A Program for the Calculation of the Top-Pair Cross-Section at Hadron Colliders*, *Comput. Phys. Commun.* **185** (2014) 2930 [arXiv:1112.5675] [INSPIRE].

[82] N. Kidonakis, *Next-to-next-to-leading-order collinear and soft gluon corrections for t-channel single top quark production*, *Phys. Rev. D* **83** (2011) 091503 [arXiv:1103.2792] [INSPIRE].

[83] N. Kidonakis, *Two-loop soft anomalous dimensions for single top quark associated production with a W^- or H^-*, *Phys. Rev. D* **82** (2010) 054018 [arXiv:1005.4451] [INSPIRE].

[84] N. Kidonakis, *NNLL resummation for s-channel single top quark production*, *Phys. Rev. D* **81** (2010) 054028 [arXiv:1001.5034] [INSPIRE].

[85] W. Beenakker, S. Dittmaier, M. Krämer, B. Plumper, M. Spira and P.M. Zerwas, *NLO QCD corrections to $t\bar{t}H$ production in hadron collisions*, *Nucl. Phys. B* **653** (2003) 151 [hep-ph/0211352] [INSPIRE].

[86] S. Dawson, C. Jackson, L.H. Orr, L. Reina and D. Wackeroth, *Associated Higgs production with top quarks at the large hadron collider: NLO QCD corrections*, *Phys. Rev. D* **68** (2003) 034022 [hep-ph/0305087] [INSPIRE].

[87] Y. Zhang, W.-G. Ma, R.-Y. Zhang, C. Chen and L. Guo, *QCD NLO and EW NLO corrections to $t\bar{t}H$ production with top quark decays at hadron collider*, *Phys. Lett. B* **738** (2014) 1 [arXiv:1407.1110] [INSPIRE].

[88] S. Frixione, V. Hirschi, D. Pagani, H.-S. Shao and M. Zaro, *Electroweak and QCD corrections to top-pair hadroproduction in association with heavy bosons*, *JHEP* **06** (2015) 184 [arXiv:1504.03446] [INSPIRE].

[89] D.J. Lange, *The EvtGen particle decay simulation package*, *Nucl. Instrum. Meth. A* **462** (2001) 152 [INSPIRE].

JHEP05(2021)093

[90] ATLAS collaboration, *The ATLAS Simulation Infrastructure*, *Eur. Phys. J. C* **70** (2010) 823 [arXiv:1005.4568] [INSPIRE].

[91] GEANT4 collaboration, *GEANT4 — a simulation toolkit*, *Nucl. Instrum. Meth. A* **506** (2003) 250 [INSPIRE].

[92] ATLAS collaboration, *The simulation principle and performance of the ATLAS fast calorimeter simulation FastCaloSim*, ATL-PHYS-PUB-2010-013 (2010).

[93] ATLAS collaboration, *Summary of ATLAS PYTHIA 8 tunes*, ATL-PHYS-PUB-2012-003 (2012).

[94] ATLAS collaboration, *Reconstruction of primary vertices at the ATLAS experiment in Run 1 proton-proton collisions at the LHC*, *Eur. Phys. J. C* **77** (2017) 332 [arXiv:1611.10235] [INSPIRE].

[95] ATLAS collaboration, *Vertex Reconstruction Performance of the ATLAS Detector at* $\sqrt{s} = 13$ *TeV*, ATL-PHYS-PUB-2015-026 (2015).

[96] ATLAS collaboration, *Performance of the ATLAS Track Reconstruction Algorithms in Dense Environments in LHC Run 2*, *Eur. Phys. J. C* **77** (2017) 673 [arXiv:1704.07983] [INSPIRE].

[97] M. Cacciari, G.P. Salam and G. Soyez, *The anti-*k_t *jet clustering algorithm*, *JHEP* **04** (2008) 063 [arXiv:0802.1189] [INSPIRE].

[98] M. Cacciari, G.P. Salam and G. Soyez, *FastJet User Manual*, *Eur. Phys. J. C* **72** (2012) 1896 [arXiv:1111.6097] [INSPIRE].

[99] ATLAS collaboration, *Topological cell clustering in the ATLAS calorimeters and its performance in LHC Run 1*, *Eur. Phys. J. C* **77** (2017) 490 [arXiv:1603.02934] [INSPIRE].

[100] ATLAS collaboration, *Jet reconstruction and performance using particle flow with the ATLAS Detector*, *Eur. Phys. J. C* **77** (2017) 466 [arXiv:1703.10485] [INSPIRE].

[101] ATLAS collaboration, *Jet energy scale and resolution measured in proton-proton collisions at* $\sqrt{s} = 13$ *TeV with the ATLAS detector*, arXiv:2007.02645 [INSPIRE].

[102] ATLAS collaboration, *Characterisation and mitigation of beam-induced backgrounds observed in the ATLAS detector during the 2011 proton-proton run*, 2013 *JINST* **8** P07004 [arXiv:1303.0223] [INSPIRE].

[103] ATLAS collaboration, *Performance of pile-up mitigation techniques for jets in pp collisions at* $\sqrt{s} = 8$ *TeV using the ATLAS detector*, *Eur. Phys. J. C* **76** (2016) 581 [arXiv:1510.03823] [INSPIRE].

[104] ATLAS collaboration, *ATLAS b-jet identification performance and efficiency measurement with* $t\bar{t}$ *events in pp collisions at* $\sqrt{s} = 13$ *TeV*, *Eur. Phys. J. C* **79** (2019) 970 [arXiv:1907.05120] [INSPIRE].

[105] ATLAS collaboration, *Soft b-hadron tagging for compressed SUSY scenarios*, ATLAS-CONF-2019-027 (2019).

[106] ATLAS collaboration, *Search for long-lived, massive particles in events with a displaced vertex and a muon with large impact parameter in pp collisions at* $\sqrt{s} = 13$ *TeV with the ATLAS detector*, *Phys. Rev. D* **102** (2020) 032006 [arXiv:2003.11956] [INSPIRE].

[107] ATLAS collaboration, *Muon reconstruction performance of the ATLAS detector in proton-proton collision data at* $\sqrt{s} = 13$ *TeV*, *Eur. Phys. J. C* **76** (2016) 292 [arXiv:1603.05598] [INSPIRE].

JHEP05(2021)093

[108] ATLAS collaboration, *Muon reconstruction and identification efficiency in ATLAS using the full Run 2 pp collision data set at* $\sqrt{s} = 13$ *TeV*, arXiv:2012.00578 [INSPIRE].

[109] ATLAS collaboration, *Electron and photon performance measurements with the ATLAS detector using the 2015–2017 LHC proton-proton collision data*, 2019 *JINST* **14** P12006 [arXiv:1908.00005] [INSPIRE].

[110] ATLAS collaboration, *Electron reconstruction and identification in the ATLAS experiment using the 2015 and 2016 LHC proton-proton collision data at* $\sqrt{s} = 13$ *TeV*, *Eur. Phys. J. C* **79** (2019) 639 [arXiv:1902.04655] [INSPIRE].

[111] ATLAS collaboration, E_T^{miss} *performance in the ATLAS detector using 2015–2016 LHC pp collisions*, ATLAS-CONF-2018-023 (2018).

[112] ATLAS collaboration, *Performance of missing transverse momentum reconstruction with the ATLAS detector using proton-proton collisions at* $\sqrt{s} = 13$ *TeV*, *Eur. Phys. J. C* **78** (2018) 903 [arXiv:1802.08168] [INSPIRE].

[113] ATLAS collaboration, *Measurement of the photon identification efficiencies with the ATLAS detector using LHC Run 2 data collected in 2015 and 2016*, *Eur. Phys. J. C* **79** (2019) 205 [arXiv:1810.05087] [INSPIRE].

[114] ATLAS collaboration, *Search for scalar bottom quark pair production with the ATLAS detector in pp Collisions at* $\sqrt{s} = 7$ *TeV*, *Phys. Rev. Lett.* **108** (2012) 181802 [arXiv:1112.3832] [INSPIRE].

[115] ATLAS collaboration, *Search for direct third-generation squark pair production in final states with missing transverse momentum and two b-jets in* $\sqrt{s} = 8$ *TeV pp collisions with the ATLAS detector*, *JHEP* **10** (2013) 189 [arXiv:1308.2631] [INSPIRE].

[116] ATLAS collaboration, *Search for bottom squark pair production in proton-proton collisions at* $\sqrt{s} = 13$ *TeV with the ATLAS detector*, *Eur. Phys. J. C* **76** (2016) 547 [arXiv:1606.08772] [INSPIRE].

[117] T. Chen and C. Guestrin, *XGBoost: A scalable tree boosting system*, in proceedings of the *22nd ACM SIGKDD International Conference on Knowledge Discovery and Data Mining (KDD '16)*, San Francisco, CA, U.S.A., 13–17 August 2016, ACM, New York NY U.S.A. (2016), pp. 785–794 [arXiv:1603.02754] [INSPIRE].

[118] A.L. Read, *Presentation of search results: The* CL_s *technique*, *J. Phys. G* **28** (2002) 2693 [INSPIRE].

[119] M. Baak, G.J. Besjes, D. Côté, A. Koutsman, J. Lorenz and D. Short, *HistFitter software framework for statistical data analysis*, *Eur. Phys. J. C* **75** (2015) 153 [arXiv:1410.1280] [INSPIRE].

[120] ATLAS collaboration, *Object-based missing transverse momentum significance in the ATLAS detector*, ATLAS-CONF-2018-038 (2018).

[121] D.R. Tovey, *On measuring the masses of pair-produced semi-invisibly decaying particles at hadron colliders*, *JHEP* **04** (2008) 034 [arXiv:0802.2879] [INSPIRE].

[122] U. Haisch, P. Pani and G. Polesello, *Determining the CP nature of spin-0 mediators in associated production of dark matter and* $t\bar{t}$ *pairs*, *JHEP* **02** (2017) 131 [arXiv:1611.09841] [INSPIRE].

[123] ATLAS collaboration, *Jet energy scale measurements and their systematic uncertainties in proton-proton collisions at* $\sqrt{s} = 13$ *TeV with the ATLAS detector*, *Phys. Rev. D* **96** (2017) 072002 [arXiv:1703.09665] [INSPIRE].

JHEP05(2021)093

[124] ATLAS collaboration, *Jet energy resolution in proton-proton collisions at $\sqrt{s} = 7$ TeV recorded in 2010 with the ATLAS detector*, *Eur. Phys. J. C* **73** (2013) 2306 [arXiv:1210.6210] [INSPIRE].

[125] M. Bähr et al., *HERWIG++ Physics and Manual*, *Eur. Phys. J. C* **58** (2008) 639 [arXiv:0803.0883] [INSPIRE].

[126] J. Bellm et al., *HERWIG 7.0/HERWIG++ 3.0 release note*, *Eur. Phys. J. C* **76** (2016) 196 [arXiv:1512.01178] [INSPIRE].

[127] ATLAS collaboration, *Improvements in $t\bar{t}$ modelling using NLO+PS Monte Carlo generators for Run2*, ATL-PHYS-PUB-2018-009 (2018).

[128] E. Bothmann, M. Schönherr and S. Schumann, *Reweighting QCD matrix-element and parton-shower calculations*, *Eur. Phys. J. C* **76** (2016) 590 [arXiv:1606.08753] [INSPIRE].

[129] ATLAS collaboration, *Measurements of the production cross-section for a Z boson in association with b-jets in proton-proton collisions at $\sqrt{s} = 13$ TeV with the ATLAS detector*, *JHEP* **07** (2020) 044 [arXiv:2003.11960] [INSPIRE].

[130] R.D. Cousins, J.T. Linnemann and J. Tucker, *Evaluation of three methods for calculating statistical significance when incorporating a systematic uncertainty into a test of the background-only hypothesis for a Poisson process*, *Nucl. Instrum. Meth. A* **595** (2008) 480 [physics/0702156] [INSPIRE].

[131] G. Cowan, K. Cranmer, E. Gross and O. Vitells, *Asymptotic formulae for likelihood-based tests of new physics*, *Eur. Phys. J. C* **71** (2011) 1554 [*Erratum ibid.* **73** (2013) 2501] [arXiv:1007.1727] [INSPIRE].

[132] ATLAS collaboration, *ATLAS Computing Acknowledgements*, ATL-SOFT-PUB-2020-001 (2020).

JHEP05(2021)093

The ATLAS collaboration

G. Aad[101], B. Abbott[127], D.C. Abbott[102], A. Abed Abud[36], K. Abeling[53], D.K. Abhayasinghe[93], S.H. Abidi[29], O.S. AbouZeid[40], N.L. Abraham[155], H. Abramowicz[160], H. Abreu[159], Y. Abulaiti[6], B.S. Acharya[66a,66b,o], B. Achkar[53], L. Adam[99], C. Adam Bourdarios[5], L. Adamczyk[83a], L. Adamek[165], J. Adelman[120], A. Adiguzel[12c,ae], S. Adorni[54], T. Adye[142], A.A. Affolder[144], Y. Afik[159], C. Agapopoulou[64], M.N. Agaras[38], A. Aggarwal[118], C. Agheorghiesei[27c], J.A. Aguilar-Saavedra[138f,138a,ad], A. Ahmad[36], F. Ahmadov[79], W.S. Ahmed[103], X. Ai[46], G. Aielli[73a,73b], S. Akatsuka[85], M. Akbiyik[99], T.P.A. Åkesson[96], E. Akilli[54], A.V. Akimov[110], K. Al Khoury[39], G.L. Alberghi[23b,23a], J. Albert[174], M.J. Alconada Verzini[160], S. Alderweireldt[36], M. Aleksa[36], I.N. Aleksandrov[79], C. Alexa[27b], T. Alexopoulos[10], A. Alfonsi[119], F. Alfonsi[23b,23a], M. Alhroob[127], B. Ali[140], S. Ali[157], M. Aliev[164], G. Alimonti[68a], C. Allaire[36], B.M.M. Allbrooke[155], P.P. Allport[21], A. Aloisio[69a,69b], F. Alonso[88], C. Alpigiani[147], E. Alunno Camelia[73a,73b], M. Alvarez Estevez[98], M.G. Alviggi[69a,69b], Y. Amaral Coutinho[80b], A. Ambler[103], L. Ambroz[133], C. Amelung[36], D. Amidei[105], S.P. Amor Dos Santos[138a], S. Amoroso[46], C.S. Amrouche[54], C. Anastopoulos[148], N. Andari[143], T. Andeen[11], J.K. Anders[20], S.Y. Andrean[45a,45b], A. Andreazza[68a,68b], V. Andrei[61a], C.R. Anelli[174], S. Angelidakis[9], A. Angerami[39], A.V. Anisenkov[121b,121a], A. Annovi[71a], C. Antel[54], M.T. Anthony[148], E. Antipov[128], M. Antonelli[51], D.J.A. Antrim[18], F. Anulli[72a], M. Aoki[81], J.A. Aparisi Pozo[172], M.A. Aparo[155], L. Aperio Bella[46], N. Aranzabal[36], V. Araujo Ferraz[80a], C. Arcangeletti[51], A.T.H. Arce[49], J-F. Arguin[109], S. Argyropoulos[52], J.-H. Arling[46], A.J. Armbruster[36], O. Arnaez[165], H. Arnold[36], Z.P. Arrubarrena Tame[113], G. Artoni[133], H. Asada[116], K. Asai[125], S. Asai[162], T. Asawatavonvanich[163], N.A. Asbah[59], E.M. Asimakopoulou[170], L. Asquith[155], J. Assahsah[35e], K. Assamagan[29], R. Astalos[28a], R.J. Atkin[33a], M. Atkinson[171], N.B. Atlay[19], P.A. Atmasiddha[105], K. Augsten[140], V.A. Austrup[180], G. Avolio[36], M.K. Ayoub[15c], G. Azuelos[109,al], D. Babal[28a], H. Bachacou[143], K. Bachas[161], F. Backman[45a,45b], P. Bagnaia[72a,72b], H. Bahrasemani[151], A.J. Bailey[172], V.R. Bailey[171], J.T. Baines[142], C. Bakalis[10], O.K. Baker[181], P.J. Bakker[119], E. Bakos[16], D. Bakshi Gupta[8], S. Balaji[156], R. Balasubramanian[119], E.M. Baldin[121b,121a], P. Balek[178], F. Balli[143], W.K. Balunas[133], J. Balz[99], E. Banas[84], M. Bandieramonte[137], A. Bandyopadhyay[19], L. Barak[160], W.M. Barbe[38], E.L. Barberio[104], D. Barberis[55b,55a], M. Barbero[101], G. Barbour[94], T. Barillari[114], M-S. Barisits[36], J. Barkeloo[130], T. Barklow[152], B.M. Barnett[142], R.M. Barnett[18], Z. Barnovska-Blenessy[60a], A. Baroncelli[60a], G. Barone[29], A.J. Barr[133], L. Barranco Navarro[45a,45b], F. Barreiro[98], J. Barreiro Guimarães da Costa[15a], U. Barron[160], S. Barsov[136], F. Bartels[61a], R. Bartoldus[152], G. Bartolini[101], A.E. Barton[89], P. Bartos[28a], A. Basalaev[46], A. Basan[99], A. Bassalat[64,ai], M.J. Basso[165], C.R. Basson[100], R.L. Bates[57], S. Batlamous[35f], J.R. Batley[32], B. Batool[150], M. Battaglia[144], M. Bauce[72a,72b], F. Bauer[143,*], P. Bauer[24], H.S. Bawa[31], A. Bayirli[12c], J.B. Beacham[49], T. Beau[134], P.H. Beauchemin[168], F. Becherer[52], P. Bechtle[24], H.P. Beck[20,q], K. Becker[176], C. Becot[46], A.J. Beddall[12a], V.A. Bednyakov[79], C.P. Bee[154], T.A. Beermann[180], M. Begalli[80b], M. Begel[29], A. Behera[154], J.K. Behr[46], F. Beisiegel[24], M. Belfkir[5], G. Bella[160], L. Bellagamba[23b], A. Bellerive[34], P. Bellos[21], K. Beloborodov[121b,121a], K. Belotskiy[111], N.L. Belyaev[111], D. Benchekroun[35a], N. Benekos[10], Y. Benhammou[160], D.P. Benjamin[6], M. Benoit[29], J.R. Bensinger[26], S. Bentvelsen[119], L. Beresford[133], M. Beretta[51], D. Berge[19], E. Bergeaas Kuutmann[170], N. Berger[5], B. Bergmann[140], L.J. Bergsten[26], J. Beringer[18], S. Berlendis[7], G. Bernardi[134], C. Bernius[152], F.U. Bernlochner[24], T. Berry[93], P. Berta[46], A. Berthold[48], I.A. Bertram[89], O. Bessidskaia Bylund[180], S. Bethke[114], A. Betti[42], A.J. Bevan[92], S. Bhatta[154], D.S. Bhattacharya[175], P. Bhattarai[26], V.S. Bhopatkar[6], R. Bi[137], R.M. Bianchi[137], O. Biebel[113], R. Bielski[36], K. Bierwagen[99], M. Biglietti[74a], T.R.V. Billoud[140], M. Bindi[53],

JHEP05(2021)093

A. Bingul[12d], C. Bini[72a,72b], S. Biondi[23b,23a], C.J. Birch-sykes[100], M. Birman[178], T. Bisanz[36], J.P. Biswal[3], D. Biswas[179,j], A. Bitadze[100], C. Bittrich[48], K. Bjørke[132], T. Blazek[28a], I. Bloch[46], C. Blocker[26], A. Blue[57], U. Blumenschein[92], G.J. Bobbink[119], V.S. Bobrovnikov[121b,121a], D. Bogavac[14], A.G. Bogdanchikov[121b,121a], C. Bohm[45a], V. Boisvert[93], P. Bokan[170,53], T. Bold[83a], M. Bomben[134], M. Bona[92], J.S. Bonilla[130], M. Boonekamp[143], C.D. Booth[93], A.G. Borbély[57], H.M. Borecka-Bielska[90], L.S. Borgna[94], G. Borissov[89], D. Bortoletto[133], D. Boscherini[23b], M. Bosman[14], J.D. Bossio Sola[103], K. Bouaouda[35a], J. Boudreau[137], E.V. Bouhova-Thacker[89], D. Boumediene[38], R. Bouquet[134], A. Boveia[126], J. Boyd[36], D. Boye[29], I.R. Boyko[79], A.J. Bozson[93], J. Bracinik[21], N. Brahimi[60d,60c], G. Brandt[180], O. Brandt[32], F. Braren[46], B. Brau[102], J.E. Brau[130], W.D. Breaden Madden[57], K. Brendlinger[46], R. Brener[159], L. Brenner[36], R. Brenner[170], S. Bressler[178], B. Brickwedde[99], D.L. Briglin[21], D. Britton[57], D. Britzger[114], I. Brock[24], R. Brock[106], G. Brooijmans[39], W.K. Brooks[145d], E. Brost[29], P.A. Bruckman de Renstrom[84], B. Brüers[46], D. Bruncko[28b], A. Bruni[23b], G. Bruni[23b], M. Bruschi[23b], N. Bruscino[72a,72b], L. Bryngemark[152], T. Buanes[17], Q. Buat[154], P. Buchholz[150], A.G. Buckley[57], I.A. Budagov[79], M.K. Bugge[132], O. Bulekov[111], B.A. Bullard[59], T.J. Burch[120], S. Burdin[90], C.D. Burgard[46], A.M. Burger[128], B. Burghgrave[8], J.T.P. Burr[46], C.D. Burton[11], J.C. Burzynski[102], V. Büscher[99], E. Buschmann[53], P.J. Bussey[57], J.M. Butler[25], C.M. Buttar[57], J.M. Butterworth[94], W. Buttinger[142], C.J. Buxo Vazquez[106], A.R. Buzykaev[121b,121a], G. Cabras[23b,23a], S. Cabrera Urbán[172], D. Caforio[56], H. Cai[137], V.M.M. Cairo[152], O. Cakir[4a], N. Calace[36], P. Calafiura[18], G. Calderini[134], P. Calfayan[65], G. Callea[57], L.P. Caloba[80b], A. Caltabiano[73a,73b], S. Calvente Lopez[98], D. Calvet[38], S. Calvet[38], T.P. Calvet[101], M. Calvetti[71a,71b], R. Camacho Toro[134], S. Camarda[36], D. Camarero Munoz[98], P. Camarri[73a,73b], M.T. Camerlingo[74a,74b], D. Cameron[132], C. Camincher[36], M. Campanelli[94], A. Camplani[40], V. Canale[69a,69b], A. Canesse[103], M. Cano Bret[77], J. Cantero[128], Y. Cao[171], M. Capua[41b,41a], R. Cardarelli[73a], F. Cardillo[172], G. Carducci[41b,41a], T. Carli[36], G. Carlino[69a], B.T. Carlson[137], E.M. Carlson[174,166a], L. Carminati[68a,68b], R.M.D. Carney[152], S. Caron[118], E. Carquin[145d], S. Carrá[46], G. Carratta[23b,23a], J.W.S. Carter[165], T.M. Carter[50], M.P. Casado[14,g], A.F. Casha[165], E.G. Castiglia[181], F.L. Castillo[172], L. Castillo Garcia[14], V. Castillo Gimenez[172], N.F. Castro[138a,138e], A. Catinaccio[36], J.R. Catmore[132], A. Cattai[36], V. Cavaliere[29], V. Cavasinni[71a,71b], E. Celebi[12b], F. Celli[133], K. Cerny[129], A.S. Cerqueira[80a], A. Cerri[155], L. Cerrito[73a,73b], F. Cerutti[18], A. Cervelli[23b,23a], S.A. Cetin[12b], Z. Chadi[35a], D. Chakraborty[120], J. Chan[179], W.S. Chan[119], W.Y. Chan[90], J.D. Chapman[32], B. Chargeishvili[158b], D.G. Charlton[21], T.P. Charman[92], M. Chatterjee[20], C.C. Chau[34], S. Chekanov[6], S.V. Chekulaev[166a], G.A. Chelkov[79,ag], B. Chen[78], C. Chen[60a], C.H. Chen[78], H. Chen[15c], H. Chen[29], J. Chen[60a], J. Chen[39], J. Chen[26], S. Chen[135], S.J. Chen[15c], X. Chen[15b], Y. Chen[60a], Y-H. Chen[46], H.C. Cheng[62a], H.J. Cheng[15a], A. Cheplakov[79], E. Cheremushkina[122], R. Cherkaoui El Moursli[35f], E. Cheu[7], K. Cheung[63], L. Chevalier[143], V. Chiarella[51], G. Chiarelli[71a], G. Chiodini[67a], A.S. Chisholm[21], A. Chitan[27b], I. Chiu[162], Y.H. Chiu[174], M.V. Chizhov[79,t], K. Choi[11], A.R. Chomont[72a,72b], Y. Chou[102], Y.S. Chow[119], L.D. Christopher[33f], M.C. Chu[62a], X. Chu[15a,15d], J. Chudoba[139], J.J. Chwastowski[84], D. Cieri[114], K.M. Ciesla[84], V. Cindro[91], I.A. Cioară[27b], A. Ciocio[18], F. Cirotto[69a,69b], Z.H. Citron[178,k], M. Citterio[68a], D.A. Ciubotaru[27b], B.M. Ciungu[165], A. Clark[54], P.J. Clark[50], S.E. Clawson[100], C. Clement[45a,45b], L. Clissa[23b,23a], Y. Coadou[101], M. Cobal[66a,66c], A. Coccaro[55b], J. Cochran[78], R. Coelho Lopes De Sa[102], H. Cohen[160], A.E.C. Coimbra[36], B. Cole[39], J. Collot[58], P. Conde Muiño[138a,138h], S.H. Connell[33c], I.A. Connelly[57], F. Conventi[69a,am], A.M. Cooper-Sarkar[133], F. Cormier[173], L.D. Corpe[94], M. Corradi[72a,72b], E.E. Corrigan[96], F. Corriveau[103,ab], M.J. Costa[172], F. Costanza[5], D. Costanzo[148], G. Cowan[93], J.W. Cowley[32], J. Crane[100], K. Cranmer[124], R.A. Creager[135], S. Crépé-Renaudin[58], F. Crescioli[134], M. Cristinziani[24], M. Cristoforetti[75a,75b], V. Croft[168], G. Crosetti[41b,41a], A. Cueto[5], T. Cuhadar Donszelmann[169], H. Cui[15a,15d], A.R. Cukierman[152],

JHEP05(2021)093

W.R. Cunningham[57], S. Czekierda[84], P. Czodrowski[36], M.M. Czurylo[61b], M.J. Da Cunha Sargedas De Sousa[60b], J.V. Da Fonseca Pinto[80b], C. Da Via[100], W. Dabrowski[83a], T. Dado[47], S. Dahbi[33f], T. Dai[105], C. Dallapiccola[102], M. Dam[40], G. D'amen[29], V. D'Amico[74a,74b], J. Damp[99], J.R. Dandoy[135], M.F. Daneri[30], M. Danninger[151], V. Dao[36], G. Darbo[55b], A. Dattagupta[130], S. D'Auria[68a,68b], C. David[166b], T. Davidek[141], D.R. Davis[49], I. Dawson[148], K. De[8], R. De Asmundis[69a], M. De Beurs[119], S. De Castro[23b,23a], N. De Groot[118], P. de Jong[119], H. De la Torre[106], A. De Maria[15c], D. De Pedis[72a], A. De Salvo[72a], U. De Sanctis[73a,73b], A. De Santo[155], J.B. De Vivie De Regie[58], D.V. Dedovich[79], A.M. Deiana[42], J. Del Peso[98], Y. Delabat Diaz[46], F. Deliot[143], C.M. Delitzsch[7], M. Della Pietra[69a,69b], D. Della Volpe[54], A. Dell'Acqua[36], L. Dell'Asta[73a,73b], M. Delmastro[5], C. Delporte[64], P.A. Delsart[58], S. Demers[181], M. Demichev[79], G. Demontigny[109], S.P. Denisov[122], L. D'Eramo[120], D. Derendarz[84], J.E. Derkaoui[35e], F. Derue[134], P. Dervan[90], K. Desch[24], K. Dette[165], C. Deutsch[24], P.O. Deviveiros[36], F.A. Di Bello[72a,72b], A. Di Ciaccio[73a,73b], L. Di Ciaccio[5], C. Di Donato[69a,69b], A. Di Girolamo[36], G. Di Gregorio[71a,71b], A. Di Luca[75a,75b], B. Di Micco[74a,74b], R. Di Nardo[74a,74b], R. Di Sipio[165], C. Diaconu[101], F.A. Dias[119], T. Dias Do Vale[138a], M.A. Diaz[145a], F.G. Diaz Capriles[24], J. Dickinson[18], M. Didenko[164], E.B. Diehl[105], J. Dietrich[19], S. Díez Cornell[46], C. Diez Pardos[150], A. Dimitrievska[18], W. Ding[15b], J. Dingfelder[24], S.J. Dittmeier[61b], F. Dittus[36], F. Djama[101], T. Djobava[158b], J.I. Djuvsland[17], M.A.B. Do Vale[146], M. Dobre[27b], D. Dodsworth[26], C. Doglioni[96], J. Dolejsi[141], Z. Dolezal[141], M. Donadelli[80c], B. Dong[60c], J. Donini[38], A. D'onofrio[15c], M. D'Onofrio[90], J. Dopke[142], A. Doria[69a], M.T. Dova[88], A.T. Doyle[57], E. Drechsler[151], E. Dreyer[151], T. Dreyer[53], A.S. Drobac[168], D. Du[60b], T.A. du Pree[119], Y. Duan[60d], F. Dubinin[110], M. Dubovsky[28a], A. Dubreuil[54], E. Duchovni[178], G. Duckeck[113], O.A. Ducu[36,27b], D. Duda[114], A. Dudarev[36], A.C. Dudder[99], M. D'uffizi[100], L. Duflot[64], M. Dührssen[36], C. Dülsen[180], M. Dumancic[178], A.E. Dumitriu[27b], M. Dunford[61a], S. Dungs[47], A. Duperrin[101], H. Duran Yildiz[4a], M. Düren[56], A. Durglishvili[158b], B. Dutta[46], D. Duvnjak[1], G.I. Dyckes[135], M. Dyndal[36], S. Dysch[100], B.S. Dziedzic[84], M.G. Eggleston[49], T. Eifert[8], G. Eigen[17], K. Einsweiler[18], T. Ekelof[170], H. El Jarrari[35f], A. El Moussaouy[35a], V. Ellajosyula[170], M. Ellert[170], F. Ellinghaus[180], A.A. Elliot[92], N. Ellis[36], J. Elmsheuser[29], M. Elsing[36], D. Emeliyanov[142], A. Emerman[39], Y. Enari[162], J. Erdmann[47], A. Ereditato[20], P.A. Erland[84], M. Errenst[180], M. Escalier[64], C. Escobar[172], O. Estrada Pastor[172], E. Etzion[160], G. Evans[138a], H. Evans[65], M.O. Evans[155], A. Ezhilov[136], F. Fabbri[57], L. Fabbri[23b,23a], V. Fabiani[118], G. Facini[176], R.M. Fakhrutdinov[122], S. Falciano[72a], P.J. Falke[24], S. Falke[36], J. Faltova[141], Y. Fang[15a], Y. Fang[15a], G. Fanourakis[44], M. Fanti[68a,68b], M. Faraj[60c], A. Farbin[8], A. Farilla[74a], E.M. Farina[70a,70b], T. Farooque[106], S.M. Farrington[50], P. Farthouat[36], F. Fassi[35f], D. Fassouliotis[9], M. Faucci Giannelli[73a,73b], W.J. Fawcett[32], L. Fayard[64], O.L. Fedin[136,p], A. Fehr[20], M. Feickert[171], L. Feligioni[101], A. Fell[148], C. Feng[60b], M. Feng[49], M.J. Fenton[169], A.B. Fenyuk[122], S.W. Ferguson[43], J. Ferrando[46], A. Ferrari[170], P. Ferrari[119], R. Ferrari[70a], D. Ferrere[54], C. Ferretti[105], F. Fiedler[99], A. Filipčič[91], F. Filthaut[118], K.D. Finelli[25], M.C.N. Fiolhais[138a,138c,a], L. Fiorini[172], F. Fischer[113], J. Fischer[99], W.C. Fisher[106], T. Fitschen[21], I. Fleck[150], P. Fleischmann[105], T. Flick[180], B.M. Flierl[113], L. Flores[135], L.R. Flores Castillo[62a], F.M. Follega[75a,75b], N. Fomin[17], J.H. Foo[165], G.T. Forcolin[75a,75b], B.C. Forland[65], A. Formica[143], F.A. Förster[14], A.C. Forti[100], E. Fortin[101], M.G. Foti[133], D. Fournier[64], H. Fox[89], P. Francavilla[71a,71b], S. Francescato[72a,72b], M. Franchini[23b,23a], S. Franchino[61a], D. Francis[36], L. Franco[5], L. Franconi[20], M. Franklin[59], G. Frattari[72a,72b], P.M. Freeman[21], B. Freund[109], W.S. Freund[80b], E.M. Freundlich[47], D.C. Frizzell[127], D. Froidevaux[36], J.A. Frost[133], M. Fujimoto[125], E. Fullana Torregrosa[172], T. Fusayasu[115], J. Fuster[172], A. Gabrielli[23b,23a], A. Gabrielli[36], P. Gadow[114], G. Gagliardi[55b,55a], L.G. Gagnon[109], G.E. Gallardo[133], E.J. Gallas[133], B.J. Gallop[142], R. Gamboa Goni[92], K.K. Gan[126], S. Ganguly[178], J. Gao[60a], Y. Gao[50], Y.S. Gao[31,m], F.M. Garay Walls[145a], C. García[172], J.E. García Navarro[172],

JHEP05(2021)093

J.A. García Pascual[15a], M. Garcia-Sciveres[18], R.W. Gardner[37], S. Gargiulo[52], C.A. Garner[165], V. Garonne[132], S.J. Gasiorowski[147], P. Gaspar[80b], G. Gaudio[70a], P. Gauzzi[72a,72b], I.L. Gavrilenko[110], A. Gavrilyuk[123], C. Gay[173], G. Gaycken[46], E.N. Gazis[10], A.A. Geanta[27b], C.M. Gee[144], C.N.P. Gee[142], J. Geisen[96], M. Geisen[99], C. Gemme[55b], M.H. Genest[58], C. Geng[105], S. Gentile[72a,72b], S. George[93], T. Geralis[44], L.O. Gerlach[53], P. Gessinger-Befurt[99], G. Gessner[47], M. Ghasemi Bostanabad[174], M. Ghneimat[150], A. Ghosh[64], A. Ghosh[77], B. Giacobbe[23b], S. Giagu[72a,72b], N. Giangiacomi[165], P. Giannetti[71a], A. Giannini[69a,69b], G. Giannini[14], S.M. Gibson[93], M. Gignac[144], D.T. Gil[83b], B.J. Gilbert[39], D. Gillberg[34], G. Gilles[180], N.E.K. Gillwald[46], D.M. Gingrich[3,al], M.P. Giordani[66a,66c], P.F. Giraud[143], G. Giugliarelli[66a,66c], D. Giugni[68a], F. Giuli[73a,73b], S. Gkaitatzis[161], I. Gkialas[9,h], E.L. Gkougkousis[14], P. Gkountoumis[10], L.K. Gladilin[112], C. Glasman[98], G.R. Gledhill[130], I. Gnesi[41b,c], M. Goblirsch-Kolb[26], D. Godin[109], S. Goldfarb[104], T. Golling[54], D. Golubkov[122], A. Gomes[138a,138b], R. Goncalves Gama[53], R. Gonçalo[138a,138c], G. Gonella[130], L. Gonella[21], A. Gongadze[79], F. Gonnella[21], J.L. Gonski[39], S. González de la Hoz[172], S. Gonzalez Fernandez[14], R. Gonzalez Lopez[90], C. Gonzalez Renteria[18], R. Gonzalez Suarez[170], S. Gonzalez-Sevilla[54], G.R. Gonzalvo Rodriguez[172], L. Goossens[36], N.A. Gorasia[21], P.A. Gorbounov[123], H.A. Gordon[29], B. Gorini[36], E. Gorini[67a,67b], A. Gorišek[91], A.T. Goshaw[49], M.I. Gostkin[79], C.A. Gottardo[118], M. Gouighri[35b], A.G. Goussiou[147], N. Govender[33c], C. Goy[5], I. Grabowska-Bold[83a], E. Gramstad[132], S. Grancagnolo[19], M. Grandi[155], V. Gratchev[136], P.M. Gravila[27f], F.G. Gravili[67a,67b], C. Gray[57], H.M. Gray[18], C. Grefe[24], I.M. Gregor[46], P. Grenier[152], K. Grevtsov[46], C. Grieco[14], N.A. Grieser[127], A.A. Grillo[144], K. Grimm[31,l], S. Grinstein[14,x], J.-F. Grivaz[64], S. Groh[99], E. Gross[178], J. Grosse-Knetter[53], Z.J. Grout[94], C. Grud[105], A. Grummer[117], J.C. Grundy[133], L. Guan[105], W. Guan[179], C. Gubbels[173], J. Guenther[36], J.G.R. Guerrero Rojas[172], F. Guescini[114], D. Guest[76,19], R. Gugel[99], A. Guida[46], T. Guillemin[5], S. Guindon[36], J. Guo[60c], Z. Guo[101], R. Gupta[46], S. Gurbuz[24], G. Gustavino[127], M. Guth[52], P. Gutierrez[127], L.F. Gutierrez Zagazeta[135], C. Gutschow[94], C. Guyot[143], C. Gwenlan[133], C.B. Gwilliam[90], E.S. Haaland[132], A. Haas[124], C. Haber[18], H.K. Hadavand[8], A. Hadef[99], M. Haleem[175], J. Haley[128], J.J. Hall[148], G. Halladjian[106], G.D. Hallewell[101], K. Hamano[174], H. Hamdaoui[35f], M. Hamer[24], G.N. Hamity[50], K. Han[60a], L. Han[15c], L. Han[60a], S. Han[18], Y.F. Han[165], K. Hanagaki[81,v], M. Hance[144], M.D. Hank[37], R. Hankache[100], E. Hansen[96], J.B. Hansen[40], J.D. Hansen[40], M.C. Hansen[24], P.H. Hansen[40], E.C. Hanson[100], K. Hara[167], T. Harenberg[180], S. Harkusha[107], P.F. Harrison[176], N.M. Hartman[152], N.M. Hartmann[113], Y. Hasegawa[149], A. Hasib[50], S. Hassani[143], S. Haug[20], R. Hauser[106], M. Havranek[140], C.M. Hawkes[21], R.J. Hawkings[36], S. Hayashida[116], D. Hayden[106], C. Hayes[105], R.L. Hayes[173], C.P. Hays[133], J.M. Hays[92], H.S. Hayward[90], S.J. Haywood[142], F. He[60a], Y. He[163], M.P. Heath[50], V. Hedberg[96], A.L. Heggelund[132], N.D. Hehir[92], C. Heidegger[52], K.K. Heidegger[52], W.D. Heidorn[78], J. Heilman[34], S. Heim[46], T. Heim[18], B. Heinemann[46,aj], J.G. Heinlein[135], J.J. Heinrich[130], L. Heinrich[36], J. Hejbal[139], L. Helary[46], A. Held[124], S. Hellesund[132], C.M. Helling[144], S. Hellman[45a,45b], C. Helsens[36], R.C.W. Henderson[89], L. Henkelmann[32], A.M. Henriques Correia[36], H. Herde[152], Y. Hernández Jiménez[33f], H. Herr[99], M.G. Herrmann[113], T. Herrmann[48], G. Herten[52], R. Hertenberger[113], L. Hervas[36], N.P. Hessey[166a], H. Hibi[82], S. Higashino[81], E. Higón-Rodriguez[172], K. Hildebrand[37], K.K. Hill[29], K.H. Hiller[46], S.J. Hillier[21], M. Hils[48], I. Hinchliffe[18], F. Hinterkeuser[24], M. Hirose[131], S. Hirose[167], D. Hirschbuehl[180], B. Hiti[91], O. Hladik[139], J. Hobbs[154], R. Hobincu[27e], N. Hod[178], M.C. Hodgkinson[148], A. Hoecker[36], D. Hohn[52], D. Hohov[64], T. Holm[24], T.R. Holmes[37], M. Holzbock[114], L.B.A.H. Hommels[32], T.M. Hong[137], J.C. Honig[52], A. Hönle[114], B.H. Hooberman[171], W.H. Hopkins[6], Y. Horii[116], P. Horn[48], L.A. Horyn[37], S. Hou[157], J. Howarth[57], J. Hoya[88], M. Hrabovsky[129], A. Hrynevich[108], T. Hryn'ova[5], P.J. Hsu[63], S.-C. Hsu[147], Q. Hu[39], S. Hu[60c], Y.F. Hu[15a,15d,an], D.P. Huang[94], X. Huang[15c], Y. Huang[60a], Y. Huang[15a], Z. Hubacek[140],

JHEP05(2021)093

F. Hubaut[101], M. Huebner[24], F. Huegging[24], T.B. Huffman[133], M. Huhtinen[36], R. Hulsken[58], R.F.H. Hunter[34], N. Huseynov[79,ac], J. Huston[106], J. Huth[59], R. Hyneman[152], S. Hyrych[28a], G. Iacobucci[54], G. Iakovidis[29], I. Ibragimov[150], L. Iconomidou-Fayard[64], P. Iengo[36], R. Ignazzi[40], R. Iguchi[162], T. Iizawa[54], Y. Ikegami[81], N. Ilic[165,165], H. Imam[35a], G. Introzzi[70a,70b], M. Iodice[74a], K. Iordanidou[166a], V. Ippolito[72a,72b], M.F. Isacson[170], M. Ishino[162], W. Islam[128], C. Issever[19,46], S. Istin[12c], J.M. Iturbe Ponce[62a], R. Iuppa[75a,75b], A. Ivina[178], J.M. Izen[43], V. Izzo[69a], P. Jacka[139], P. Jackson[1], R.M. Jacobs[46], B.P. Jaeger[151], G. Jäkel[180], K.B. Jakobi[99], K. Jakobs[52], T. Jakoubek[178], J. Jamieson[57], K.W. Janas[83a], P.A. Janus[83a], G. Jarlskog[96], A.E. Jaspan[90], N. Javadov[79,ac], T. Javůrek[36], M. Javurkova[102], F. Jeanneau[143], L. Jeanty[130], J. Jejelava[158a], P. Jenni[52,d], S. Jézéquel[5], J. Jia[154], Z. Jia[15c], Y. Jiang[60a], S. Jiggins[52], F.A. Jimenez Morales[38], J. Jimenez Pena[114], S. Jin[15c], A. Jinaru[27b], O. Jinnouchi[163], H. Jivan[33f], P. Johansson[148], K.A. Johns[7], C.A. Johnson[65], E. Jones[176], R.W.L. Jones[89], T.J. Jones[90], J. Jovicevic[36], X. Ju[18], J.J. Junggeburth[114], A. Juste Rozas[14,x], A. Kaczmarska[84], M. Kado[72a,72b], H. Kagan[126], M. Kagan[152], A. Kahn[39], C. Kahra[99], T. Kaji[177], E. Kajomovitz[159], C.W. Kalderon[29], A. Kaluza[99], A. Kamenshchikov[122], M. Kaneda[162], N.J. Kang[144], S. Kang[78], Y. Kano[116], J. Kanzaki[81], D. Kar[33f], K. Karava[133], M.J. Kareem[166b], I. Karkanias[161], S.N. Karpov[79], Z.M. Karpova[79], V. Kartvelishvili[89], A.N. Karyukhin[122], E. Kasimi[161], C. Kato[60d], J. Katzy[46], K. Kawade[149], K. Kawagoe[87], T. Kawaguchi[116], T. Kawamoto[143], G. Kawamura[53], E.F. Kay[174], F.I. Kaya[168], S. Kazakos[14], V.F. Kazanin[121b,121a], Y. Ke[154], J.M. Keaveney[33a], R. Keeler[174], J.S. Keller[34], D. Kelsey[155], J.J. Kempster[21], J. Kendrick[21], K.E. Kennedy[39], O. Kepka[139], S. Kersten[180], B.P. Kerševan[91], S. Ketabchi Haghighat[165], F. Khalil-Zada[13], M. Khandoga[143], A. Khanov[128], A.G. Kharlamov[121b,121a], T. Kharlamova[121b,121a], E.E. Khoda[173], T.J. Khoo[76,19], G. Khoriauli[175], E. Khramov[79], J. Khubua[158b], S. Kido[82], M. Kiehn[36], A. Kilgallon[130], E. Kim[163], Y.K. Kim[37], N. Kimura[94], A. Kirchhoff[53], D. Kirchmeier[48], J. Kirk[142], A.E. Kiryunin[114], T. Kishimoto[162], D.P. Kisliuk[165], V. Kitali[46], C. Kitsaki[10], O. Kivernyk[24], T. Klapdor-Kleingrothaus[52], M. Klassen[61a], C. Klein[34], L. Klein[175], M.H. Klein[105], M. Klein[90], U. Klein[90], P. Klimek[36], A. Klimentov[29], F. Klimpel[36], T. Klingl[24], T. Klioutchnikova[36], F.F. Klitzner[113], P. Kluit[119], S. Kluth[114], E. Kneringer[76], A. Knue[52], D. Kobayashi[87], M. Kobel[48], M. Kocian[152], T. Kodama[162], P. Kodys[141], D.M. Koeck[155], P.T. Koenig[24], T. Koffas[34], N.M. Köhler[36], M. Kolb[143], I. Koletsou[5], T. Komarek[129], K. Köneke[52], A.X.Y. Kong[1], T. Kono[125], V. Konstantinides[94], N. Konstantinidis[94], B. Konya[96], R. Kopeliansky[65], S. Koperny[83a], K. Korcyl[84], K. Kordas[161], G. Koren[160], A. Korn[94], I. Korolkov[14], E.V. Korolkova[148], N. Korotkova[112], O. Kortner[114], S. Kortner[114], V.V. Kostyukhin[148,164], A. Kotsokechagia[64], A. Kotwal[49], A. Koulouris[10], A. Kourkoumeli-Charalampidi[70a,70b], C. Kourkoumelis[9], E. Kourlitis[6], R. Kowalewski[174], W. Kozanecki[143], A.S. Kozhin[122], V.A. Kramarenko[112], G. Kramberger[91], D. Krasnopevtsev[60a], M.W. Krasny[134], A. Krasznahorkay[36], J.A. Kremer[99], J. Kretzschmar[90], K. Kreul[19], P. Krieger[165], F. Krieter[113], S. Krishnamurthy[102], A. Krishnan[61b], M. Krivos[141], K. Krizka[18], K. Kroeninger[47], H. Kroha[114], J. Kroll[139], J. Kroll[135], K.S. Krowpman[106], U. Kruchonak[79], H. Krüger[24], N. Krumnack[78], M.C. Kruse[49], J.A. Krzysiak[84], A. Kubota[163], O. Kuchinskaia[164], S. Kuday[4b], D. Kuechler[46], J.T. Kuechler[46], S. Kuehn[36], T. Kuhl[46], V. Kukhtin[79], Y. Kulchitsky[107,af], S. Kuleshov[145b], M. Kumar[33f], M. Kuna[58], A. Kupco[139], T. Kupfer[47], O. Kuprash[52], H. Kurashige[82], L.L. Kurchaninov[166a], Y.A. Kurochkin[107], A. Kurova[111], M.G. Kurth[15a,15d], E.S. Kuwertz[36], M. Kuze[163], A.K. Kvam[147], J. Kvita[129], T. Kwan[103], C. Lacasta[172], F. Lacava[72a,72b], D.P.J. Lack[100], H. Lacker[19], D. Lacour[134], E. Ladygin[79], R. Lafaye[5], B. Laforge[134], T. Lagouri[145c], S. Lai[53], I.K. Lakomiec[83a], J.E. Lambert[127], S. Lammers[65], W. Lampl[7], C. Lampoudis[161], E. Lançon[29], U. Landgraf[52], M.P.J. Landon[92], V.S. Lang[52], J.C. Lange[53], R.J. Langenberg[102], A.J. Lankford[169], F. Lanni[29], K. Lantzsch[24], A. Lanza[70a], A. Lapertosa[55b,55a], J.F. Laporte[143], T. Lari[68a], F. Lasagni Manghi[23b,23a], M. Lassnig[36], V. Latonova[139], T.S. Lau[62a], A. Laudrain[99], A. Laurier[34],

JHEP05(2021)093

M. Lavorgna[69a,69b], S.D. Lawlor[93], M. Lazzaroni[68a,68b], B. Le[100], A. Lebedev[78], M. LeBlanc[7], T. LeCompte[6], F. Ledroit-Guillon[58], A.C.A. Lee[94], C.A. Lee[29], G.R. Lee[17], L. Lee[59], S.C. Lee[157], S. Lee[78], L.L. Leeuw[33c], B. Lefebvre[166a], H.P. Lefebvre[93], M. Lefebvre[174], C. Leggett[18], K. Lehmann[151], N. Lehmann[20], G. Lehmann Miotto[36], W.A. Leight[46], A. Leisos[161,w], M.A.L. Leite[80c], C.E. Leitgeb[113], R. Leitner[141], K.J.C. Leney[42], T. Lenz[24], S. Leone[71a], C. Leonidopoulos[50], A. Leopold[134], C. Leroy[109], R. Les[106], C.G. Lester[32], M. Levchenko[136], J. Levêque[5], D. Levin[105], L.J. Levinson[178], D.J. Lewis[21], B. Li[15b], B. Li[105], C-Q. Li[60c,60d], F. Li[60c], H. Li[60a], H. Li[60b], J. Li[60c], K. Li[147], L. Li[60c], M. Li[15a,15d], Q.Y. Li[60a], S. Li[60d,60c,b], X. Li[46], Y. Li[46], Z. Li[60b], Z. Li[133], Z. Li[103], Z. Li[90], Z. Liang[15a], M. Liberatore[46], B. Liberti[73a], K. Lie[62c], C.Y. Lin[32], K. Lin[106], R.A. Linck[65], R.E. Lindley[7], J.H. Lindon[21], A. Linss[46], A.L. Lionti[54], E. Lipeles[135], A. Lipniacka[17], T.M. Liss[171,ak], A. Lister[173], J.D. Little[8], B. Liu[15a], B.X. Liu[151], J.B. Liu[60a], J.K.K. Liu[37], K. Liu[60d,60c], M. Liu[60a], M.Y. Liu[60a], P. Liu[15a], X. Liu[60a], Y. Liu[46], Y. Liu[15a,15d], Y.L. Liu[105], Y.W. Liu[60a], M. Livan[70a,70b], A. Lleres[58], J. Llorente Merino[151], S.L. Lloyd[92], E.M. Lobodzinska[46], P. Loch[7], S. Loffredo[73a,73b], T. Lohse[19], K. Lohwasser[148], M. Lokajicek[139], J.D. Long[171], R.E. Long[89], I. Longarini[72a,72b], L. Longo[36], R. Longo[171], I. Lopez Paz[14], A. Lopez Solis[46], J. Lorenz[113], N. Lorenzo Martinez[5], A.M. Lory[113], A. Lösle[52], X. Lou[45a,45b], X. Lou[15a], A. Lounis[64], J. Love[6], P.A. Love[89], J.J. Lozano Bahilo[172], M. Lu[60a], S. Lu[135], Y.J. Lu[63], H.J. Lubatti[147], C. Luci[72a,72b], F.L. Lucio Alves[15c], A. Lucotte[58], F. Luehring[65], I. Luise[154], L. Luminari[72a], B. Lund-Jensen[153], N.A. Luongo[130], M.S. Lutz[160], D. Lynn[29], H. Lyons[90], R. Lysak[139], E. Lytken[96], F. Lyu[15a], V. Lyubushkin[79], T. Lyubushkina[79], H. Ma[29], L.L. Ma[60b], Y. Ma[94], D.M. Mac Donell[174], G. Maccarrone[51], C.M. Macdonald[148], J.C. MacDonald[148], J. Machado Miguens[135], R. Madar[38], W.F. Mader[48], M. Madugoda Ralalage Don[128], N. Madysa[48], J. Maeda[82], T. Maeno[29], M. Maerker[48], V. Magerl[52], J. Magro[66a,66c,r], D.J. Mahon[39], C. Maidantchik[80b], A. Maio[138a,138b,138d], K. Maj[83a], O. Majersky[28a], S. Majewski[130], N. Makovec[64], B. Malaescu[134], Pa. Malecki[84], V.P. Maleev[136], F. Malek[58], D. Malito[41b,41a], U. Mallik[77], C. Malone[32], S. Maltezos[10], S. Malyukov[79], J. Mamuzic[172], G. Mancini[51], J.P. Mandalia[92], I. Mandić[91], L. Manhaes de Andrade Filho[80a], I.M. Maniatis[161], J. Manjarres Ramos[48], K.H. Mankinen[96], A. Mann[113], A. Manousos[76], B. Mansoulie[143], I. Manthos[161], S. Manzoni[119], A. Marantis[161], L. Marchese[133], G. Marchiori[134], M. Marcisovsky[139], L. Marcoccia[73a,73b], C. Marcon[96], M. Marjanovic[127], Z. Marshall[18], M.U.F. Martensson[170], S. Marti-Garcia[172], T.A. Martin[176], V.J. Martin[50], B. Martin dit Latour[17], L. Martinelli[74a,74b], M. Martinez[14,x], P. Martinez Agullo[172], V.I. Martinez Outschoorn[102], S. Martin-Haugh[142], V.S. Martoiu[27b], A.C. Martyniuk[94], A. Marzin[36], S.R. Maschek[114], L. Masetti[99], T. Mashimo[162], R. Mashinistov[110], J. Masik[100], A.L. Maslennikov[121b,121a], L. Massa[23b,23a], P. Massarotti[69a,69b], P. Mastrandrea[71a,71b], A. Mastroberardino[41b,41a], T. Masubuchi[162], D. Matakias[29], T. Mathisen[170], A. Matic[113], N. Matsuzawa[162], J. Maurer[27b], B. Maček[91], D.A. Maximov[121b,121a], R. Mazini[157], I. Maznas[161], S.M. Mazza[144], C. Mc Ginn[29], J.P. Mc Gowan[103], S.P. Mc Kee[105], T.G. McCarthy[114], W.P. McCormack[18], E.F. McDonald[104], A.E. McDougall[119], J.A. Mcfayden[18], G. Mchedlidze[158b], M.A. McKay[42], K.D. McLean[174], S.J. McMahon[142], P.C. McNamara[104], R.A. McPherson[174,ab], J.E. Mdhluli[33f], Z.A. Meadows[102], S. Meehan[36], T. Megy[38], S. Mehlhase[113], A. Mehta[90], B. Meirose[43], D. Melini[159], B.R. Mellado Garcia[33f], F. Meloni[46], A. Melzer[24], E.D. Mendes Gouveia[138a,138e], A.M. Mendes Jacques Da Costa[21], H.Y. Meng[165], L. Meng[36], S. Menke[114], E. Meoni[41b,41a], S.A.M. Merkt[137], C. Merlassino[133], P. Mermod[54,*], L. Merola[69a,69b], C. Meroni[68a], G. Merz[105], O. Meshkov[112,110], J.K.R. Meshreki[150], J. Metcalfe[6], A.S. Mete[6], C. Meyer[65], J-P. Meyer[143], M. Michetti[19], R.P. Middleton[142], L. Mijović[50], G. Mikenberg[178], M. Mikestikova[139], M. Mikuž[91], H. Mildner[148], A. Milic[165], C.D. Milke[42], D.W. Miller[37], L.S. Miller[34], A. Milov[178], D.A. Milstead[45a,45b], A.A. Minaenko[122], I.A. Minashvili[158b], L. Mince[57], A.I. Mincer[124], B. Mindur[83a], M. Mineev[79], Y. Minegishi[162], Y. Mino[85], L.M. Mir[14],

JHEP05(2021)093

M. Mironova[133], T. Mitani[177], J. Mitrevski[113], V.A. Mitsou[172], M. Mittal[60c], O. Miu[165], A. Miucci[20], P.S. Miyagawa[92], A. Mizukami[81], J.U. Mjörnmark[96], T. Mkrtchyan[61a], M. Mlynarikova[120], T. Moa[45a,45b], S. Mobius[53], K. Mochizuki[109], P. Moder[46], P. Mogg[113], S. Mohapatra[39], G. Mokgatitswane[33f], B. Mondal[150], S. Mondal[140], K. Mönig[46], E. Monnier[101], A. Montalbano[151], J. Montejo Berlingen[36], M. Montella[94], F. Monticelli[88], N. Morange[64], A.L. Moreira De Carvalho[138a], M. Moreno Llácer[172], C. Moreno Martinez[14], P. Morettini[55b], M. Morgenstern[159], S. Morgenstern[176], D. Mori[151], M. Morii[59], M. Morinaga[177], V. Morisbak[132], A.K. Morley[36], A.P. Morris[94], L. Morvaj[36], P. Moschovakos[36], B. Moser[119], M. Mosidze[158b], T. Moskalets[143], P. Moskvitina[118], J. Moss[31,n], E.J.W. Moyse[102], S. Muanza[101], J. Mueller[137], D. Muenstermann[89], G.A. Mullier[96], J.J. Mullin[135], D.P. Mungo[68a,68b], J.L. Munoz Martinez[14], F.J. Munoz Sanchez[100], P. Murin[28b], W.J. Murray[176,142], A. Murrone[68a,68b], J.M. Muse[127], M. Muškinja[18], C. Mwewa[33a], A.G. Myagkov[122,ag], A.A. Myers[137], G. Myers[65], J. Myers[130], M. Myska[140], B.P. Nachman[18], O. Nackenhorst[47], A.Nag Nag[48], K. Nagai[133], K. Nagano[81], J.L. Nagle[29], E. Nagy[101], A.M. Nairz[36], Y. Nakahama[116], K. Nakamura[81], H. Nanjo[131], F. Napolitano[61a], R.F. Naranjo Garcia[46], R. Narayan[42], I. Naryshkin[136], M. Naseri[34], T. Naumann[46], G. Navarro[22a], J. Navarro-Gonzalez[172], P.Y. Nechaeva[110], F. Nechansky[46], T.J. Neep[21], A. Negri[70a,70b], M. Negrini[23b], C. Nellist[118], C. Nelson[103], K. Nelson[105], M.E. Nelson[45a,45b], S. Nemecek[139], M. Nessi[36,f], M.S. Neubauer[171], F. Neuhaus[99], M. Neumann[180], R. Newhouse[173], P.R. Newman[21], C.W. Ng[137], Y.S. Ng[19], Y.W.Y. Ng[169], B. Ngair[35f], H.D.N. Nguyen[101], T. Nguyen Manh[109], E. Nibigira[38], R.B. Nickerson[133], R. Nicolaidou[143], D.S. Nielsen[40], J. Nielsen[144], M. Niemeyer[53], N. Nikiforou[11], V. Nikolaenko[122,ag], I. Nikolic-Audit[134], K. Nikolopoulos[21], P. Nilsson[29], H.R. Nindhito[54], A. Nisati[72a], N. Nishu[60c], R. Nisius[114], T. Nitta[177], T. Nobe[162], D.L. Noel[32], Y. Noguchi[85], I. Nomidis[134], M.A. Nomura[29], R.R.B. Norisam[94], J. Novak[91], T. Novak[46], O. Novgorodova[48], R. Novotny[117], L. Nozka[129], K. Ntekas[169], E. Nurse[94], F.G. Oakham[34,al], J. Ocariz[134], A. Ochi[82], I. Ochoa[138a], J.P. Ochoa-Ricoux[145a], K. O'Connor[26], S. Odaka[81], S. Oerdek[53], A. Ogrodnik[83a], A. Oh[100], C.C. Ohm[153], H. Oide[163], R. Oishi[162], M.L. Ojeda[165], Y. Okazaki[85], M.W. O'Keefe[90], Y. Okumura[162], A. Olariu[27b], L.F. Oleiro Seabra[138a], S.A. Olivares Pino[145a], D. Oliveira Damazio[29], J.L. Oliver[1], M.J.R. Olsson[169], A. Olszewski[84], J. Olszowska[84], Ö.O. Öncel[24], D.C. O'Neil[151], A.P. O'neill[133], A. Onofre[138a,138e], P.U.E. Onyisi[11], H. Oppen[132], R.G. Oreamuno Madriz[120], M.J. Oreglia[37], G.E. Orellana[88], D. Orestano[74a,74b], N. Orlando[14], R.S. Orr[165], V. O'Shea[57], R. Ospanov[60a], G. Otero y Garzon[30], H. Otono[87], P.S. Ott[61a], G.J. Ottino[18], M. Ouchrif[35e], J. Ouellette[29], F. Ould-Saada[132], A. Ouraou[143,*], Q. Ouyang[15a], M. Owen[57], R.E. Owen[142], V.E. Ozcan[12c], N. Ozturk[8], J. Pacalt[129], H.A. Pacey[32], K. Pachal[49], A. Pacheco Pages[14], C. Padilla Aranda[14], S. Pagan Griso[18], G. Palacino[65], S. Palazzo[50], S. Palestini[36], M. Palka[83b], P. Palni[83a], D.K. Panchal[11], C.E. Pandini[54], J.G. Panduro Vazquez[93], P. Pani[46], G. Panizzo[66a,66c], L. Paolozzi[54], C. Papadatos[109], S. Parajuli[42], A. Paramonov[6], C. Paraskevopoulos[10], D. Paredes Hernandez[62b], S.R. Paredes Saenz[133], B. Parida[178], T.H. Park[165], A.J. Parker[31], M.A. Parker[32], F. Parodi[55b,55a], E.W. Parrish[120], J.A. Parsons[39], U. Parzefall[52], L. Pascual Dominguez[134], V.R. Pascuzzi[18], J.M.P. Pasner[144], F. Pasquali[119], E. Pasqualucci[72a], S. Passaggio[55b], F. Pastore[93], P. Pasuwan[45a,45b], J.R. Pater[100], A. Pathak[179,j], J. Patton[90], T. Pauly[36], J. Pearkes[152], M. Pedersen[132], L. Pedraza Diaz[118], R. Pedro[138a], T. Peiffer[53], S.V. Peleganchuk[121b,121a], O. Penc[139], C. Peng[62b], H. Peng[60a], M. Penzin[164], B.S. Peralva[80a], M.M. Perego[64], A.P. Pereira Peixoto[138a], L. Pereira Sanchez[45a,45b], D.V. Perepelitsa[29], E. Perez Codina[166a], L. Perini[68a,68b], H. Pernegger[36], S. Perrella[36], A. Perrevoort[119], K. Peters[46], R.F.Y. Peters[100], B.A. Petersen[36], T.C. Petersen[40], E. Petit[101], V. Petousis[140], C. Petridou[161], P. Petroff[64], F. Petrucci[74a,74b], M. Pettee[181], N.E. Pettersson[102], K. Petukhova[141], A. Peyaud[143], R. Pezoa[145d], L. Pezzotti[70a,70b], G. Pezzullo[181], T. Pham[104], P.W. Phillips[142], M.W. Phipps[171], G. Piacquadio[154], E. Pianori[18], A. Picazio[102], R. Piegaia[30],

JHEP05(2021)093

D. Pietreanu[27b], J.E. Pilcher[37], A.D. Pilkington[100], M. Pinamonti[66a,66c], J.L. Pinfold[3], C. Pitman Donaldson[94], L. Pizzimento[73a,73b], A. Pizzini[119], M.-A. Pleier[29], V. Plesanovs[52], V. Pleskot[141], E. Plotnikova[79], P. Podberezko[121b,121a], R. Poettgen[96], R. Poggi[54], L. Poggioli[134], I. Pogrebnyak[106], D. Pohl[24], I. Pokharel[53], G. Polesello[70a], A. Poley[151,166a], A. Policicchio[72a,72b], R. Polifka[141], A. Polini[23b], C.S. Pollard[46], V. Polychronakos[29], D. Ponomarenko[111], L. Pontecorvo[36], S. Popa[27a], G.A. Popeneciu[27d], L. Portales[5], D.M. Portillo Quintero[58], S. Pospisil[140], P. Postolache[27c], K. Potamianos[133], I.N. Potrap[79], C.J. Potter[32], H. Potti[11], T. Poulsen[96], J. Poveda[172], T.D. Powell[148], G. Pownall[46], M.E. Pozo Astigarraga[36], A. Prades Ibanez[172], P. Pralavorio[101], M.M. Prapa[44], S. Prell[78], D. Price[100], M. Primavera[67a], M.L. Proffitt[147], N. Proklova[111], K. Prokofiev[62c], F. Prokoshin[79], S. Protopopescu[29], J. Proudfoot[6], M. Przybycien[83a], D. Pudzha[136], A. Puri[171], P. Puzo[64], D. Pyatiizbyantseva[111], J. Qian[105], Y. Qin[100], A. Quadt[53], M. Queitsch-Maitland[36], G. Rabanal Bolanos[59], F. Ragusa[68a,68b], G. Rahal[97], J.A. Raine[54], S. Rajagopalan[29], K. Ran[15a,15d], D.F. Rassloff[61a], D.M. Rauch[46], S. Rave[99], B. Ravina[57], I. Ravinovich[178], M. Raymond[36], A.L. Read[132], N.P. Readioff[148], M. Reale[67a,67b], D.M. Rebuzzi[70a,70b], G. Redlinger[29], K. Reeves[43], D. Reikher[160], A. Reiss[99], A. Rej[150], C. Rembser[36], A. Renardi[46], M. Renda[27b], M.B. Rendel[114], A.G. Rennie[57], S. Resconi[68a], E.D. Resseguie[18], S. Rettie[94], B. Reynolds[126], E. Reynolds[21], O.L. Rezanova[121b,121a], P. Reznicek[141], E. Ricci[75a,75b], R. Richter[114], S. Richter[46], E. Richter-Was[83b], M. Ridel[134], P. Rieck[114], O. Rifki[46], M. Rijssenbeek[154], A. Rimoldi[70a,70b], M. Rimoldi[46], L. Rinaldi[23b], T.T. Rinn[171], G. Ripellino[153], I. Riu[14], P. Rivadeneira[46], J.C. Rivera Vergara[174], F. Rizatdinova[128], E. Rizvi[92], C. Rizzi[36], S.H. Robertson[103,ab], M. Robin[46], D. Robinson[32], C.M. Robles Gajardo[145d], M. Robles Manzano[99], A. Robson[57], A. Rocchi[73a,73b], C. Roda[71a,71b], S. Rodriguez Bosca[172], A. Rodriguez Rodriguez[52], A.M. Rodríguez Vera[166b], S. Roe[36], J. Roggel[180], O. Røhne[132], R.A. Rojas[145d], B. Roland[52], C.P.A. Roland[65], J. Roloff[29], A. Romaniouk[111], M. Romano[23b,23a], N. Rompotis[90], M. Ronzani[124], L. Roos[134], S. Rosati[72a], G. Rosin[102], B.J. Rosser[135], E. Rossi[46], E. Rossi[5], E. Rossi[69a,69b], L.P. Rossi[55b], L. Rossini[46], R. Rosten[126], M. Rotaru[27b], B. Rottler[52], D. Rousseau[64], G. Rovelli[70a,70b], A. Roy[11], A. Rozanov[101], Y. Rozen[159], X. Ruan[33f], A.J. Ruby[90], T.A. Ruggeri[1], F. Rühr[52], A. Ruiz-Martinez[172], A. Rummler[36], Z. Rurikova[52], N.A. Rusakovich[79], H.L. Russell[36], L. Rustige[38], J.P. Rutherfoord[7], E.M. Rüttinger[148], M. Rybar[141], E.B. Rye[132], A. Ryzhov[122], J.A. Sabater Iglesias[46], P. Sabatini[172], L. Sabetta[72a,72b], H.F-W. Sadrozinski[144], R. Sadykov[79], F. Safai Tehrani[72a], B. Safarzadeh Samani[155], M. Safdari[152], P. Saha[120], S. Saha[103], M. Sahinsoy[114], A. Sahu[180], M. Saimpert[36], M. Saito[162], T. Saito[162], D. Salamani[54], G. Salamanna[74a,74b], A. Salnikov[152], J. Salt[172], A. Salvador Salas[14], D. Salvatore[41b,41a], F. Salvatore[155], A. Salzburger[36], D. Sammel[52], D. Sampsonidis[161], D. Sampsonidou[60d,60c], J. Sánchez[172], A. Sanchez Pineda[66a,36,66c], H. Sandaker[132], C.O. Sander[46], I.G. Sanderswood[89], M. Sandhoff[180], C. Sandoval[22b], D.P.C. Sankey[142], M. Sannino[55b,55a], Y. Sano[116], A. Sansoni[51], C. Santoni[38], H. Santos[138a,138b], S.N. Santpur[18], A. Santra[178], K.A. Saoucha[148], A. Sapronov[79], J.G. Saraiva[138a,138d], O. Sasaki[81], K. Sato[167], F. Sauerburger[52], E. Sauvan[5], P. Savard[165,al], R. Sawada[162], C. Sawyer[142], L. Sawyer[95], I. Sayago Galvan[172], C. Sbarra[23b], A. Sbrizzi[66a,66c], T. Scanlon[94], J. Schaarschmidt[147], P. Schacht[114], D. Schaefer[37], L. Schaefer[135], U. Schäfer[99], A.C. Schaffer[64], D. Schaile[113], R.D. Schamberger[154], E. Schanet[113], C. Scharf[19], N. Scharmberg[100], V.A. Schegelsky[136], D. Scheirich[141], F. Schenck[19], M. Schernau[169], C. Schiavi[55b,55a], L.K. Schildgen[24], Z.M. Schillaci[26], E.J. Schioppa[67a,67b], M. Schioppa[41b,41a], K.E. Schleicher[52], S. Schlenker[36], K.R. Schmidt-Sommerfeld[114], K. Schmieden[99], C. Schmitt[99], S. Schmitt[46], L. Schoeffel[143], A. Schoening[61b], P.G. Scholer[52], E. Schopf[133], M. Schott[99], J. Schovancova[36], S. Schramm[54], F. Schroeder[180], A. Schulte[99], H-C. Schultz-Coulon[61a], M. Schumacher[52], B.A. Schumm[144], Ph. Schune[143], A. Schwartzman[152], T.A. Schwarz[105], Ph. Schwemling[143], R. Schwienhorst[106], A. Sciandra[144], G. Sciolla[26], F. Scuri[71a], F. Scutti[104],

JHEP05(2021)093

C.D. Sebastiani[90], K. Sedlaczek[47], P. Seema[19], S.C. Seidel[117], A. Seiden[144], B.D. Seidlitz[29], T. Seiss[37], C. Seitz[46], J.M. Seixas[80b], G. Sekhniaidze[69a], S.J. Sekula[42], N. Semprini-Cesari[23b,23a], S. Sen[49], C. Serfon[29], L. Serin[64], L. Serkin[66a,66b], M. Sessa[60a], H. Severini[127], S. Sevova[152], F. Sforza[55b,55a], A. Sfyrla[54], E. Shabalina[53], J.D. Shahinian[135], N.W. Shaikh[45a,45b], D. Shaked Renous[178], L.Y. Shan[15a], M. Shapiro[18], A. Sharma[36], A.S. Sharma[1], P.B. Shatalov[123], K. Shaw[155], S.M. Shaw[100], M. Shehade[178], Y. Shen[127], P. Sherwood[94], L. Shi[94], C.O. Shimmin[181], Y. Shimogama[177], M. Shimojima[115], J.D. Shinner[93], I.P.J. Shipsey[133], S. Shirabe[163], M. Shiyakova[79,z], J. Shlomi[178], M.J. Shochet[37], J. Shojaii[104], D.R. Shope[153], S. Shrestha[126], E.M. Shrif[33f], M.J. Shroff[174], E. Shulga[178], P. Sicho[139], A.M. Sickles[171], E. Sideras Haddad[33f], O. Sidiropoulou[36], A. Sidoti[23b,23a], F. Siegert[48], Dj. Sijacki[16], M.V. Silva Oliveira[36], S.B. Silverstein[45a], S. Simion[64], R. Simoniello[36], S. Simsek[12b], P. Sinervo[165], V. Sinetckii[112], S. Singh[151], S. Sinha[33f], M. Sioli[23b,23a], I. Siral[130], S.Yu. Sivoklokov[112], J. Sjölin[45a,45b], A. Skaf[53], E. Skorda[96], P. Skubic[127], M. Slawinska[84], K. Sliwa[168], V. Smakhtin[178], B.H. Smart[142], J. Smiesko[141], S.Yu. Smirnov[111], Y. Smirnov[111], L.N. Smirnova[112,s], O. Smirnova[96], E.A. Smith[37], H.A. Smith[133], M. Smizanska[89], K. Smolek[140], A. Smykiewicz[84], A.A. Snesarev[110], H.L. Snoek[119], I.M. Snyder[130], S. Snyder[29], R. Sobie[174,ab], A. Soffer[160], A. Søgaard[50], F. Sohns[53], C.A. Solans Sanchez[36], E.Yu. Soldatov[111], U. Soldevila[172], A.A. Solodkov[122], A. Soloshenko[79], O.V. Solovyanov[122], V. Solovyev[136], P. Sommer[148], H. Son[168], A. Sonay[14], W.Y. Song[166b], A. Sopczak[140], A.L. Sopio[94], F. Sopkova[28b], S. Sottocornola[70a,70b], R. Soualah[66a,66c], A.M. Soukharev[121b,121a], Z. Soumaimi[35f], D. South[46], S. Spagnolo[67a,67b], M. Spalla[114], M. Spangenberg[176], F. Spanò[93], D. Sperlich[52], T.M. Spieker[61a], G. Spigo[36], M. Spina[155], D.P. Spiteri[57], M. Spousta[141], A. Stabile[68a,68b], B.L. Stamas[120], R. Stamen[61a], M. Stamenkovic[119], A. Stampekis[21], E. Stanecka[84], B. Stanislaus[133], M.M. Stanitzki[46], M. Stankaityte[133], B. Stapf[119], E.A. Starchenko[122], G.H. Stark[144], J. Stark[58], P. Staroba[139], P. Starovoitov[61a], S. Stärz[103], R. Staszewski[84], G. Stavropoulos[44], P. Steinberg[29], A.L. Steinhebel[130], B. Stelzer[151,166a], H.J. Stelzer[137], O. Stelzer-Chilton[166a], H. Stenzel[56], T.J. Stevenson[155], G.A. Stewart[36], M.C. Stockton[36], G. Stoicea[27b], M. Stolarski[138a], S. Stonjek[114], A. Straessner[48], J. Strandberg[153], S. Strandberg[45a,45b], M. Strauss[127], T. Strebler[101], P. Strizenec[28b], R. Ströhmer[175], D.M. Strom[130], R. Stroynowski[42], A. Strubig[45a,45b], S.A. Stucci[29], B. Stugu[17], J. Stupak[127], N.A. Styles[46], D. Su[152], W. Su[60d,147,60c], X. Su[60a], N.B. Suarez[137], V.V. Sulin[110], M.J. Sullivan[90], D.M.S. Sultan[54], S. Sultansoy[4c], T. Sumida[85], S. Sun[105], X. Sun[100], C.J.E. Suster[156], M.R. Sutton[155], M. Svatos[139], M. Swiatlowski[166a], S.P. Swift[2], T. Swirski[175], A. Sydorenko[99], I. Sykora[28a], M. Sykora[141], T. Sykora[141], D. Ta[99], K. Tackmann[46,y], A. Taffard[169], R. Tafirout[166a], E. Tagiev[122], R.H.M. Taibah[134], R. Takashima[86], K. Takeda[82], T. Takeshita[149], E.P. Takeva[50], Y. Takubo[81], M. Talby[101], A.A. Talyshev[121b,121a], K.C. Tam[62b], N.M. Tamir[160], J. Tanaka[162], R. Tanaka[64], S. Tapia Araya[171], S. Tapprogge[99], A. Tarek Abouelfadl Mohamed[106], S. Tarem[159], K. Tariq[60b], G. Tarna[27b,e], G.F. Tartarelli[68a], P. Tas[141], M. Tasevsky[139], E. Tassi[41b,41a], G. Tateno[162], Y. Tayalati[35f], G.N. Taylor[104], W. Taylor[166b], H. Teagle[90], A.S. Tee[89], R. Teixeira De Lima[152], P. Teixeira-Dias[93], H. Ten Kate[36], J.J. Teoh[119], K. Terashi[162], J. Terron[98], S. Terzo[14], M. Testa[51], R.J. Teuscher[165,ab], N. Themistokleous[50], T. Theveneaux-Pelzer[19], D.W. Thomas[93], J.P. Thomas[21], E.A. Thompson[46], P.D. Thompson[21], E. Thomson[135], E.J. Thorpe[92], V.O. Tikhomirov[110,ah], Yu.A. Tikhonov[121b,121a], S. Timoshenko[111], P. Tipton[181], S. Tisserant[101], A. Tnourji[38], K. Todome[23b,23a], S. Todorova-Nova[141], S. Todt[48], J. Tojo[87], S. Tokár[28a], K. Tokushuku[81], E. Tolley[126], R. Tombs[32], M. Tomoto[81,116], L. Tompkins[152], P. Tornambe[102], E. Torrence[130], H. Torres[48], E. Torró Pastor[172], M. Toscani[30], C. Tosciri[37], J. Toth[101,aa], D.R. Tovey[148], A. Traeet[17], C.J. Treado[124], T. Trefzger[175], A. Tricoli[29], I.M. Trigger[166a], S. Trincaz-Duvoid[134], D.A. Trischuk[173], W. Trischuk[165], B. Trocmé[58], A. Trofymov[64], C. Troncon[68a], F. Trovato[155], L. Truong[33c], M. Trzebinski[84], A. Trzupek[84], F. Tsai[46],

JHEP05(2021)093

P.V. Tsiareshka[107,af], A. Tsirigotis[161,w], V. Tsiskaridze[154], E.G. Tskhadadze[158a], M. Tsopoulou[161], I.I. Tsukerman[123], V. Tsulaia[18], S. Tsuno[81], D. Tsybychev[154], Y. Tu[62b], A. Tudorache[27b], V. Tudorache[27b], A.N. Tuna[36], S. Turchikhin[79], D. Turgeman[178], I. Turk Cakir[4b,u], R.J. Turner[21], R. Turra[68a], P.M. Tuts[39], S. Tzamarias[161], E. Tzovara[99], K. Uchida[162], F. Ukegawa[167], G. Unal[36], M. Unal[11], A. Undrus[29], G. Unel[169], F.C. Ungaro[104], K. Uno[162], J. Urban[28b], P. Urquijo[104], G. Usai[8], Z. Uysal[12d], V. Vacek[140], B. Vachon[103], K.O.H. Vadla[132], T. Vafeiadis[36], C. Valderanis[113], E. Valdes Santurio[45a,45b], M. Valente[166a], S. Valentinetti[23b,23a], A. Valero[172], L. Valéry[46], R.A. Vallance[21], A. Vallier[36], J.A. Valls Ferrer[172], T.R. Van Daalen[14], P. Van Gemmeren[6], S. Van Stroud[94], I. Van Vulpen[119], M. Vanadia[73a,73b], W. Vandelli[36], M. Vandenbroucke[143], E.R. Vandewall[128], D. Vannicola[72a,72b], R. Vari[72a], E.W. Varnes[7], C. Varni[55b,55a], T. Varol[157], D. Varouchas[64], K.E. Varvell[156], M.E. Vasile[27b], G.A. Vasquez[174], F. Vazeille[38], D. Vazquez Furelos[14], T. Vazquez Schroeder[36], J. Veatch[53], V. Vecchio[100], M.J. Veen[119], L.M. Veloce[165], F. Veloso[138a,138c], S. Veneziano[72a], A. Ventura[67a,67b], A. Verbytskyi[114], M. Verducci[71a,71b], C. Vergis[24], W. Verkerke[119], A.T. Vermeulen[119], J.C. Vermeulen[119], C. Vernieri[152], P.J. Verschuuren[93], M.L. Vesterbacka[124], M.C. Vetterli[151,al], N. Viaux Maira[145d], T. Vickey[148], O.E. Vickey Boeriu[148], G.H.A. Viehhauser[133], L. Vigani[61b], M. Villa[23b,23a], M. Villaplana Perez[172], E.M. Villhauer[50], E. Vilucchi[51], M.G. Vincter[34], G.S. Virdee[21], A. Vishwakarma[50], C. Vittori[23b,23a], I. Vivarelli[155], M. Vogel[180], P. Vokac[140], J. Von Ahnen[46], S.E. von Buddenbrock[33f], E. Von Toerne[24], V. Vorobel[141], K. Vorobev[111], M. Vos[172], J.H. Vossebeld[90], M. Vozak[100], N. Vranjes[16], M. Vranjes Milosavljevic[16], V. Vrba[140,*], M. Vreeswijk[119], N.K. Vu[101], R. Vuillermet[36], I. Vukotic[37], S. Wada[167], C. Wagner[102], P. Wagner[24], W. Wagner[180], S. Wahdan[180], H. Wahlberg[88], R. Wakasa[167], V.M. Walbrecht[114], J. Walder[142], R. Walker[113], S.D. Walker[93], W. Walkowiak[150], V. Wallangen[45a,45b], A.M. Wang[59], A.Z. Wang[179], C. Wang[60a], C. Wang[60c], H. Wang[18], J. Wang[62a], P. Wang[42], R.-J. Wang[99], R. Wang[60a], R. Wang[120], S.M. Wang[157], S. Wang[60b], T. Wang[60a], W.T. Wang[60a], W.X. Wang[60a], Y. Wang[60a], Z. Wang[105], C. Wanotayaroj[36], A. Warburton[103], C.P. Ward[32], R.J. Ward[21], N. Warrack[57], A.T. Watson[21], M.F. Watson[21], G. Watts[147], B.M. Waugh[94], A.F. Webb[11], C. Weber[29], M.S. Weber[20], S.A. Weber[34], S.M. Weber[61a], Y. Wei[133], A.R. Weidberg[133], J. Weingarten[47], M. Weirich[99], C. Weiser[52], P.S. Wells[36], T. Wenaus[29], B. Wendland[47], T. Wengler[36], S. Wenig[36], N. Wermes[24], M. Wessels[61a], T.D. Weston[20], K. Whalen[130], A.M. Wharton[89], A.S. White[105], A. White[8], M.J. White[1], D. Whiteson[169], W. Wiedenmann[179], C. Wiel[48], M. Wielers[142], N. Wieseotte[99], C. Wiglesworth[40], L.A.M. Wiik-Fuchs[52], H.G. Wilkens[36], L.J. Wilkins[93], D.M. Williams[39], H.H. Williams[135], S. Williams[32], S. Willocq[102], P.J. Windischhofer[133], I. Wingerter-Seez[5], F. Winklmeier[130], B.T. Winter[52], M. Wittgen[152], M. Wobisch[95], A. Wolf[99], R. Wölker[133], J. Wollrath[52], M.W. Wolter[84], H. Wolters[138a,138c], V.W.S. Wong[173], A.F. Wongel[46], N.L. Woods[144], S.D. Worm[46], B.K. Wosiek[84], K.W. Woźniak[84], K. Wraight[57], S.L. Wu[179], X. Wu[54], Y. Wu[60a], J. Wuerzinger[133], T.R. Wyatt[100], B.M. Wynne[50], S. Xella[40], J. Xiang[62c], X. Xiao[105], X. Xie[60a], I. Xiotidis[155], D. Xu[15a], H. Xu[60a], H. Xu[60a], L. Xu[29], R. Xu[135], T. Xu[143], W. Xu[105], Y. Xu[15b], Z. Xu[60b], Z. Xu[152], B. Yabsley[156], S. Yacoob[33a], D.P. Yallup[94], N. Yamaguchi[87], Y. Yamaguchi[163], M. Yamatani[162], H. Yamauchi[167], T. Yamazaki[18], Y. Yamazaki[82], J. Yan[60c], Z. Yan[25], H.J. Yang[60c,60d], H.T. Yang[18], S. Yang[60a], T. Yang[62c], X. Yang[60a], X. Yang[15a], Y. Yang[162], Z. Yang[105,60a], W-M. Yao[18], Y.C. Yap[46], H. Ye[15c], J. Ye[42], S. Ye[29], I. Yeletskikh[79], M.R. Yexley[89], P. Yin[39], K. Yorita[177], K. Yoshihara[78], C.J.S. Young[36], C. Young[152], R. Yuan[60b,i], X. Yue[61a], M. Zaazoua[35f], B. Zabinski[84], G. Zacharis[10], E. Zaffaroni[54], J. Zahreddine[134], A.M. Zaitsev[122,ag], T. Zakareishvili[158b], N. Zakharchuk[34], S. Zambito[36], D. Zanzi[52], S.V. Zeißner[47], C. Zeitnitz[180], G. Zemaityte[133], J.C. Zeng[171], O. Zenin[122], T. Ženiš[28a], S. Zenz[92], S. Zerradi[35a], D. Zerwas[64], M. Zgubič[133], B. Zhang[15c], D.F. Zhang[15b], G. Zhang[15b], J. Zhang[6], K. Zhang[15a], L. Zhang[15c], L. Zhang[60a], M. Zhang[171], R. Zhang[179], S. Zhang[105], X. Zhang[60c], X. Zhang[60b], Z. Zhang[64], P. Zhao[49],

JHEP05(2021)093

Y. Zhao[144], Z. Zhao[60a], A. Zhemchugov[79], Z. Zheng[105], D. Zhong[171], B. Zhou[105], C. Zhou[179], H. Zhou[7], M. Zhou[154], N. Zhou[60c], Y. Zhou[7], C.G. Zhu[60b], C. Zhu[15a,15d], H.L. Zhu[60a], H. Zhu[15a], J. Zhu[105], Y. Zhu[60a], X. Zhuang[15a], K. Zhukov[110], V. Zhulanov[121b,121a], D. Zieminska[65], N.I. Zimine[79], S. Zimmermann[52,*], Z. Zinonos[114], M. Ziolkowski[150], L. Živković[16], A. Zoccoli[23b,23a], K. Zoch[53], T.G. Zorbas[148], R. Zou[37], W. Zou[39], L. Zwalinski[36]

[1] *Department of Physics, University of Adelaide, Adelaide, Australia*
[2] *Physics Department, SUNY Albany, Albany NY, U.S.A.*
[3] *Department of Physics, University of Alberta, Edmonton AB, Canada*
[4] [(a)] *Department of Physics, Ankara University, Ankara;* [(b)] *Istanbul Aydin University, Application and Research Center for Advanced Studies, Istanbul;* [(c)] *Division of Physics, TOBB University of Economics and Technology, Ankara, Turkey*
[5] *LAPP, Univ. Savoie Mont Blanc, CNRS/IN2P3, Annecy , France*
[6] *High Energy Physics Division, Argonne National Laboratory, Argonne IL, U.S.A.*
[7] *Department of Physics, University of Arizona, Tucson AZ, U.S.A.*
[8] *Department of Physics, University of Texas at Arlington, Arlington TX, U.S.A.*
[9] *Physics Department, National and Kapodistrian University of Athens, Athens, Greece*
[10] *Physics Department, National Technical University of Athens, Zografou, Greece*
[11] *Department of Physics, University of Texas at Austin, Austin TX, U.S.A.*
[12] [(a)] *Bahcesehir University, Faculty of Engineering and Natural Sciences, Istanbul;* [(b)] *Istanbul Bilgi University, Faculty of Engineering and Natural Sciences, Istanbul;* [(c)] *Department of Physics, Bogazici University, Istanbul;* [(d)] *Department of Physics Engineering, Gaziantep University, Gaziantep, Turkey*
[13] *Institute of Physics, Azerbaijan Academy of Sciences, Baku, Azerbaijan*
[14] *Institut de Física d'Altes Energies (IFAE), Barcelona Institute of Science and Technology, Barcelona, Spain*
[15] [(a)] *Institute of High Energy Physics, Chinese Academy of Sciences, Beijing;* [(b)] *Physics Department, Tsinghua University, Beijing;* [(c)] *Department of Physics, Nanjing University, Nanjing;* [(d)] *University of Chinese Academy of Science (UCAS), Beijing, China*
[16] *Institute of Physics, University of Belgrade, Belgrade, Serbia*
[17] *Department for Physics and Technology, University of Bergen, Bergen, Norway*
[18] *Physics Division, Lawrence Berkeley National Laboratory and University of California, Berkeley CA, U.S.A.*
[19] *Institut für Physik, Humboldt Universität zu Berlin, Berlin, Germany*
[20] *Albert Einstein Center for Fundamental Physics and Laboratory for High Energy Physics, University of Bern, Bern, Switzerland*
[21] *School of Physics and Astronomy, University of Birmingham, Birmingham, U.K.*
[22] [(a)] *Facultad de Ciencias y Centro de Investigaciónes, Universidad Antonio Nariño, Bogotá;* [(b)] *Departamento de Física, Universidad Nacional de Colombia, Bogotá, Colombia, Colombia*
[23] [(a)] *INFN Bologna and Universita' di Bologna, Dipartimento di Fisica;* [(b)] *INFN Sezione di Bologna, Italy*
[24] *Physikalisches Institut, Universität Bonn, Bonn, Germany*
[25] *Department of Physics, Boston University, Boston MA, U.S.A.*
[26] *Department of Physics, Brandeis University, Waltham MA, U.S.A.*
[27] [(a)] *Transilvania University of Brasov, Brasov;* [(b)] *Horia Hulubei National Institute of Physics and Nuclear Engineering, Bucharest;* [(c)] *Department of Physics, Alexandru Ioan Cuza University of Iasi, Iasi;* [(d)] *National Institute for Research and Development of Isotopic and Molecular Technologies, Physics Department, Cluj-Napoca;* [(e)] *University Politehnica Bucharest, Bucharest;* [(f)] *West University in Timisoara, Timisoara, Romania*
[28] [(a)] *Faculty of Mathematics, Physics and Informatics, Comenius University, Bratislava;* [(b)] *Department of Subnuclear Physics, Institute of Experimental Physics of the Slovak Academy of Sciences, Kosice, Slovak Republic*
[29] *Physics Department, Brookhaven National Laboratory, Upton NY, U.S.A.*

JHEP05(2021)093

[30] Departamento de Física, Universidad de Buenos Aires, Buenos Aires, Argentina
[31] California State University, CA, U.S.A.
[32] Cavendish Laboratory, University of Cambridge, Cambridge, U.K.
[33] [(a)] Department of Physics, University of Cape Town, Cape Town; [(b)] iThemba Labs, Western Cape; [(c)] Department of Mechanical Engineering Science, University of Johannesburg, Johannesburg; [(d)] National Institute of Physics, University of the Philippines Diliman; [(e)] University of South Africa, Department of Physics, Pretoria; [(f)] School of Physics, University of the Witwatersrand, Johannesburg, South Africa
[34] Department of Physics, Carleton University, Ottawa ON, Canada
[35] [(a)] Faculté des Sciences Ain Chock, Réseau Universitaire de Physique des Hautes Energies — Université Hassan II, Casablanca; [(b)] Faculté des Sciences, Université Ibn-Tofail, Kénitra; [(c)] Faculté des Sciences Semlalia, Université Cadi Ayyad, LPHEA-Marrakech; [(d)] Moroccan Foundation for Advanced Science Innovation and Research (MAScIR), Rabat; [(e)] LPMR, Faculté des Sciences, Université Mohamed Premier, Oujda; [(f)] Faculté des sciences, Université Mohammed V, Rabat, Morocco
[36] CERN, Geneva, Switzerland
[37] Enrico Fermi Institute, University of Chicago, Chicago IL, U.S.A.
[38] LPC, Université Clermont Auvergne, CNRS/IN2P3, Clermont-Ferrand, France
[39] Nevis Laboratory, Columbia University, Irvington NY, U.S.A.
[40] Niels Bohr Institute, University of Copenhagen, Copenhagen, Denmark
[41] [(a)] Dipartimento di Fisica, Università della Calabria, Rende; [(b)] INFN Gruppo Collegato di Cosenza, Laboratori Nazionali di Frascati, Italy
[42] Physics Department, Southern Methodist University, Dallas TX, U.S.A.
[43] Physics Department, University of Texas at Dallas, Richardson TX, U.S.A.
[44] National Centre for Scientific Research "Demokritos", Agia Paraskevi, Greece
[45] [(a)] Department of Physics, Stockholm University; [(b)] Oskar Klein Centre, Stockholm, Sweden
[46] Deutsches Elektronen-Synchrotron DESY, Hamburg and Zeuthen, Germany
[47] Lehrstuhl für Experimentelle Physik IV, Technische Universität Dortmund, Dortmund, Germany
[48] Institut für Kern und Teilchenphysik, Technische Universität Dresden, Dresden, Germany
[49] Department of Physics, Duke University, Durham NC, U.S.A.
[50] SUPA — School of Physics and Astronomy, University of Edinburgh, Edinburgh, U.K.
[51] INFN e Laboratori Nazionali di Frascati, Frascati, Italy
[52] Physikalisches Institut, Albert-Ludwigs-Universität Freiburg, Freiburg, Germany
[53] II. Physikalisches Institut, Georg-August-Universität Göttingen, Göttingen, Germany
[54] Département de Physique Nucléaire et Corpusculaire, Université de Genève, Genève, Switzerland
[55] [(a)] Dipartimento di Fisica, Università di Genova, Genova; [(b)] INFN Sezione di Genova, Italy
[56] II. Physikalisches Institut, Justus-Liebig-Universität Giessen, Giessen, Germany
[57] SUPA — School of Physics and Astronomy, University of Glasgow, Glasgow, U.K.
[58] LPSC, Université Grenoble Alpes, CNRS/IN2P3, Grenoble INP, Grenoble, France
[59] Laboratory for Particle Physics and Cosmology, Harvard University, Cambridge MA, U.S.A.
[60] [(a)] Department of Modern Physics and State Key Laboratory of Particle Detection and Electronics, University of Science and Technology of China, Hefei; [(b)] Institute of Frontier and Interdisciplinary Science and Key Laboratory of Particle Physics and Particle Irradiation (MOE), Shandong University, Qingdao; [(c)] School of Physics and Astronomy, Shanghai Jiao Tong University, Key Laboratory for Particle Astrophysics and Cosmology (MOE), SKLPPC, Shanghai; [(d)] Tsung-Dao Lee Institute, Shanghai, China
[61] [(a)] Kirchhoff-Institut für Physik, Ruprecht-Karls-Universität Heidelberg, Heidelberg; [(b)] Physikalisches Institut, Ruprecht-Karls-Universität Heidelberg, Heidelberg, Germany
[62] [(a)] Department of Physics, Chinese University of Hong Kong, Shatin, N.T., Hong Kong; [(b)] Department of Physics, University of Hong Kong, Hong Kong; [(c)] Department of Physics and Institute for Advanced Study, Hong Kong University of Science and Technology, Clear Water Bay, Kowloon, Hong Kong, China
[63] Department of Physics, National Tsing Hua University, Hsinchu, Taiwan

JHEP05(2021)093

[64] IJCLab, Université Paris-Saclay, CNRS/IN2P3, 91405, Orsay, France
[65] Department of Physics, Indiana University, Bloomington IN, U.S.A.
[66] [(a)] INFN Gruppo Collegato di Udine, Sezione di Trieste, Udine; [(b)] ICTP, Trieste; [(c)] Dipartimento Politecnico di Ingegneria e Architettura, Università di Udine, Udine, Italy
[67] [(a)] INFN Sezione di Lecce; [(b)] Dipartimento di Matematica e Fisica, Università del Salento, Lecce, Italy
[68] [(a)] INFN Sezione di Milano; [(b)] Dipartimento di Fisica, Università di Milano, Milano, Italy
[69] [(a)] INFN Sezione di Napoli; [(b)] Dipartimento di Fisica, Università di Napoli, Napoli, Italy
[70] [(a)] INFN Sezione di Pavia; [(b)] Dipartimento di Fisica, Università di Pavia, Pavia, Italy
[71] [(a)] INFN Sezione di Pisa; [(b)] Dipartimento di Fisica E. Fermi, Università di Pisa, Pisa, Italy
[72] [(a)] INFN Sezione di Roma; [(b)] Dipartimento di Fisica, Sapienza Università di Roma, Roma, Italy
[73] [(a)] INFN Sezione di Roma Tor Vergata; [(b)] Dipartimento di Fisica, Università di Roma Tor Vergata, Roma, Italy
[74] [(a)] INFN Sezione di Roma Tre; [(b)] Dipartimento di Matematica e Fisica, Università Roma Tre, Roma, Italy
[75] [(a)] INFN-TIFPA; [(b)] Università degli Studi di Trento, Trento, Italy
[76] Institut für Astro und Teilchenphysik, Leopold-Franzens-Universität, Innsbruck, Austria
[77] University of Iowa, Iowa City IA, U.S.A.
[78] Department of Physics and Astronomy, Iowa State University, Ames IA, U.S.A.
[79] Joint Institute for Nuclear Research, Dubna, Russia
[80] [(a)] Departamento de Engenharia Elétrica, Universidade Federal de Juiz de Fora (UFJF), Juiz de Fora; [(b)] Universidade Federal do Rio De Janeiro COPPE/EE/IF, Rio de Janeiro; [(c)] Instituto de Física, Universidade de São Paulo, São Paulo, Brazil
[81] KEK, High Energy Accelerator Research Organization, Tsukuba, Japan
[82] Graduate School of Science, Kobe University, Kobe, Japan
[83] [(a)] AGH University of Science and Technology, Faculty of Physics and Applied Computer Science, Krakow; [(b)] Marian Smoluchowski Institute of Physics, Jagiellonian University, Krakow, Poland
[84] Institute of Nuclear Physics Polish Academy of Sciences, Krakow, Poland
[85] Faculty of Science, Kyoto University, Kyoto, Japan
[86] Kyoto University of Education, Kyoto, Japan
[87] Research Center for Advanced Particle Physics and Department of Physics, Kyushu University, Fukuoka , Japan
[88] Instituto de Física La Plata, Universidad Nacional de La Plata and CONICET, La Plata, Argentina
[89] Physics Department, Lancaster University, Lancaster, U.K.
[90] Oliver Lodge Laboratory, University of Liverpool, Liverpool, U.K.
[91] Department of Experimental Particle Physics, Jožef Stefan Institute and Department of Physics, University of Ljubljana, Ljubljana, Slovenia
[92] School of Physics and Astronomy, Queen Mary University of London, London, U.K.
[93] Department of Physics, Royal Holloway University of London, Egham, U.K.
[94] Department of Physics and Astronomy, University College London, London, U.K.
[95] Louisiana Tech University, Ruston LA, U.S.A.
[96] Fysiska institutionen, Lunds universitet, Lund, Sweden
[97] Centre de Calcul de l'Institut National de Physique Nucléaire et de Physique des Particules (IN2P3), Villeurbanne, France
[98] Departamento de Física Teorica C-15 and CIAFF, Universidad Autónoma de Madrid, Madrid, Spain
[99] Institut für Physik, Universität Mainz, Mainz, Germany
[100] School of Physics and Astronomy, University of Manchester, Manchester, U.K.
[101] CPPM, Aix-Marseille Université, CNRS/IN2P3, Marseille, France
[102] Department of Physics, University of Massachusetts, Amherst MA, U.S.A.
[103] Department of Physics, McGill University, Montreal QC, Canada
[104] School of Physics, University of Melbourne, Victoria, Australia
[105] Department of Physics, University of Michigan, Ann Arbor MI, U.S.A.

JHEP05(2021)093

[106] Department of Physics and Astronomy, Michigan State University, East Lansing MI, U.S.A.
[107] B.I. Stepanov Institute of Physics, National Academy of Sciences of Belarus, Minsk, Belarus
[108] Research Institute for Nuclear Problems of Byelorussian State University, Minsk, Belarus
[109] Group of Particle Physics, University of Montreal, Montreal QC, Canada
[110] P.N. Lebedev Physical Institute of the Russian Academy of Sciences, Moscow, Russia
[111] National Research Nuclear University MEPhI, Moscow, Russia
[112] D.V. Skobeltsyn Institute of Nuclear Physics, M.V. Lomonosov Moscow State University, Moscow, Russia
[113] Fakultät für Physik, Ludwig-Maximilians-Universität München, München, Germany
[114] Max-Planck-Institut für Physik (Werner-Heisenberg-Institut), München, Germany
[115] Nagasaki Institute of Applied Science, Nagasaki, Japan
[116] Graduate School of Science and Kobayashi-Maskawa Institute, Nagoya University, Nagoya, Japan
[117] Department of Physics and Astronomy, University of New Mexico, Albuquerque NM, U.S.A.
[118] Institute for Mathematics, Astrophysics and Particle Physics, Radboud University/Nikhef, Nijmegen, Netherlands
[119] Nikhef National Institute for Subatomic Physics and University of Amsterdam, Amsterdam, Netherlands
[120] Department of Physics, Northern Illinois University, DeKalb IL, U.S.A.
[121] [(a)] Budker Institute of Nuclear Physics and NSU, SB RAS, Novosibirsk; [(b)] Novosibirsk State University Novosibirsk, Russia
[122] Institute for High Energy Physics of the National Research Centre Kurchatov Institute, Protvino, Russia
[123] Institute for Theoretical and Experimental Physics named by A.I. Alikhanov of National Research Centre "Kurchatov Institute", Moscow, Russia
[124] Department of Physics, New York University, New York NY, U.S.A.
[125] Ochanomizu University, Otsuka, Bunkyo-ku, Tokyo, Japan
[126] Ohio State University, Columbus OH, U.S.A.
[127] Homer L. Dodge Department of Physics and Astronomy, University of Oklahoma, Norman OK, U.S.A.
[128] Department of Physics, Oklahoma State University, Stillwater OK, U.S.A.
[129] Palacký University, RCPTM, Joint Laboratory of Optics, Olomouc, Czech Republic
[130] Institute for Fundamental Science, University of Oregon, Eugene, OR, U.S.A.
[131] Graduate School of Science, Osaka University, Osaka, Japan
[132] Department of Physics, University of Oslo, Oslo, Norway
[133] Department of Physics, Oxford University, Oxford, U.K.
[134] LPNHE, Sorbonne Université, Université de Paris, CNRS/IN2P3, Paris, France
[135] Department of Physics, University of Pennsylvania, Philadelphia PA, U.S.A.
[136] Konstantinov Nuclear Physics Institute of National Research Centre "Kurchatov Institute", PNPI, St. Petersburg, Russia
[137] Department of Physics and Astronomy, University of Pittsburgh, Pittsburgh PA, U.S.A.
[138] [(a)] Laboratório de Instrumentação e Física Experimental de Partículas — LIP, Lisboa; [(b)] Departamento de Física, Faculdade de Ciências, Universidade de Lisboa, Lisboa; [(c)] Departamento de Física, Universidade de Coimbra, Coimbra; [(d)] Centro de Física Nuclear da Universidade de Lisboa, Lisboa; [(e)] Departamento de Física, Universidade do Minho, Braga; [(f)] Departamento de Física Teórica y del Cosmos, Universidad de Granada, Granada (Spain); [(g)] Departamento de Física and CEFITEC of Faculdade de Ciências e Tecnologia, Universidade Nova de Lisboa, Caparica; [(h)] Instituto Superior Técnico, Universidade de Lisboa, Lisboa, Portugal
[139] Institute of Physics of the Czech Academy of Sciences, Prague, Czech Republic
[140] Czech Technical University in Prague, Prague, Czech Republic
[141] Charles University, Faculty of Mathematics and Physics, Prague, Czech Republic
[142] Particle Physics Department, Rutherford Appleton Laboratory, Didcot, U.K.
[143] IRFU, CEA, Université Paris-Saclay, Gif-sur-Yvette, France

JHEP05(2021)093

[144] Santa Cruz Institute for Particle Physics, University of California Santa Cruz, Santa Cruz CA, U.S.A.
[145] [(a)] Departamento de Física, Pontificia Universidad Católica de Chile, Santiago; [(b)] Universidad Andres Bello, Department of Physics, Santiago; [(c)] Instituto de Alta Investigación, Universidad de Tarapacá; [(d)] Departamento de Física, Universidad Técnica Federico Santa María, Valparaíso, Chile
[146] Universidade Federal de São João del Rei (UFSJ), São João del Rei, Brazil
[147] Department of Physics, University of Washington, Seattle WA, U.S.A.
[148] Department of Physics and Astronomy, University of Sheffield, Sheffield, U.K.
[149] Department of Physics, Shinshu University, Nagano, Japan
[150] Department Physik, Universität Siegen, Siegen, Germany
[151] Department of Physics, Simon Fraser University, Burnaby BC, Canada
[152] SLAC National Accelerator Laboratory, Stanford CA, U.S.A.
[153] Physics Department, Royal Institute of Technology, Stockholm, Sweden
[154] Departments of Physics and Astronomy, Stony Brook University, Stony Brook NY, U.S.A.
[155] Department of Physics and Astronomy, University of Sussex, Brighton, U.K.
[156] School of Physics, University of Sydney, Sydney, Australia
[157] Institute of Physics, Academia Sinica, Taipei, Taiwan
[158] [(a)] E. Andronikashvili Institute of Physics, Iv. Javakhishvili Tbilisi State University, Tbilisi; [(b)] High Energy Physics Institute, Tbilisi State University, Tbilisi, Georgia
[159] Department of Physics, Technion, Israel Institute of Technology, Haifa, Israel
[160] Raymond and Beverly Sackler School of Physics and Astronomy, Tel Aviv University, Tel Aviv, Israel
[161] Department of Physics, Aristotle University of Thessaloniki, Thessaloniki, Greece
[162] International Center for Elementary Particle Physics and Department of Physics, University of Tokyo, Tokyo, Japan
[163] Department of Physics, Tokyo Institute of Technology, Tokyo, Japan
[164] Tomsk State University, Tomsk, Russia
[165] Department of Physics, University of Toronto, Toronto ON, Canada
[166] [(a)] TRIUMF, Vancouver BC; [(b)] Department of Physics and Astronomy, York University, Toronto ON, Canada
[167] Division of Physics and Tomonaga Center for the History of the Universe, Faculty of Pure and Applied Sciences, University of Tsukuba, Tsukuba, Japan
[168] Department of Physics and Astronomy, Tufts University, Medford MA, U.S.A.
[169] Department of Physics and Astronomy, University of California Irvine, Irvine CA, U.S.A.
[170] Department of Physics and Astronomy, University of Uppsala, Uppsala, Sweden
[171] Department of Physics, University of Illinois, Urbana IL, U.S.A.
[172] Instituto de Física Corpuscular (IFIC), Centro Mixto Universidad de Valencia — CSIC, Valencia, Spain
[173] Department of Physics, University of British Columbia, Vancouver BC, Canada
[174] Department of Physics and Astronomy, University of Victoria, Victoria BC, Canada
[175] Fakultät für Physik und Astronomie, Julius-Maximilians-Universität Würzburg, Würzburg, Germany
[176] Department of Physics, University of Warwick, Coventry, U.K.
[177] Waseda University, Tokyo, Japan
[178] Department of Particle Physics and Astrophysics, Weizmann Institute of Science, Rehovot, Israel
[179] Department of Physics, University of Wisconsin, Madison WI, U.S.A.
[180] Fakultät für Mathematik und Naturwissenschaften, Fachgruppe Physik, Bergische Universität Wuppertal, Wuppertal, Germany
[181] Department of Physics, Yale University, New Haven CT, U.S.A.

[a] Also at Borough of Manhattan Community College, City University of New York, New York NY, U.S.A.
[b] Also at Center for High Energy Physics, Peking University, China
[c] Also at Centro Studi e Ricerche Enrico Fermi, Italy

JHEP05(2021)093

[d] Also at CERN, Geneva, Switzerland
[e] Also at CPPM, Aix-Marseille Université, CNRS/IN2P3, Marseille, France
[f] Also at Département de Physique Nucléaire et Corpusculaire, Université de Genève, Genève, Switzerland
[g] Also at Departament de Fisica de la Universitat Autonoma de Barcelona, Barcelona, Spain
[h] Also at Department of Financial and Management Engineering, University of the Aegean, Chios, Greece
[i] Also at Department of Physics and Astronomy, Michigan State University, East Lansing MI, U.S.A.
[j] Also at Department of Physics and Astronomy, University of Louisville, Louisville, KY, U.S.A.
[k] Also at Department of Physics, Ben Gurion University of the Negev, Beer Sheva, Israel
[l] Also at Department of Physics, California State University, East Bay, U.S.A.
[m] Also at Department of Physics, California State University, Fresno, U.S.A.
[n] Also at Department of Physics, California State University, Sacramento, U.S.A.
[o] Also at Department of Physics, King's College London, London, U.K.
[p] Also at Department of Physics, St. Petersburg State Polytechnical University, St. Petersburg, Russia
[q] Also at Department of Physics, University of Fribourg, Fribourg, Switzerland
[r] Also at Dipartimento di Matematica, Informatica e Fisica, Università di Udine, Udine, Italy
[s] Also at Faculty of Physics, M.V. Lomonosov Moscow State University, Moscow, Russia
[t] Also at Faculty of Physics, Sofia University, 'St. Kliment Ohridski', Sofia, Bulgaria
[u] Also at Giresun University, Faculty of Engineering, Giresun, Turkey
[v] Also at Graduate School of Science, Osaka University, Osaka, Japan
[w] Also at Hellenic Open University, Patras, Greece
[x] Also at Institucio Catalana de Recerca i Estudis Avancats, ICREA, Barcelona, Spain
[y] Also at Institut für Experimentalphysik, Universität Hamburg, Hamburg, Germany
[z] Also at Institute for Nuclear Research and Nuclear Energy (INRNE) of the Bulgarian Academy of Sciences, Sofia, Bulgaria
[aa] Also at Institute for Particle and Nuclear Physics, Wigner Research Centre for Physics, Budapest, Hungary
[ab] Also at Institute of Particle Physics (IPP), Canada
[ac] Also at Institute of Physics, Azerbaijan Academy of Sciences, Baku, Azerbaijan
[ad] Also at Instituto de Fisica Teorica, IFT-UAM/CSIC, Madrid, Spain
[ae] Also at Istanbul University, Department of Physics, Istanbul, Turkey
[af] Also at Joint Institute for Nuclear Research, Dubna, Russia
[ag] Also at Moscow Institute of Physics and Technology State University, Dolgoprudny, Russia
[ah] Also at National Research Nuclear University MEPhI, Moscow, Russia
[ai] Also at Physics Department, An-Najah National University, Nablus, Palestine
[aj] Also at Physikalisches Institut, Albert-Ludwigs-Universität Freiburg, Freiburg, Germany
[ak] Also at The City College of New York, New York NY, U.S.A.
[al] Also at TRIUMF, Vancouver BC, Canada
[am] Also at Universita di Napoli Parthenope, Napoli, Italy
[an] Also at University of Chinese Academy of Sciences (UCAS), Beijing, China
[*] Deceased

JHEP05(2021)093